Inorganic geochemistry of lake sediments: A review of analytical techniques and guidelines for data interpretation

Sebastien Bertrand, Rik Tjallingii, Malin E Kylander, Bruno Wilhelm, Stephen J Roberts, Fabien Arnaud, Erik Brown, Richard Bindler

▶ **To cite this version:**

Sebastien Bertrand, Rik Tjallingii, Malin E Kylander, Bruno Wilhelm, Stephen J Roberts, et al.. Inorganic geochemistry of lake sediments: A review of analytical techniques and guidelines for data interpretation. Earth-Science Reviews, 2024, 249, pp.104639. 10.1016/j.earscirev.2023.104639 . hal-04460604

HAL Id: hal-04460604
https://hal.science/hal-04460604

Submitted on 15 Feb 2024

HAL is a multi-disciplinary open access archive for the deposit and dissemination of scientific research documents, whether they are published or not. The documents may come from teaching and research institutions in France or abroad, or from public or private research centers.

L'archive ouverte pluridisciplinaire **HAL**, est destinée au dépôt et à la diffusion de documents scientifiques de niveau recherche, publiés ou non, émanant des établissements d'enseignement et de recherche français ou étrangers, des laboratoires publics ou privés.

Distributed under a Creative Commons Attribution 4.0 International License

Earth-Science Reviews 249 (2024) 104639

Contents lists available at ScienceDirect

Earth-Science Reviews

journal homepage: www.elsevier.com/locate/earscirev

Inorganic geochemistry of lake sediments: A review of analytical techniques and guidelines for data interpretation

Sebastien Bertrand [a,b,*], Rik Tjallingii [c], Malin E. Kylander [d], Bruno Wilhelm [e], Stephen J. Roberts [f], Fabien Arnaud [g], Erik Brown [h], Richard Bindler [i]

[a] Renard Centre of Marine Geology, Ghent University, Gent, Belgium
[b] GEOPS, Paris-Saclay University, Orsay, France
[c] Section Climate Dynamics and Landscape Evolution, GFZ German Research Centre for Geosciences, Potsdam, Germany
[d] Department of Geological Sciences and the Bolin Centre for Climate Research, Stockholm University, Sweden
[e] Université Grenoble Alpes, Grenoble, France
[f] British Antarctic Survey, Cambridge, United Kingdom
[g] EDYTEM, Université Savoie Mont Blanc, Le Bourget du Lac, France
[h] University of Minnesota Duluth, Duluth, USA
[i] Umeå University, Umeå, Sweden

ARTICLE INFO

Keywords:
XRF core scanner
Normalization
Calibration
Compositional data
Statistical exploration
Grain size
Provenance

ABSTRACT

Inorganic geochemistry is a powerful tool in paleolimnology. It has become one of the most commonly used techniques to analyze lake sediments, particularly due to the development and increasing availability of XRF core scanners during the last two decades. It allows for the reconstruction of the continuous processes that occur in lakes and their watersheds, and it is ideally suited to identify event deposits. How earth surface processes and limnological conditions are recorded in the inorganic geochemical composition of lake sediments is, however, relatively complex. Here, we review the main techniques used for the inorganic geochemical analysis of lake sediments and we offer guidance on sample preparation and instrument selection. We then summarize the best practices to process and interpret bulk inorganic geochemical data. In particular, we emphasize that log-ratio transformation is critical for the rigorous statistical analysis of geochemical datasets, whether they are obtained by XRF core scanning or more traditional techniques. In addition, we show that accurately interpreting inorganic geochemical data requires a sound understanding of the main components of the sediment (organic matter, biogenic silica, carbonates, lithogenic particles) and mineral assemblages. Finally, we provide a series of examples illustrating the potential and limits of inorganic geochemistry in paleolimnology. Although the examples presented in this paper focus on lake and fjord sediments, the principles presented here also apply to other sedimentary environments.

1. Introduction

The inorganic geochemical composition of lake sediments contains valuable information about the processes occurring in lakes and their watersheds. Variations in the abundance of one or several elements can be used to reconstruct changes in catchment hydrology, lake productivity, pollution, lake level, wind strength, etc. (e.g., Davies et al., 2015). Inorganic geochemistry is also frequently used to identify event deposits in lake sediments, such as those caused by floods, earthquakes, tsunamis, and volcanic eruptions (e.g., Sabatier et al., 2022; Wilhelm et al., 2022).

The development and increasing availability of X-ray Fluorescence core scanners (XRF-CS) during the last two decades has resulted in a considerable increase in the use of inorganic geochemical data in paleolimnology. Researchers are now able to acquire high-resolution multi-elemental inorganic geochemical data rapidly and non-destructively on split sediment cores with minimal sample preparation. As a result, XRF-CS has become one of the most frequently used paleolimnological techniques of the 21st century and inorganic geochemistry is increasingly part of the routine measurements made before sediment core subsampling. Despite these recent technical developments, more traditional techniques such as Inductively Coupled Plasma Optical Emission

* Corresponding author at: Renard Centre of Marine Geology, Ghent University, Gent, Belgium and GEOPS, Paris-Saclay University, Orsay, France.
E-mail addresses: sebastien.bertrand@ugent.be, sebastien.bertrand@universite-paris-saclay.fr (S. Bertrand).

https://doi.org/10.1016/j.earscirev.2023.104639
Received 9 July 2023; Received in revised form 30 September 2023; Accepted 20 November 2023
Available online 1 December 2023
0012-8252/© 2023 The Author(s). Published by Elsevier B.V. This is an open access article under the CC BY license (http://creativecommons.org/licenses/by/4.0/).

Spectrometry (ICP-OES), Inductively Coupled Plasma Mass Spectrometry (ICP-MS) and Wavelength Dispersive X-ray Fluorescence (WD-XRF) still have their place in paleolimnological research, especially when quantitative results and/or a direct comparison with the composition of sediment sources are needed.

The use of XRF-CS by the paleolimnology community in the last two decades has outpaced the development of data handling and interpretation tools, resulting in frequent data mis- or over-interpretations. Unlike techniques analyzing discrete samples, such as ICP-OES, ICP-MS, and WD-XRF, XRF-CS only measures a subset of major and trace elements, most commonly those with atomic masses ranging from Si to Zr. Analytical uncertainties are particularly high for lighter elements, such as Si, Al, and Mg, although, combined, these elements constitute about 85% of the earth's crust, and by extension of detrital sediments. XRF-CS results are also influenced by variations in the water content and physical properties of the sediment, such as bulk density, and therefore require specific data processing methods.

Accurately interpreting inorganic geochemical data, independent of the technique used to acquire them, also requires a profound knowledge of the mechanisms responsible for elemental changes, which differ between catchments depending on e.g., bedrock geology, basin geomorphology, soil cover, climate, vegetation. It requires a comprehensive understanding of the associations of elements with one or several components of the sediment, such as lithogenic particles, carbonates, biogenic silica, or organic matter, and with specific minerals. The latter can be aided by multivariate statistical analysis of the geochemical datasets. In other words, interpretations of geochemical data are generally site-specific and not directly transferable from lake to lake. Therefore, they should not be taken as universally applicable.

With this in mind, the goal of this review paper is to provide guidelines to analyze, process, and interpret inorganic geochemical data obtained from lake sediments. Although these guidelines may seem familiar and routine for inorganic geochemists, they are specifically designed for the increasingly large community of paleolimnologists that use inorganic geochemical data but are relatively unfamiliar with the fundamentals of inorganic geochemistry. In this article, we specifically focus on bulk inorganic geochemical measurements, which are relatively easy to acquire, widely used in paleolimnology, and sufficient to answer most research questions. Techniques aimed at the analysis of rare earth elements, isotopes, or specific components isolated from the sediment (e.g., leaching) are not discussed. Those designed for the analysis of micro-samples and elemental mapping (e.g., SEM-EDX, micro-XRF) are also not part of this review. We focus here on major and selected trace elements that are of particular interest in paleolimnology. Although most of the examples presented in this review correspond to lake and fjord sediments, the principles presented here also apply to other sedimentary environments (e.g., marine sediments, peat). We hope that this article serves as a basis to help the paleolimnological community rigorously process and interpret inorganic geochemical data obtained on lake sediments, independent of their expertise.

2. Analytical techniques

The inorganic geochemical composition of lake sediments can be analyzed using a number of instruments, the choice of which is generally based on the required spatial resolution (number of samples), amount of sediment available for analysis, required precision, and expected concentrations (cf. detection limits). Nowadays, most sediment cores are analyzed at high (mm to cm) resolution using XRF-CS. However, traditional techniques designed to analyze discrete samples such as ICP-OES, WD-XRF, and, to a lesser extent, ICP-MS, remain abundantly used in paleolimnology, especially for applications that require quantitative measurements or for analyzing samples collected in sediment traps or after filtration of water samples. Such quantitative measurements are also required to compare the geochemical composition of sediment cores to e.g., the nature of the sediment sources (bedrock, soil, river sediment) and to calculate element fluxes.

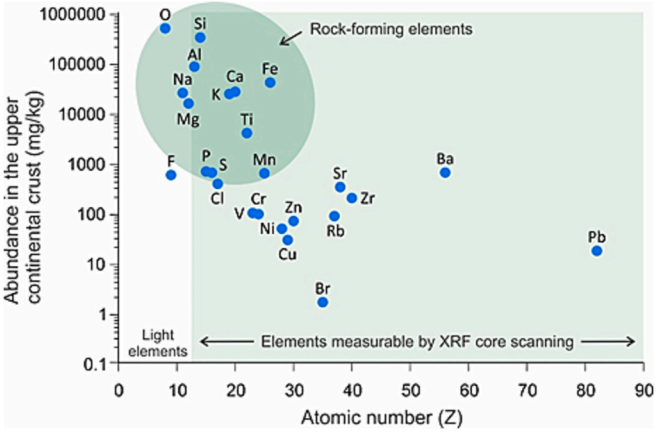

Fig. 1. Abundance of elements in the Earth's upper continental crust (from Rudnick and Gao, 2014) plotted against their atomic number. For elements with Z > 12, only those detectable by XRF core scanners are shown. Note that Na, Mg and O are important rock-forming elements but that they are not measurable by XRF-CS. Figure inspired from Rothwell and Croudace (2015).

Compared to XRF-CS, discrete sample analysis offers lower limits of detection (LOD) and higher precision (reproducibility), but it is also much more time-consuming. In addition, light elements such as Si, Al, Na and Mg are notoriously difficult or impossible to measure by XRF-CS, although they constitute the most abundant rock-forming elements in the upper continental crust (Fig. 1). Therefore, traditional techniques remain necessary for total major element[1] analysis. The text that follows briefly describes the most commonly used instruments for inorganic geochemical analysis, with a focus on helping readers select the instrument that is most appropriate for their specific objectives.

2.1. Discrete samples

Inorganic geochemical analysis of discrete sediment samples is generally done using WD-XRF or ICP-OES, which is also referred to as Inductively Coupled Plasma Atomic Emission Spectroscopy (ICP-AES). While more commonly used for trace and ultratrace element analysis, ICP-MS is also sometimes applied for the analysis of major elements. In addition, high-end Energy Dispersive X-ray Fluorescence (ED-XRF) instruments are increasingly used for the analysis of discrete samples since recent improvements in energy-dispersive detectors mean that benchtop (not portable) ED-XRF may perform almost as well as the traditional, but more costly, WD-XRF (e.g., Craigie, 2018). Although high precision elemental analysis is also possible using Atomic Absorption Spectrometry (AAS), this technique is less frequently used for multi-elemental analysis due to difficulties in measuring multiple elements (e.g., Ferreira et al., 2018). As such, ICP-OES and WD-XRF are currently the two types of instruments most frequently used for the analysis of discrete samples in paleolimnology. They offer similar performance when it comes to precision and LOD, but they mostly differ in the amount of sample required and in the type of sample preparation needed before analysis (Table 1). Readers interested in specific details about preparation techniques and/or the functioning of a specific instrument are referred to Potts (1987) and Gill (2014).

2.1.1. Wavelength dispersive X-ray fluorescence

Analyzing the inorganic geochemical composition of sediment samples by WD-XRF requires the preparation of glass beads, pressed pellets,

[1] Major elements are defined here as the 10 rock-forming elements (Si, Al, Fe, Ti, Na, Ca, K, Mg, Mn, P)

Table 1
Most common preparation techniques for the analysis of discrete sediment samples, according to analytical instrument and type of elements of interest. Note that analyzing loose powders by WD-XRF is becoming increasingly popular, despite the lower precision.

	Major elements	Trace elements
WD-XRF	Fused glass beads (0.5 g)	Pressed pellets (3 g)
ICP-OES	Fused glass beads (50 mg) dissolved in nitric acid	Multi-acid digestion (50 mg)

or loose powders. Glass beads are based on fusing the sediment sample with a flux and are preferred for major element geochemistry due to its ability to digest samples entirely, lack of matrix effect, and excellent sample homogenization. Pressed pellets are preferred for trace elements since they do not use any flux, which may add impurities, and result in higher sample dilution. Analyzing milled samples in the form of dry powders directly is a newer approach that is increasing in popularity as it exploits the non-destructive nature of the WD-XRF instrumentation (e.g., Rydberg, 2014). In all cases, the samples should first be air- or freeze-dried and homogenized with an agate mortar or ball mill. In case of samples from saltwater environments (samples from saltwater lakes or marine sediment samples), it is recommended to rinse the samples before drying to avoid salts precipitating from the porewater (e.g., Loring and Rantala, 1992).

a) The preparation of glass beads generally consists in mixing about 0.5 g of homogenized sediment with 2.5 g of flux, which decreases the melting temperature of the mix to about 1000 °C. The two most common fluxes are Li-metaborate and Li-tetraborate, to which LiBr is added as a wetting agent. Fusion generally consists in mixing the sediment-flux mixture in a Pt-Au crucible, which is then placed in a muffle furnace at 1050 °C for about 10 min. Automatic fluxing systems are also available (e.g., Claisse®).

b) Pressed pellets are generally prepared by pressing about 3 g of homogenized sediment with a 10 ton press, with or without binding agent. The pellets can be directly analyzed by WD-XRF. This preparation technique is faster than flux fusion but it results in slightly less homogenous samples.

c) Loose powders loaded into plastic cups are increasingly being used for WD-XRF analysis. Here, the sample is dried and milled to a homogenous powder, loaded into plastic sample cups with an inner diameter of 15 to 20 mm and a 2.5 μm Mylar® film at the base. Samples sizes range from 0.2 to 0.5 g. The main advantages of this method are its speed and the lack of sample contamination through the addition of flux or binding agents.

2.1.2. *Inductively coupled Plasma Optical Emission Spectrometry*

The analysis of sediment samples by ICP-OES requires digesting the samples to obtain a solution for analysis. This is generally done either by dissolving glass beads in nitric acid or using multi-acid digestion. In both cases, only about 50 mg of homogenized sediment is required (Table 1). The dissolution of glass beads is faster and commonly used for the analysis of major and some relatively abundant trace elements (e.g., Ba, Sr, Zr). Its main disadvantage is that the relatively high dilution factors may result in lowering the concentration of some low abundance trace elements below the instrument's LOD (Fig. 2). Multi-acid digestion is better suited for trace elements since it does not involve the use of flux, which limits dilution and contamination, and can be done using high-purity acids. However, it is less effective at digesting refractory minerals, such as zircon and titanite, resulting in the incomplete recovery of elements such as Ti, Cr, and Zr (Sholkovitz, 1990; Murray et al., 2000; Huang et al., 2007; Craigie, 2018). Solutions prepared using any of these techniques can also be analyzed by ICP-MS. However, using an ICP-MS is only sensible for low abundance trace elements (including rare earth elements) since for major and most trace elements, the LODs of ICP-OES instruments are far below the concentrations generally encountered in lake sediments (Fig. 2). In practice, it is common to analyze major and abundant trace elements by ICP-OES after flux fusion and glass bead dissolution, and less abundant elements by ICP-OES or ICP-MS after multi-acid digestion. Most recent ICP-OES use a combination of radial and axial analysis (also called dual view), which ensures simultaneous element analysis and low limits of detection, respectively.

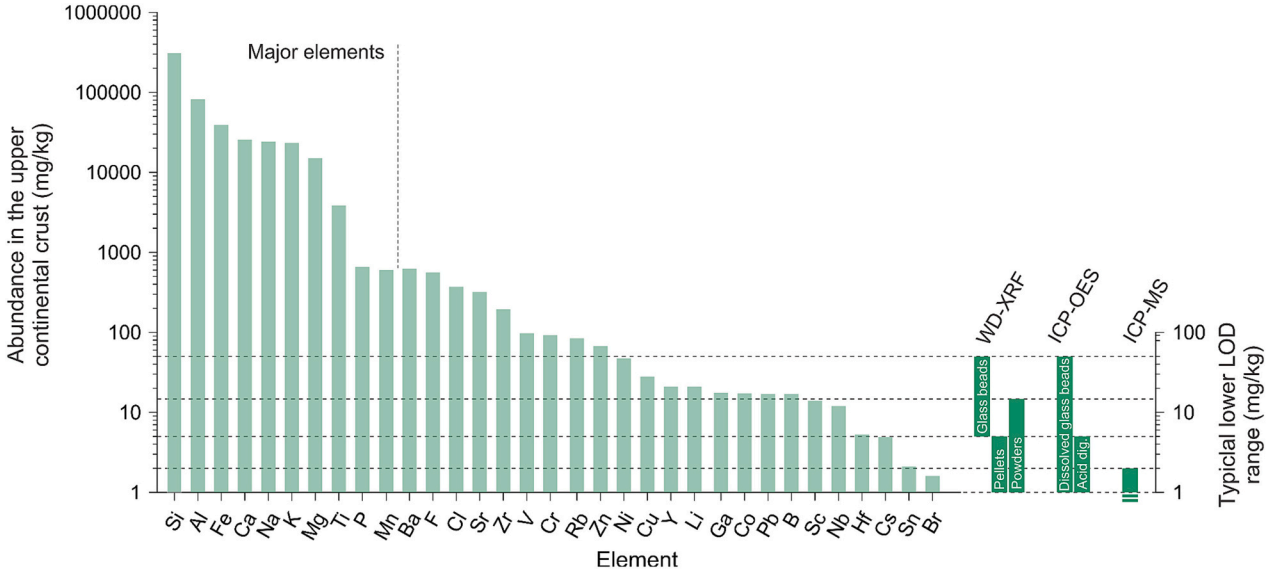

Fig. 2. Abundance of major and abundant trace elements (>1 mg/kg) in the upper continental crust (UCC; from Rudnick and Gao, 2014), compared to the average range of lower limits of detection (lower LOD) of traditional instruments (WD-XRF, ICP-OES and ICP-MS; compiled from Potts, 1987; Gill, 2014; Bertrand et al., 2012; Duchesne and Bologne, 2009; Rydberg, 2014; https://www.eag.com/app-note/icp-oes-and-icp-ms-detection-limit-guidance/ and https://actlabs.com/). For the solution-based techniques (ICP-OES and ICP-MS), the LODs consider a 4000× dilution, which is typical for the glass bead preparation technique (Murray et al., 2000). Lower dilution, and therefore better precision, can be achieved using multi-acid digestion. Note that these values are only indicative and that the real LODs depend on the exact element, instrument, sample matrix, analytical setup, etc. XRF core scanners are not included in this figure but their LODs are strongly element-dependent and typically one order of magnitude or more above the techniques presented here (see Fig. 1).

a) Glass beads are generally prepared the same way as for WD-XRF analysis, but in smaller Pt-Au crucibles since ICP-OES only requires dissolving about 50 mg of sediment. As such, it is generally done manually and not using automatic fluxing systems, which are made for larger crucibles and samples. After fusion with 200 mg of flux, the bead is dissolved in 5% nitric acid, which is then filtered, diluted, and measured by ICP-OES. This procedure is described in detail in Murray et al. (2000).

b) Multi-acid digestion using a mixture of acids such as HF, HCl and HNO_3 is the cleanest preparation technique. However, total acid digestion requires the use of HF, which is particularly hazardous. Acid digestions are often made using hotplate, hotblock or microwave systems. The latter accelerates the breakdown of geological samples through the use of high temperature and pressure. This method is preferred for trace elements close to the limit of detection of the instrument. A drawback is that the use of HF does not allow for the analysis of Si due to the formation of volatile SiF and subsequent loss of Si during digestion (e.g., Gill, 2014).

2.1.3. Choosing an instrument

As illustrated in Fig. 2, the lower LODs of all instruments for all major and abundant trace elements are well below the concentrations normally encountered in the upper continental crust, and therefore in lake sediments. As a result, the LODs of the traditional techniques (WD-XRF, ICP-OES) do not generally constitute a limitation in paleolimnology, unless specific trace and ultratrace elements are of interest. Instrument precision (i.e., repeatability), on the other hand, is generally a more important criterion to consider when selecting an instrument since variations in concentrations between samples may be relatively minor but significant. Both WD-XRF and ICP-OES typically achieve precisions of 1–2% relative standard deviation (RSD) for major elements and 2–10% RSD for trace elements. Achieving such a level of precision or better by ICP-OES requires correcting for instrument drift by measuring a matrix-matched solution in-between every sample (e.g., Murray et al., 2000; Gill, 2014). The precision reached by ICP-MS for trace elements tends to be similar. Precision for loose powders analyzed by WD-XRF is generally better than 10% for major and abundant trace elements (Rydberg, 2014), which is similar to values obtained on pressed pellets with modern bench-top ED-XRF instruments (Wien et al., 2005; Zhan, 2005), although this is highly dependent on sample preparation (Cevik et al., 2013). Such a precision may be a limitation for some applications in paleolimnology. The simultaneous acquisition of several elements by ICP-OES instruments using a CCD detector or polychromator can result in particularly good precision ($< 1\%$) for elemental ratios (e.g., Bertrand et al., 2012).

Other considerations when choosing an instrument include the amount of sample available, the number of elements required, instrument availability, and analytical costs. Also note that halogens (Cl, Br, I) can generally not be measured with a reasonable precision by ICP-OES. For more details, readers are referred to Gill (2014) and Craigie (2018).

2.1.4. Reporting inorganic geochemical results obtained on discrete samples

Independent of the selected instrument and preparation technique, inorganic geochemical results are generally expressed as a percentage (wt%, g/g, mg/g) of the total sediment weight, including organic matter, since samples are generally not combusted before preparation. This is different from total rock analysis, for which samples are generally combusted at 1000 °C, i.e., oxidized, before analysis, to remove organic matter and CO_2 from carbonates. Not combusting the samples prior to preparation permits a better comparison with measurements obtained by XRF-CS. As a result, the sum of the major elements[1] expressed in oxides is generally lower than 100% (i.e., the mass percentage of CO_2 is significant but not quantified).

Traditionally, WD-XRF data of major elements have been reported in oxides. Trace elements and major elements measured by ICP-OES or ICP-MS, however, are generally expressed as elemental concentrations. This is however not a requirement, and it mostly reflects the standards used for calibration (rock powders for WD-XRF vs elements in solution for ICP-based techniques). In any case, oxide concentrations can easily be transformed into element concentrations and vice versa (Table 2).

Table 2
Conversion factors between oxide concentrations and element concentrations for the 10 major elements. Multiplying elemental concentrations by the corresponding conversion factor provides oxide concentrations and vice versa.

Element (wt%)	Conversion factor	Oxide (wt%)
Si	2.1392	SiO_2
Al	1.8895	Al_2O_3
Fe	1.4297	Fe_2O_3
Fe	1.2865	FeO
Mn	1.2912	MnO
Ti	1.6681	TiO_2
Ca	1.3992	CaO
Na	1.3480	Na_2O
K	1.2046	K_2O
Mg	1.6582	MgO
P	2.2916	P_2O_5

When reporting quantitative data, it is important to report three aspects of quality control: limits of detection, precision, and accuracy (e.g., Gill, 2014).

For major elements, reporting LODs is not strictly necessary since they are typically several orders of magnitude below the concentrations typically encountered in lake sediments (Fig. 2). LODs should however be systematically reported for trace elements. They are calculated through the analysis of multiple procedural blanks, which are prepared identically to the samples but do not contain any sediment. LODs are defined as 3 × the standard deviation of the procedural blank.

Reporting precision and representing it on figures is particularly important to determine the significance of the variations. These values can be established using repeat measurements (generally 10) of individually prepared representative samples throughout the analytical run.

Accuracy should be reported as compared to a certified reference material (CRM). Choosing a representative CRM may be challenging in paleolimnology due to the general lack of lake sediment standards. CRMs are available from the NRC (National Research Council of Canada), BCR (Institute for Reference Materials and Measurements of the European Commission), and NIST (National Institute of Standards and Technology, USA). BCR has lake sediment CRMs (BCR-280R and 701) but values are only certified for selected trace metals. As a result, river, estuarine, or marine sediments (e.g., HISS-1, MESS-4, PACS-3, and STSD) are often used as an alternative since they allow covering the entire range of elements of interest.

Making geochemical data available to the community through online data repositories is strongly encouraged. The EarthChem Library (https://earthchem.org/ecl/) is specifically designed for geochemical datasets obtained on discrete samples. For data obtained along sediment cores, PANGAEA (https://www.pangaea.de/) and the NOAA World Data Service for Paleoclimatology (https://www.ncei.noaa.gov/products/paleoclimatology) are particularly well suited. Although best practices for reporting geochemical data are yet to be defined (Klöcking et al., 2023), most scientific journals allow referring directly to datasets hosted on these online data repositories.

2.2. XRF core scanning

Non-destructive inorganic geochemical measurements obtained directly at the split sediment core surface started in the 1980s with the development of the XRF core scanner (Jansen et al., 1998). For the first time, this development allowed the rapid and non-destructive scanning of entire sediment cores at centimeter to sub-millimeter resolution, providing near continuous geochemical records. XRF-CS analysis is based on energy-dispersive (ED) XRF. The latter allows measuring all

elements simultaneously, but it is less sensitive and less precise than WD-XRF. XRF-CS analysis therefore favors measurements at high spatial resolution over high precision. Unlike traditional geochemical analysis on discrete samples, XRF-CS measurements made on the surface of wet sediment cores are influenced by downcore variations in water content and bulk density (Jansen et al., 1998; Croudace et al., 2006; Tjallingii et al., 2007). By comparison, grain-size variations do not seem to significantly affect the quality of the measurements (Bertrand et al., 2015). Since calibrating XRF-CS measurements is not as straightforward as with traditional analytical techniques, instruments generally provide results expressed in elemental counts (or count per second) instead of concentrations.

Several types of XRF-CS have been developed during the last two decades. The basic principles behind those XRF-CS systems are similar but instrument-specific information can be found in Richter et al., 2006 (Avaatech), Croudace et al., 2006 (Itrax), Sakamoto et al., 2006 (Tatscan), and Murdmaa et al. (2021) (Geotek). In addition, instrumental developments and applications have been detailed in two specialist books (Rothwell, 2006; Croudace and Rothwell, 2015) and in a special issue of Quaternary International (Croudace et al., 2019). In parallel to XRF-CS instruments specifically designed for the analysis of sediment cores, field portable XRF (FP-XRF or P-XRF) is becoming increasingly popular in geosciences, including for sediment core analysis (e.g. Schillereff et al., 2015). However, this instrument originally developed for the mining industry generally suffers from poor LODs when applied to natural sediment mixtures, and it is not optimized to observe the mm-scale variations that are typical of most lake sediments. Its current use in paleolimnology is therefore mostly restricted to qualitative measurements.

2.2.1. Data acquisition

Sample preparation for XRF-CS analysis is limited to scraping off the split core surface to ensure a fresh and smooth surface and covering it with an XRF-transparent foil (e.g., Prolene, polypropylene, Mylar) to avoid desiccation of the core and potential contamination of the analytical equipment. The core surface is then irradiated with an X-ray source that generates secondary XRF radiation within the upper sediments. The energy (in keV) of the XRF photons re-emitted by the irradiated surface is proportional to the atomic number of the elements. The elemental range and measurement quality can be optimized by adjusting the measurement time, the X-ray source settings (kV and mA), and the type of X-ray source (e.g. Rh, Cr, Mo anode) (e.g., Jones et al., 2019).

Elements with a low atomic number (Z), i.e., light elements, generally have poor detection limits since they produce low energy radiation that is easily absorbed within the sample or by water at the core surface and air between the core surface and the detector. Heavier elements have a higher fluorescence energy and a higher penetration depth (or response or critical depth) and are less influenced by absorption of XRF radiation at the core surface (Tjallingii et al., 2007). Generally, XRF-CS instruments provide good results for elements between Si ($Z = 14$) and Zr ($Z = 40$). Performance can be improved for elements lighter than Si (e.g., Mg, Al) by using a He atmosphere or vacuum. The detection of heavier elements, however, suffers from the higher background radiation (bremsstrahlung) of the X-ray source, which can be suppressed by the use of filters.

In addition to elemental fluorescence, XRF spectra obtained by XRF-CS also record the scattering of primary X-rays, which consists of bremsstrahlung and fluorescence radiation. The two main anode fluorescence lines are the incoherent (also called Compton or inelastic) and coherent (also called Rayleigh or elastic) peaks. The intensity of these scatter peaks depends on the average atomic number of the sample. Samples with a light matrix are characterized by a low coherent and a high incoherent peak and vice versa. The ratio of the incoherent to coherent scattering thus provides a relative assessment of the average atomic number of the sample (Croudace et al., 2006). As a result, this ratio has been used to estimate relative variations in lighter (e.g. water, organic matter) and heavier (e.g. lithogenic particles) elements in sediments (e.g. Thomson et al., 2006; Woodward and Gadd, 2019).

The sampling resolution of most XRF-CS can be varied between 0.2 and 10 mm. Depending on the system, the irradiated surface is fixed by the use of a flat beam optical device generating a rectangular beam that sweeps over a specific core length (e.g., Itrax; Croudace et al., 2006), or can be adjusted with a variable slit collimation system (e.g., Avaatech; Richter et al., 2006).

The analytical quality of XRF-CS measurements increases with the number of counts, which is proportional to the measurement time and intensity of the primary X-ray beam. The latter depends on the electric current (mA) of the X-ray source. The measurement time is set by the user (generally 1–60 s) but it may not always correspond to the net acquisition time, depending on how the instrument deals with dead time, i.e., the processing time that is required to generate a XRF spectrum during a measurement (Dunlea et al., 2020).

The precision of elemental intensity data acquired by XRF scanning has been a subject of debate since the introduction of the first XRF-CS (Croudace et al., 2006; Jansen et al., 1998). The best way to calculate the analytical precision of XRF-CS measurements is by using replicate measurements of a number of points along the core (Weltje et al., 2015; Weltje and Tjallingii, 2008). The latter are easy to acquire and respect the non-destructive nature of the method. Ideally, the number of replicate measurements should be proportional to the total number of data points (5 to 10%), obtained at the same resolution, and cover the various lithologies of the sediment core. For example, replicate measurements can be acquired for every 10th measurement or at 2 or 3 selected intervals along the core.

Absolute LODs are particularly difficult to determine for XRF-CS measurements since they vary with sample composition (matrix) and physical sediment properties. Therefore, estimates based on reference materials cannot be transferred to measurements obtained on sediment cores. The best way to assess the LODs of XRF-CS measurements is by using the analytical uncertainty calculated from replicate measurements (cf previous paragraph; Weltje and Tjallingii, 2008). In practice, LODs are at least one order of magnitude higher than those obtained by the analysis of discrete samples using traditional techniques (WD-XRF, ICP-OES and ICP-MS; Fig. 2).

2.2.2. Data processing

Element intensities obtained from XRF-CS measurements are calculated by integrating the peaks observed on the XRF spectra after complete processing of the spectra, which includes background removal, peak identification, and peak overlap corrections. Generally, spectra are processed using a peak-fitting model and the quality of the calculated results is represented by the goodness-of-fit. XRF-CS results are typically presented as element intensities in totals counts or counts per second (cps). The meaning and interpretation of element intensities produced by XRF-CS has been debated since the early days of XRF-CS (e.g. Jansen et al., 1998). Since XRF-CS element intensities are not a quantitative measure, the intensities of two elements cannot be compared directly. For example, the intensities of Si are generally lower than those of Fe, but this does not mean that the concentrations of Si are lower than those of Fe. As a result, downcore variations in individual element intensities can only be used to estimate relative variations in element abundance. However, due to the lack of physical homogenization of the samples prior to analysis, variations in element intensity are also affected by downcore changes in physical sediment properties (Jansen et al., 1998), which makes the use of intensities particularly dangerous. Likewise, the absorption of XRF energy by air or pooling of water under the foil covering the core surface causes another unpredictable influence on element intensities (Kido et al., 2006; Tjallingii et al., 2007). Finally, non-linear XRF absorption and enhancement effects, or matrix effects, complicate the direct comparison between XRF scanning measurements and quantitative analyses made on discrete samples (Jansen et al., 1998; Croudace et al., 2006; Tjallingii et al., 2007; Weltje and Tjallingii, 2008).

To circumvent these issues, the XRF-CS community has developed different strategies that are detailed below. The overall goal of these methods is to reduce the influence of physical properties and matrix effects on the XRF-CS measurements, and ultimately extract representative geochemical information from these measurements. Although raw intensities may contain information that is no longer visible after processing, those variations generally reflect changes in lithology (water content, organic matter content, sediment compaction, etc), but not necessarily in inorganic geochemistry (Fig. 3). Differences between pre- and post-processing datasets tend to be high for unconsolidated sediments, particularly in the upper meters of lake sediment cores, which are typically poorly compacted. Given the rapid evolution of XRF-CS data processing techniques, it is currently recommended to report XRF-CS data in raw format in data repositories such as PANGAEA (https://www.pangaea.de/) or the NOAA World Data Service for Paleoclimatology (https://www.ncei.noaa.gov/products/paleoclimatology)

a) Normalization

Normalization of element intensities can be an effective way to eliminate effects arising from changes in physical sediment properties (density, pooling of water, etc.) or measurement times (live time). It is based on the basic principle that all the elements of a measurement are equally affected by physical properties (Weltje and Tjallingii, 2008).

Normalization of XRF-CS data has been done by dividing element intensities by (a) the intensity of a selected element (Jansen et al., 1998; Weltje and Tjallingii, 2008; Lowemark et al., 2011), (b) the incoherent (Compton; Hunt et al., 2015), coherent (Rayleigh; Hahn et al., 2014) or coherent + incoherent (Croudace et al., 2006; Kylander et al., 2012) intensity, or (c) the total count rate at the detector (labeled kcps on itrax data spreadsheets; Ohlendorf et al., 2015). Normalizing element intensities by the incoherent scatter has been suggested to compensate for matrix effects, but this application is inappropriate for the broad compositional ranges typically encountered in sediments (Croudace and Gilligan, 1990). The most appropriate normalization strategy is provided by dividing individual element intensities by the sum of all measured element intensities and expressing them as proportions (% cps, Jansen et al., 1998; Fig. 3b). In this case, it is important to note that the obtained percentages do not correspond to actual concentrations since the heavier elements yield much higher counts than light elements. Also, the sum of all measured element intensities is not the same as the total count rate (kcps), which refers to the detector input-count rate and is a measure of detector saturation. It should also be noted that dividing element intensities (counts) by the acquisition time (to obtain counts per second; cps) does not constitute a proper normalization technique. It is merely a change in scale, and it can only be done if the net acquisition time is known (Dunlea et al., 2020).

Although it has been abundantly used in the literature, normalization does not constitute a robust calibration technique (Jansen et al., 1998; Croudace et al., 2006; Richter et al., 2006; Weltje and Tjallingii, 2008; Lowemark et al., 2011; Kylander et al., 2012; Ohlendorf et al., 2015) since it does not account for non-linear matrix effects (Jenkins and de Vries, 1970; Weltje and Tjallingii, 2008).

b) Log-ratios

The use of log-ratios builds on the advantages of the normalization described above, but also accounts for non-linear matrix effects. The log-ratio approach is based on the observation that log-ratios of element intensities are linear functions of log-ratios of element concentrations (Weltje and Tjallingii, 2008). Log-ratio calibration is able to accurately estimate relative matrix effects, and its strength is proven by results that cross the origin and have a linear 1:1 relation with concentrations (Weltje and Tjallingii, 2008). This linear relation also implies that log-ratios of intensities contain the same information as log-ratios of concentrations.

The centered log-ratio (clr) approach provides a multivariate log-ratio transformation and allows the exploration of single elements, including statistical correlations (Weltje et al., 2015). In practice, the clr values are calculated by dividing the intensities of an element by the geometric mean of the intensities obtained on all selected elements of a measurement (generally all well-measured elements). For example, the geometric mean (g(z)) of all n elements of a measurement at depth z is calculated as:

$$g(z) = \sqrt[n]{counts_{element\ A\ (z)} \cdot counts_{element\ B\ (z)} \cdot \ldots counts_{element\ n\ (z)}} \quad (1)$$

and the clr of element A at depth z is calculated as:

$$\mathrm{CLR\ A\ (z)} = ln\left[\frac{counts\ element\ A\ (z)}{g(z)}\right] \quad (2)$$

Note that clr calculations are only valid for the elements included in the selection. The elements selected for the clr calculation should be well-measured (not noisy) and free of zero values. Measurements with a large amount of zero values can be left out (outliers), whereas occasional zero values can be replaced by a small value (e.g. the detection limit or half of the minimum non-zero value). Additionally, clr calculations should only include element intensities (i.e. the coherent and incoherent scattering data should not be included), and they can be applied directly to elements measured in different runs (i.e., with different X-ray source settings, kV and mA). Clr calculations are very straightforward, rapid, and they can be done either manually (see Excel example in appendix

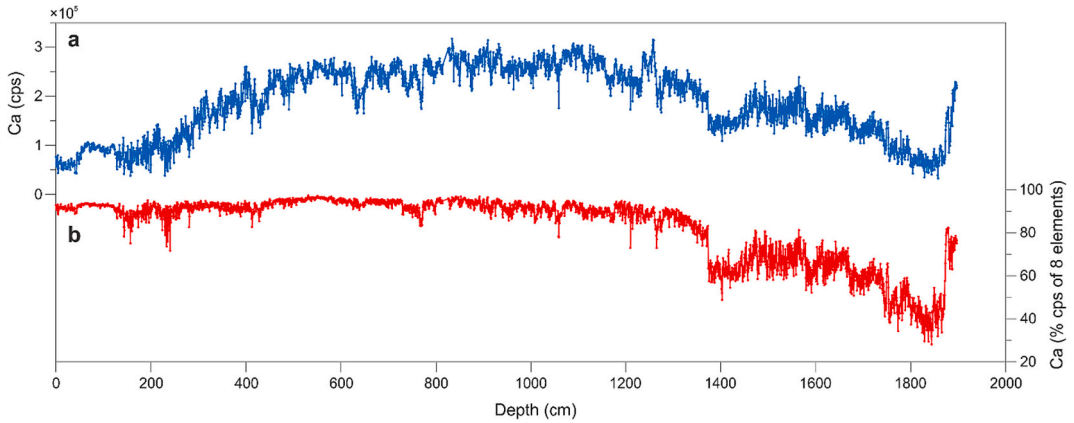

Fig. 3. Normalization of XRF-CS Ca intensities obtained on a sediment core from Lake Gościąż, Poland (Bonk et al., 2021). (a) Calcium intensity (cps) and (b) normalized Ca intensities, obtained by dividing the Ca intensities by the sum of the eight well-measured elements. The main differences between the two Ca records are explained by the high water in the upper part of the core (0–400 cm), which decreases downcore due to sediment compaction.

A), using software such as CoDaPack (http://compositionaldata.com/), or by means of a couple of lines of code in R, Matlab, or Python. The calculated clr values are dimensionless, can be positive and negative (positive for elements with high intensities and vice versa), and the sum of all clr values of a particular measurement should equal zero, which is a good test to verify the correctness of clr calculations (see checksum in appendix 1).

Centered log-ratios of XRF-CS intensities are sufficient for researchers who are merely interested in relative downcore variations in one element since they provide the same information as centered log-ratios of concentrations (Weltje et al., 2015). Centered log-ratios of XRF-CS intensities should however not be compared directly with concentrations. For specific applications making use of ratios between two elements, the equivalent approach consists in using the log-ratio of the intensities of these two elements (e.g., log (elt_A / elt_B)). It is based on the same principle as centered log-ratios but uses the intensity of one element relative to another one instead of the whole. Ratios of clr-transformed data, however, are meaningless.

c) Calibration

Quantification of XRF-CS data can be achieved by calibrating element intensities with quantitative geochemical data (i.e., expressed as concentrations) obtained through traditional discrete sample analysis (e.g., ICP-OES, WD-XRF or ICP-MS). The advantage of such a calibration is that it minimizes many of the inhomogeneity and instrument-specific differences, allowing for inter-instrument comparisons (e.g. Dunlea et al., 2020). Additionally, calibrated XRF data can be directly compared to other quantitative geochemical measurements and can be used to calculate mass accumulation rates. Although there are multiple ways to calibrate XRF-CS data (Gregory et al., 2019), calibrating element intensities directly should be avoided. The initial log-ratio calibration model of Weltje and Tjallingii (2008) was only able to provide semi-quantitative results expressed as a proportion (%) of the sum of the intensities of the measured elements (as in Fig. 3b). However, the multivariate log-ratio calibration model developed by Weltje et al. (2015) provides fully quantitative results, and generally achieves the best results (e.g., Gregory et al., 2019; Dunlea et al., 2020). Both the log-ratio and the multivariate log-ratio calibrations can be done using the free software package Xelerate (Weltje et al., 2015). In addition to calibrating element intensities, this software also has a function to optimize the amount and location (depth) of calibration samples (Weltje et al., 2015).

3. Interpretation of inorganic geochemical data

The large amount of geochemical data produced by analytical instruments, particularly XRF-CS, can be daunting to unfamiliar users. After scanning sediment cores, the first question paleolimnologists generally ask is “which element should I use”? A solution is often found by browsing the literature in order to find an example that is deemed similar, which has been facilitated by the publication of compilations of examples (e.g., Rothwell and Croudace, 2015; Davies et al., 2015). This approach is however relatively risky as interpretations of downcore changes in one element or elemental ratio are not universally applicable. Rather, we argue that they should be evaluated on a lake-by-lake basis, depending on the environmental context of each lake. Therefore, we attempt here to guide paleolimnologists through a series of fundamental steps to interpret inorganic geochemical data from lake sediments. As there is no direct answer to the question “which element should I use”, this section provides a line of thought to help users pick the most appropriate element(s), depending on the nature of the sediment, and the process(es) of interest.

The first step towards a sound interpretation of inorganic geochemical data obtained on lake sediments consists in understanding the association of elements with the main components of the sediment. A rigorous study therefore starts by quantifying (or at least estimating) the amounts of organic matter, biogenic silica, carbonates (and other authigenic minerals, if any) and lithogenic particles of the sediment (Section 3.1). This quantification can be done either at low resolution on a subset of sediment samples collected along the entire length of a sediment core, or on a short sediment core from the same site. In the former case, it is recommended to select samples that cover the entire range of chemical compositions. A principal component analysis (PCA) of the elements of interest may help select the most appropriate samples (negative and positive PC scores + one in the center of the biplot; e.g., Liu et al., 2019). Paleolimnologists particularly interested in the lithogenic fraction of the sediment may also analyze the mineralogical composition of the sediment (by e.g., X-ray diffraction) to rigorously associate elements with the main rock-forming minerals (see Section 3.2.2). Such a comprehensive approach is particularly recommended when starting to investigate a new lake or lakes in a new region.

An alternative, less time-consuming, approach is to analyze the correlation or co-variability of elements measured on a lake sediment core, using either a correlation matrix or a principal component analysis (PCA; Section 3.2). This may provide enough information for simple lake systems but may not be sufficient for lakes in which sediment composition is driven by a complex mixture of processes. When the objective is to reconstruct a specific process, it is also advised to compare downcore elemental variations obtained on well-dated short sediment cores with the climate or environmental variable of interest (calibration-in-time approach; e.g., Grosjean et al., 2009). Although it is tempting to formulate an interpretation based on XRF-CS data only, this frequently leads to misinterpretations, which we hope this section will help avoid.

3.1. Association of elements with the four main components of the sediment

Most lake sediments are composed of a mixture of lithogenic particles, organic matter, biogenic silica (opal), and carbonates (and/or other authigenic minerals) in variable proportions. As inorganic elements can be associated with one or several of these components (Fig. 4), their abundance is particularly important to quantify. This is especially important for the interpretation of Si and Ca, which can each belong to two of the four sediment components (Fig. 4). This poses a challenging equiafinity problem since their downcore variations can result from distinct processes, depending on which sediment component these elements are associated with. Interpreting XRF-CS data constitutes an even greater challenge since pore water may constitute up to 90% of the analyzed volume, in addition to the four components mentioned above. Although the influence of water content (i.e., dilution) is significantly reduced when working with log-ratios (see Section 2.2.2), pore water may still be responsible for downcore variations in elements occurring in dissolved form in the interstitial water itself (mostly halogens: Cl, Br).

Several techniques are available to quantify each of the four components of the sediment. They are summarized below. These techniques generally focus on extracting and measuring either the component itself or a conservative element representing the component (e.g., organic carbon for organic matter). In addition to the quantitative techniques presented below, qualitative estimates of the abundance of these components can also be obtained from the analysis of smear slides (e.g., Myrbo et al., 2011).

3.1.1. Organic matter

The most frequently used technique to estimate the organic matter content of lake sediments is Loss-On-Ignition at 550 °C (LOI_{550}), which implies measuring sediment weight loss after igniting 1 g of dry (105 °C) sediment during 4 h at 550 °C (Heiri et al., 2001). This technique provides good estimates of organic matter content but it is only semi-quantitative due to weight loss by dehydration of some clay minerals in the same temperature range. LOI_{550} values therefore tend to overestimate organic matter content.

The most accurate technique to quantify organic matter content in

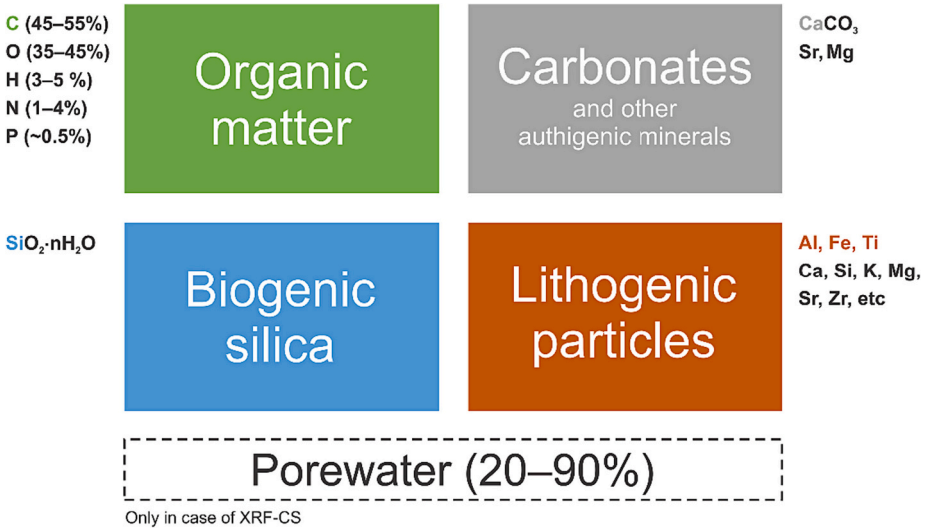

Fig. 4. The four main components of lake sediments, with indication of the main geochemical elements contained in each group. The elements in color are those that are generally used to quantify each component (see text). In case of XRF core scanning, a large fraction of the analyzed volume is composed of porewater, which may hold halogen elements (Br, Cl).

sediments is the analysis of Total Organic Carbon (TOC) with an elemental analyzer, after the removal of carbonates (Verardo et al., 1990; Brodie et al., 2011). This technique also uses less sediment (~50 mg) than LOI (1 g). Since organic carbon only constitutes about 50% of total organic matter (the rest of the weight is due to O, H, N, P), TOC values should be multiplied by two to obtain organic matter content. This multiplication factor however varies with the nature and selective degradation of the preserved organic matter (Pribyl, 2010; Arndt et al., 2013), which constitutes a limitation to quantify organic matter content in sediments.

An alternative technique is Rock-Eval pyrolysis, which consists in measuring the hydrocarbons, CO, and CO_2 that are formed during the progressive burning of sediment samples (Lafargue et al., 1998). The technique was originally designed as a tool to characterize the type and maturity of organic matter for the oil industry (Espitalie et al., 1985). It is rarely used in paleolimnology to estimate organic matter content only since it is relatively time-consuming and that TOC is an indirect measurement that can be biased by the presence of carbonates (Baudin et al., 2015; Ordoñez et al., 2019).

In terms of bulk inorganic geochemistry, the main influence of organic matter is dilution of the other three components of the sediment. Organic matter may however also control variations in halogen elements such as Br and Cl, and in some trace metals (e.g., Cd, Zn), which tend to be organic-bound (e.g., El Bilali et al., 2002; Gilfedder et al., 2011; Jokinen et al., 2020). Finally, it is worth noting that downcore variations in organic matter content can sometimes be estimated using the inc/coh scattering ratio measured by XRF-CS instruments (e.g., Woodward and Gadd, 2019). This ratio, however, also varies with water content, bulk sediment composition, etc. since it essentially reflects the mean atomic number of the analyzed material. This proxy is therefore not universally applicable and requires careful ground truthing (Chawchai et al., 2016).

3.1.2. *Biogenic silica*

Biogenic silica (often abbreviated BSi or bioSi) is contained in the shells/frustules of organisms such as diatoms and radiolarians as well as in phytoliths. The most accurate technique to quantify bioSi in lake sediments is alkaline extraction, which consists of placing 50 mg of sediment in a centrifuge tube with a strong base (NaOH or Na_2CO_3) at 85 °C for 5 h. The extracted Si can then be quantified using blue spectrophotometry (Mortlock and Froelich, 1989) or ICP-OES (Ohlendorf and Sturm, 2007). Since the extraction procedure also results in the dissolution of non-biogenic silica phases, such as clay minerals and volcanic glass, not all extracted Si can be considered biogenic. A lithogenic Si correction, generally obtained by measuring Al on the extracts and assuming a fixed Si:Al ratio, is highly recommended (e.g., Bertrand et al., 2012).

Frustules are composed of opal, i.e., hydrated amorphous silica ($SiO_2.nH_2O$). Obtaining opal abundances for proper sediment budget calculations by weight therefore requires multiplying the (Al-corrected) bioSi concentrations by 2.4 (Mortlock and Froelich, 1989).

In terms of bulk inorganic geochemistry, variations in opal content are reflected as changes in total Si. However, a significant fraction of Si in lake sediments is of lithogenic origin (siliciclastic particles). This has resulted in the development of indices to estimate changes in opal abundance in lake sediments based on bulk inorganic geochemical data. The "excess Si" method is the most common. It consists in subtracting the amount of silica linked to the lithogenic fraction of the sediment from total silica concentrations ($bioSiO_2 = SiO_2$ tot - x * Al_2O_3, where x is the SiO_2/Al_2O_3 ratio of terrigenous particles; Leinen, 1977; Bertrand et al., 2005). A derivative of this method for uncalibrated XRF-CS data is the use of Si:Al or Si:Ti ratios. Values above a certain threshold are considered as representing silica of biogenic origin (e.g., Brown, 2015, see Section 4.1.2 for an example).

3.1.3. *Carbonates (and other authigenic minerals)*

The amount of carbonates in lake sediments varies widely. Carbonate minerals can be (a) biogenic, i.e., the shells of aquatic organisms, (b) authigenic, i.e., produced by precipitation within the water column, or (c) detrital (lithogenic), i.e., originating from the erosion of soils or bedrock. Their abundance can be estimated by loss-on-ignition between 950 °C and 550 °C (LOI_{950}; Heiri et al., 2001). This technique is however mostly qualitative since measurements are affected by refractory organic matter that requires temperatures above 550 °C to be oxidized. As a result, sediment samples containing no carbonate frequently display LOI_{950} values of ~2%.

A more accurate way to measure the carbonate content of sediments is by coulometry, which quantifies the amount of CO_2 evolved from the dissolution of carbonates in acid (e.g., Mörth and Backman, 2011). In addition to being highly accurate, this technique only requires 50 mg of sediment, and it has excellent limits of detection (~0.03% $CaCO_3$; Rebolledo et al., 2019).

Another technique that is commonly used, particularly for sediments rich in $CaCO_3$ (>10%), is pressure calcimetry. This technique measures the pressure of the CO_2 released from the dissolution of carbonates in

acid. Compared to coulometry, it is easier to set up but it requires larger samples (0.1–3 g, depending on $CaCO_3$ concentrations) and it has higher limits of detection (Cantera and Ozán, 2022). It is therefore generally only used for carbonate-rich sediments.

An additional approach that is often used to quantify carbonate content in sediments consists in measuring total carbon (TC) and total organic carbon (TOC) and calculating the total inorganic carbon (TIC) by difference. The latter is assumed to originate only from carbonates. In practice, this requires two measurements per sample on an elemental analyzer, i.e., before (TC) and after (TOC) sample acidification. This technique is therefore rather inaccurate, relatively time consuming, and only applicable to samples that contain relatively high amounts of carbonates (>2–3%). Note, however, that manufacturers of elemental analyzers recently developed preparation modules that allow for the direct analysis of TIC, with a performance that should be similar to the coulometry-based technique (e.g., Bonk et al., 2023).

Finally, rock-eval pyrolysis has also been used to quantify the carbonate content of sediments, based on the decomposition of calcite and aragonite at temperatures above 750 °C (Pillot et al., 2014). The accuracy of the method is however known to be affected by the presence of clay minerals (Wattripont et al., 2019).

The choice of technique ultimately depends on the required accuracy, $CaCO_3$ abundance, and the amount of sample available for analysis. The advantages and limits of each of these techniques are further discussed in Kennedy and Woods (2013).

Since carbon only constitutes 12% of the mass of calcium carbonate ($CaCO_3$), C concentrations measured by coulometry or elemental analysis should be multiplied by 100/12 to obtain carbonate content. This relies on the assumption that all of the measured C is evolved from carbonates, which is generally the case.

Note that none of the techniques presented above differentiates between biogenic, authigenic and lithogenic carbonates. Analyzing smear slides or thin sections can rapidly provide information about the nature of the carbonate particles. A detailed understanding of the limnological processes at play and of the regional geology is also required to accurately interpret variations in carbonate content. In terms of bulk inorganic geochemistry, variations in carbonate content are reflected in total Ca variations. In most lakes, however, a significant amount of calcium is of siliciclastic (lithogenic) origin (Fig. 4), mainly in the form of plagioclase (anorthite), amphibole, and pyroxene.

In addition to carbonates, lake sediments may also contain other authigenic minerals such as sulfates, clay minerals, or iron sulfides (pyrite, greigite). These minerals may form in the water column or in the sediment. Their abundance tends to be low in freshwater lakes but they can become significant in saline lakes (Wilkin et al., 1996; Last, 2002; Deocampo and Jones, 2014).

3.1.4. Lithogenic particles

The proportion of lithogenic (technically siliciclastic) particles in lake sediments is generally quantified by difference (100% – organic matter – opal – carbonates). In this case, it is important to convert TOC values into organic matter content (2 x TOC), biogenic silica into opal (2.4 x bioSi) and inorganic carbon into carbonate content (8.33 x TIC) since this calculation uses the mass of each component. The lithogenic particles are generally those that hold most of the inorganic elements (e.g., Al, Fe, Ti, Na, K, …), in addition to significant amounts of Si and Ca (Fig. 4).

The concentration of inorganic geochemical elements in the lithogenic fraction of the sediment is mostly controlled by mineralogy, which can be investigated using X-ray diffraction. As a result, concentrations in purely lithogenic elements in bulk sediment samples reflect the abundance of the lithogenic fraction but they are also strongly affected by changes in sediment grain size and/or provenance (see Section 3.3). The elements that are the least affected by these processes, i.e., those that best represent the lithogenic particles, are known as conservative elements. In lake sediments, Al, Ti, Rb, and Sc are generally considered conservative, and can therefore be used to estimate downcore changes in the proportion of lithogenic particles (e.g., Boës et al., 2011). Accurately quantifying changes in the abundance of lithogenic particles is particularly important to calculate fluxes of detrital sediments, which is frequently used to reconstruct watershed hydrology and erosion (e.g., Arnaud et al., 2016).

3.2. Statistics and data exploration

The association of inorganic geochemical elements with any of the four components of the sediment (Fig. 4), or with mineral assemblages, can be explored using simple multivariate statistics. These tools also facilitate the selection of element(s) that best represents the process of interest, for example sediment transport, provenance, productivity, redox conditions, etc.

3.2.1. Exploring compositional data

A relatively easy way to explore element associations is through the use of principal component analysis (PCA). PCA is a statistical data reduction technique that groups correlated elements, which can in turn provide an idea of the processes driving their variation. Although similar results can be achieved by using a correlation matrix, a PCA biplot is particularly useful to visually explore element associations (Fig. 5). In addition, a PCA allows reducing the dataset to a lower number of important variables.

As indicated in Section 2, elemental abundances are generally reported as proportions of the total sample mass (in %, ‰, or ppm). In other words, elemental abundances are compositional in nature and the total of all elements is a constant (e.g., 1, 100, 10^6). Therefore, the concentration of any element is always relative to the concentration of the other elements. As a result, a change in the concentration of one element automatically results in a change in the concentration of all the others, whether the process(es) driving the supply of that element has (have) changed or not. This is known as a closed-sum constraint (Aitchison, 1986).

Because of the closed-sum constraint, geochemical variables are not independent and violate some of the basic assumptions upon which standard statistical analyses are based. Statistical analyses assume, for example, that all variables are independent, unconstrained (vary between $+\infty$ and $-\infty$), normally distributed (mean = 0, std. dev = 1) and symmetrical (A/B = -B/A) (Schuenemeyer and Drew, 2011). Chemical concentrations, as any other compositional data, are not independent, unconstrained, normally distributed, or symmetrical. A log-ratio transformation should therefore systematically be applied to all compositional data to fulfill the preconditions for statistical analysis. As shown by Aitchison (1982, 1986), applying a log-ratio transformation to elemental concentrations largely discards the constant-sum constraints. In other words, calculating log ratios of concentrations opens the dataset and makes concentrations independent from each other, and therefore fully compatible with statistical requirements.

Transforming compositional data into centered log-ratio (clr) prior to statistical operation (e.g. PCA, z-score, standard deviation) is crucial to obtain rigorous statistical results. As mentioned previously, clr transformation can be done either manually (see 2.2.2), or using simple software packages for compositional data analysis. Note that log-ratios can always be transformed back to concentrations after processing.

(a) Exploring concentrations

The effect of the clr transformation on the interpretation of geochemical data can be illustrated by comparing the results of PCA analyses obtained on raw versus clr-transformed concentrations. The example shown in Fig. 6 uses quantitative ED-XRF data obtained on 98 discrete samples from Lake Le Bourget, France, in which sedimentation is dominated by authigenic carbonates (Arnaud, 2005). The PCA obtained on the raw concentrations of all 10 major elements shows that

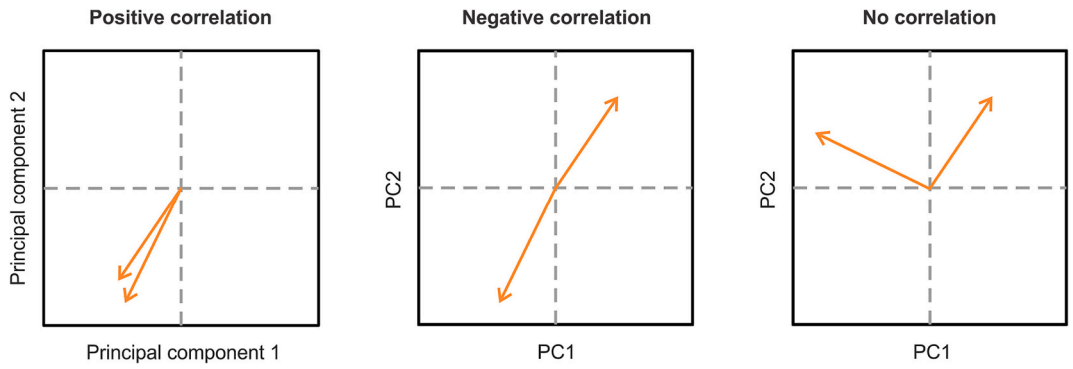

Fig. 5. Interpretation of the relations between variables based on a PCA biplot.

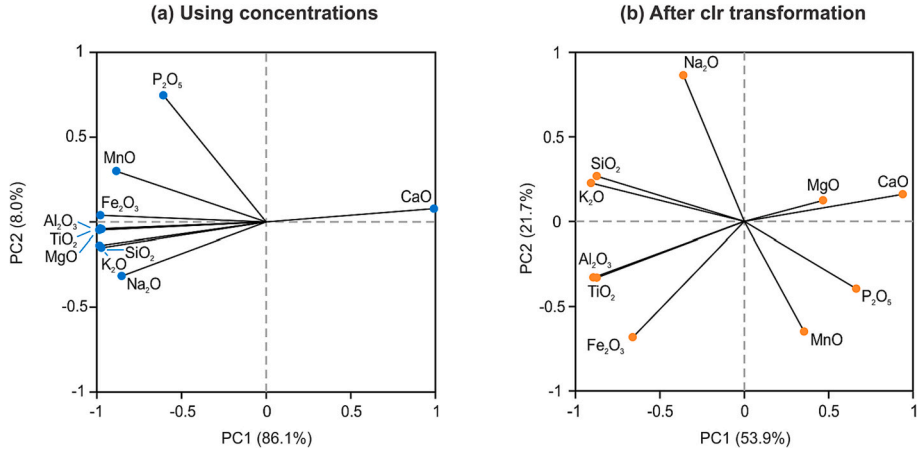

Fig. 6. Comparison of PCA results obtained on (a) raw concentrations and (b) clr-transformed data from the sediments of Lake Le Bourget (data from Arnaud et al., 2005).

variations in the concentration of all elements are essentially driven by changes in the element with the highest concentration, in this case Ca, which is the only element with a positive loading on principal component 1 (PC1; Fig. 6a). All the other elements show strong negative PC1 loadings, which reflects their dilution by authigenic carbonates. Therefore, the PCA analysis obtained on raw concentrations (Fig. 6a) is dominated by closed-sum constraints, i.e., the variability of the entire dataset is driven by CaO variations.

Investigating the element correlations after clr-transformation (Fig. 6b) reveals more information on the correlation between the elements. For example, it shows that MgO and, to a lesser extent P_2O_5, are positively correlated with CaO, which reflects the presence of MgO in carbonates. In addition, all lithogenic elements (SiO_2, K_2O, Al_2O_3, TiO_2, Fe_2O_3) show negative PC1 loadings, indicating that they are positively correlated with each other and are probably associated with the detrital sediment fraction. The negative correlation between lithogenic elements

Table 3
Correlation matrix using (a) raw concentrations (in blue) and (b) clr-transformed data (in orange) for the sediments of Lake Le Bourget (data from Arnaud et al., 2005). The data are the same as those presented in Fig. 5. Values in bold are significant at $p < 0.001$.

	SiO_2	Al_2O_3	Fe_2O_3	MnO	MgO	CaO	Na_2O	K_2O	TiO_2	P_2O_5
SiO_2	**1**	**0.945**	**0.920**	**0.806**	**0.915**	**-0.990**	**0.935**	**0.974**	**0.933**	**0.510**
Al_2O_3	**0.644**	**1**	**0.988**	**0.852**	**0.980**	**-0.974**	**0.794**	**0.973**	**0.995**	**0.537**
Fe_2O_3	**0.346**	**0.817**	**1**	**0.892**	**0.975**	**-0.958**	**0.753**	**0.951**	**0.984**	**0.583**
MnO	**-0.361**	-0.232	0.129	**1**	**0.840**	**-0.845**	**0.631**	**0.813**	**0.841**	**0.688**
MgO	**-0.583**	-0.308	-0.275	-0.227	**1**	**-0.949**	**0.771**	**0.961**	**0.986**	**0.526**
CaO	**-0.819**	**-0.827**	**-0.706**	0.128	**0.554**	**1**	**-0.891**	**-0.984**	**-0.964**	**-0.558**
Na_2O	**0.594**	-0.040	**-0.355**	**-0.529**	-0.252	-0.278	**1**	**0.888**	**0.782**	**0.374**
K_2O	**0.812**	**0.691**	**0.427**	**-0.408**	**-0.417**	**-0.867**	**0.534**	**1**	**0.969**	**0.505**
TiO_2	**0.599**	**0.964**	**0.815**	-0.268	-0.223	**-0.828**	-0.047	**0.682**	**1**	**0.540**
P_2O_5	**-0.586**	**-0.548**	-0.223	**0.463**	-0.035	**0.432**	**-0.489**	**-0.650**	**-0.504**	**1**

(a) Raw concentrations

(b) clr-transformed data

and CaO reveals a clear separation of detrital sediments and authigenic carbonates, which confirms that these sediment fractions are deposited independently.

Similarly, a correlation matrix based on raw concentrations of the same dataset reveals that all elements are significantly anti-correlated to Ca and significantly positively correlated to each other (Table 3a). These strong positive correlations are however artificial (intrinsic correlations) since they mostly reflect their common dilution by Ca. This also means that plotting the concentration of any element versus depth will virtually show a mirror of Ca concentrations, which is of very limited use in paleolimnology. A correlation matrix based on clr-transformed data, on the other hand, allows comparing the associations of elements independent of closed-sum effects (Table 2b).

PCA biplots and correlation matrices of clr-transformed data are particularly useful to select the element(s) to plot downcore. For Instance, the (log)ratio of two negatively correlated elements reveals the maximum variation in the data. The (log)ratio of two positively correlated elements, on the other hand, provides information on variations within a specific sediment fraction (e.g., the lithogenic fraction). For example, the (log)ratio of K_2O and TiO_2 in the example above could be used to represent variations in mineralogy. Finally, the ratio between two uncorrelated elements does not contain much information since the elements vary independent of each other. The interpretation of such a ratio would therefore be complex since it is affected by several processes. However, it is important to remember that correlations between elements may vary among lithofacies.

(b) Exploring XRF core scanner intensities

Using clr-transformed data is an even more important requirement when working with XRF core scanner measurements since the measurements are highly dependent on matrix effects (water content, physical properties, etc). In the following example, XRF core scanner data from Les Echets, a paleolake located in SE France, is used (Kylander et al., 2011). The sediment is heterogeneous, with documented differences in grain size, and organic, biogenic silica and carbonate contents (Wohlfarth et al., 2008), which all have the potential to influence XRF-CS measurements. To illustrate the influence of clr-transformation on the data, a PCA was applied to the XRF counts before and after clr-transformation (Fig. 7).

While at a first glance these two analyses look similar, there are key differences. For example, the elements K, Ti, and Rb, which are all associated with the detrital fraction, have very positive loadings on PC1 in both cases, but Si is more positively associated with PC2 when using the raw data set, and with PC1 using the clr-transformed data (Fig. 7). Thus, using the raw data, the predominant association of Si with the detrital faction of the sediment is missed. Given the relatively low biogenic silica concentrations in the sediments of Les Echets (< 4%), the largest part of the Si is expected to be hosted by siliciclastic minerals, which is correctly reflected as covariations with K, Ti, and Rb on the clr-transformed biplot (Fig. 7b). Likewise, the sign of the PC1 score for Sr and Mn varies depending on data handling, and the transformation impacts the associations of Ca, Fe, Zr, and S which can all lead to the misidentification of processes within the lake. In this example, the clr-transformation mostly made a difference for elements showing variations on the order of several magnitudes, namely S, Ca, and Mn (Fig. 7).

(c) Downcore plots

Downcore plots of concentrations or clr-transformed intensities are not independent of dilution either and should therefore be interpreted as such. A robust approach to circumvent the closed-sum effects is plotting downcore variations in element intensities as log-ratios between two elements. Note that even when concentrations are available, log-ratios

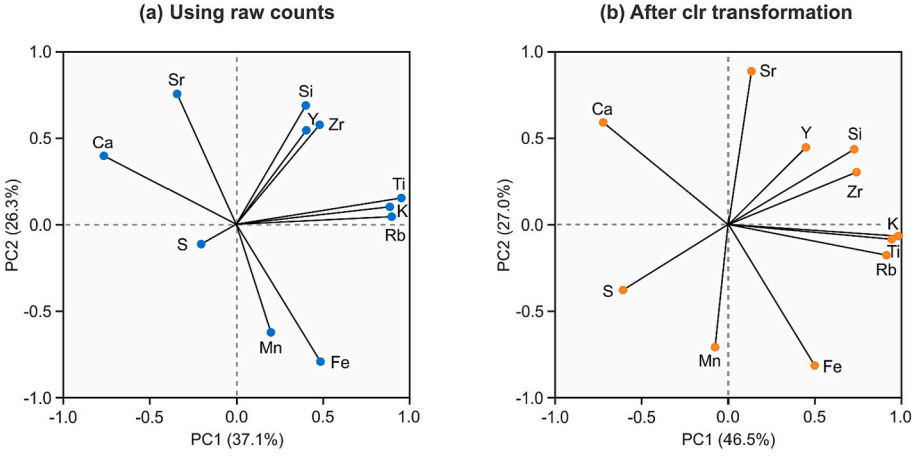

PC	1	2	3	4
% variance	37.1	26.3	11.4	10.9
K	**0.89**	0.10	0.31	0.01
Ti	**0.95**	0.15	0.11	-0.04
Rb	**0.90**	0.04	-0.07	0.24
Si	0.40	**0.69**	0.06	-0.33
Sr	-0.34	**0.75**	0.42	0.30
Mn	0.20	**-0.62**	0.45	0.45
Ca	**-0.76**	0.40	0.34	0.30
Fe	0.49	**-0.79**	0.10	0.12
Zr	0.48	**0.58**	-0.41	0.01
S	-0.20	-0.12	**-0.68**	**0.55**
Y	0.41	**-0.54**	-0.03	**0.58**

PC	1	2	3	4
% variance	46.5	27.0	11.5	7.9
K	**0.94**	-0.09	0.15	-0.15
Ti	**0.98**	-0.07	0.02	-0.07
Rb	**0.91**	-0.18	-0.13	0.15
Si	**0.73**	0.44	-0.06	-0.43
Sr	0.13	**0.89**	0.36	-0.05
Mn	-0.07	**-0.71**	**0.63**	0.15
Ca	**-0.72**	**0.59**	0.25	-0.16
Fe	**0.50**	**-0.82**	0.15	-0.11
Zr	**0.74**	0.30	-0.38	-0.03
S	**-0.61**	0.38	**-0.68**	-0.05
Y	0.45	0.45	-0.07	**0.75**

Fig. 7. Comparison of PCA results using raw and clr-transformed counts, including the relative variance explained by each PC (%) and the loading of each element (values in bold are greater than 0.50 or lesser than -0.50).

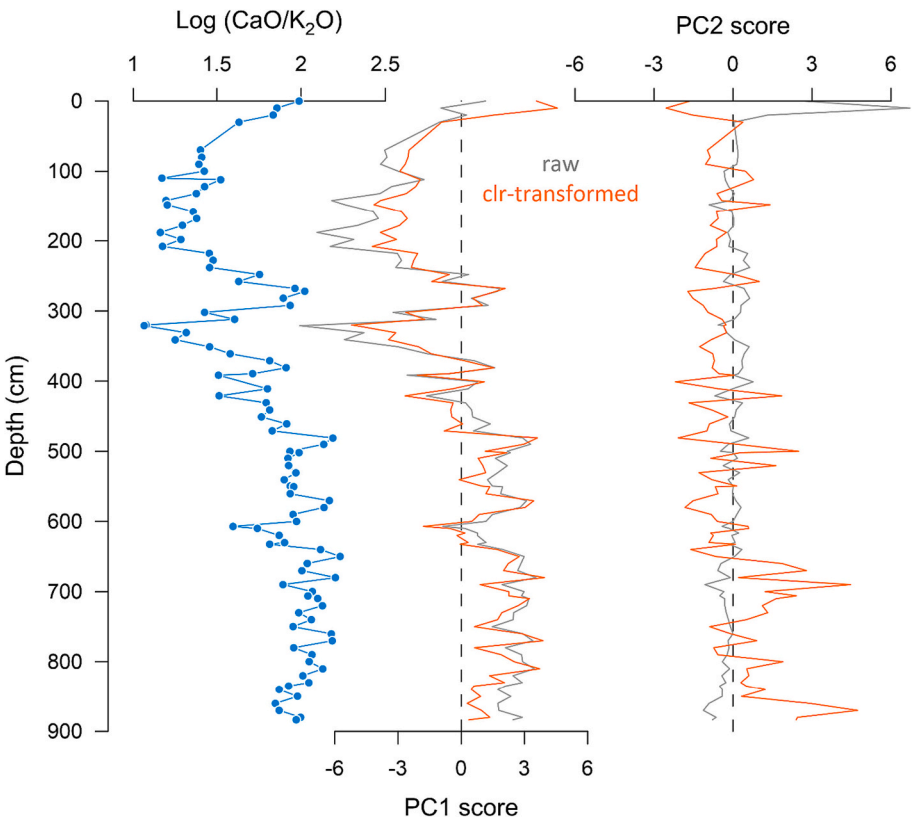

Fig. 8. Log (CaO/K_2O) of a sediment core from Lake Le Bourget compared with principal component 1 and 2 scores computed with raw and clr-transformed data (data from Arnaud et al., 2012). This figure illustrates that plotting PC1 scores downcore provides similar information as plotting the log-ratio between two elements with opposite PC1 loadings (CaO and K_2O; see Fig. 6). In addition, it illustrates the difference between PC scores based on raw and clr-transformed data, highlighting the ability of the clr-transformation to extract more information from geochemical datasets (see PC2 scores).

are preferred over ratios since they are symmetrical, i.e., conclusions made on A/B are equal to those obtained from B/A. Alternatively, one can also plot downcore variations in PC scores, which summarizes the information contained in the elements loading significantly on the selected principal component. In the case of Lake Bourget, for example, downcore variations in either the PC1 score, or log (CaO/K_2O) reflect the relative importance of carbonate productivity versus detrital input (Fig. 8) since CaO and K_2O have high positive and negative loadings on PC1, respectively (Fig. 6).

The influence of the clr-transformation can also be seen when PC1 and PC2 scores are plotted against depth (Fig. 8). In this example, the PC1 scores are relatively similar, but the PC2 scores vary significantly. Those calculated on raw data show almost no variations with depth, whereas those calculated on clr-transformed data show significant changes downcore. This difference reflects the higher variance along PC2 after clr transformation (Fig. 6). The PC2 scores computed from clr-transformed data show changes that are particularly marked at the base of the core, reflecting variations in sediment grain size (Arnaud et al., 2012). These changes would not have been visible without clr transformation (Fig. 8). This example therefore highlights the capability of clr transformation to extract additional information from geochemical datasets.

The third approach to circumvent the closed-sum effects is to calculate mass accumulations, which requires having access to concentrations and a high-resolution core chronology (see Section 3.2.3).

The text above was mostly aimed at raising awareness on the influence of data pre-processing on the results of multivariate statistical analysis. One drawback of using (centered) log-ratios is that the information contained in the absolute values (concentrations) is discarded. In the clr space, variations between 10 and 100%, for example, are equal to variations between 0.01 and 0.1%. Absolute concentrations, however, also contain useful information (e.g., Baxter and Freestone, 2006). For instance, they permit identifying the dominant process(es) at play in a lake, such as carbonate sedimentation in Lake Le Bourget above. As a result, absolute concentrations should not be entirely discarded but they should be investigated in parallel with log ratios.

3.2.2. *Association of elements with sediment components and minerals*

The previous section investigated correlations between geochemical elements only. In some cases, this may be sufficient to understand the sediment components with which they are associated, and to interpret the processes controlling their variations. However, linking geochemistry with components of the sediment (see Section 3.1) or mineralogy (e.g. after X-ray diffraction analysis) can be done more rigorously by including such data in the PCA. This additional information should be projected as supplementary quantitative variables in the PCA biplot, meaning that they have no influence on the principal components but are there to help interpret the dimensions of variability. Just like for the geochemical data, the concentrations in the four components of the sediment or mineralogy should be transformed before being projected in the PCA. However, centered log ratios become inappropriate for datasets with few (< 5) variables, such as sediment components. In this case, the log ratios of the variable can be calculated using the logarithm of the variable divided by "total – the variable" (e.g., log (TOC[%]/(100-TOC [%])). Note that it is not necessary to express TOC in organic matter content, bioSi in opal content, and TIC in carbonate content (Section 3.1) in this case, as this does not affect the log ratios.

This approach is illustrated below using ICP-OES data obtained on fjord sediment core PC29A (Bertrand et al., 2014). The sediment of core PC29A is dominated by lithogenic particles (83–86 wt%), with significantly lower amounts of biogenic silica (4.9–6.2 wt%) and organic carbon (0.9–1.5 wt%). Carbonate concentrations are very low (<0.1 wt

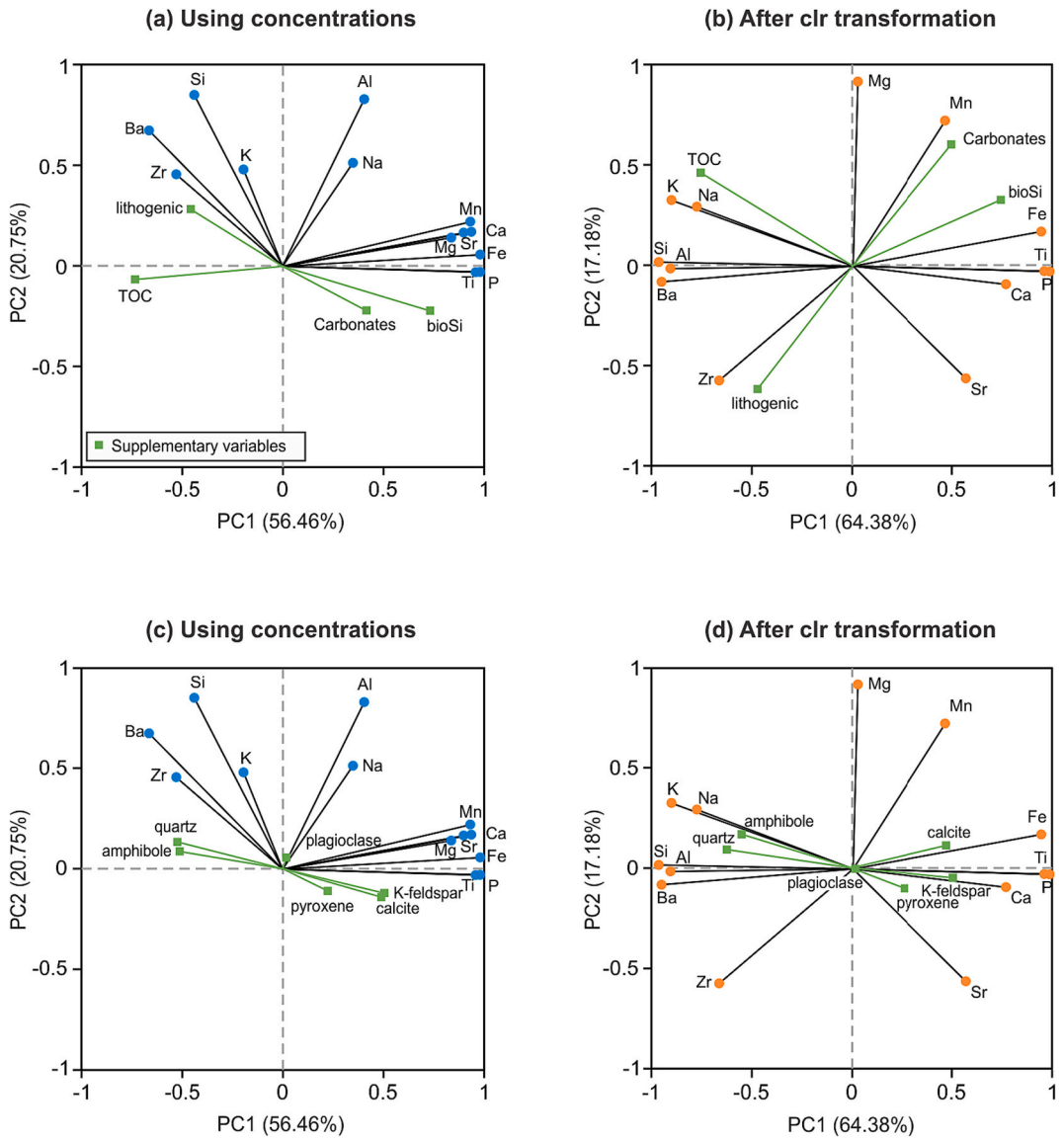

Fig. 9. PCA of the geochemical composition of fjord sediment core PC29A, with sediment composition (a–b) and mineralogy (c–d) plotted as supplementary variables. Data from Bertrand et al. (2014).

%) but significant. As for Figs. 6 and 7, PCAs were constructed on the raw and clr-transformed geochemical data (here the 10 major elements + Zr, Ba and Sr). The four components of the sediment (Fig. 9 a,b) and its bulk mineralogical composition (Fig. 9 c,d) were then projected as supplementary variables.

The PCA results obtained on untransformed concentrations show that more than half of the chemical elements (Ca, Mg, Fe, Mn, P, Sr, Ti) have a strongly positive PC1 loading (Fig. 9a). After projecting the four components of the sediment on the same PCA, it becomes clear that these variations mostly reflect dilution by organic matter (Fig. 9a). The results also clearly illustrate that total Si concentrations do not reflect changes in biogenic silica but are mostly associated with the lithogenic fraction of the sediment, and that Zr is the best element to represent the lithogenic fraction of the sediment (Fig. 9a). In addition, they suggest that Al is not correlated to the lithogenic content of the sediment.

The PCA based on clr-transformed data (Fig. 9b) provides additional insight into the relation between elements and their associations with the four components of the sediment. It confirms most of the observations made on the non-transformed data but it also shows that Al is positively correlated to the lithogenic content, and anti-correlated with Fe and Ti. This supports the use of Al as a normalizing element in this specific sediment core (Bertrand et al., 2014). The anti-correlation between Fe and Ti and the lithogenic fraction reflects the influence of grain size, i.e., the concentrations of Fe and Ti within the lithogenic fraction vary with particle size, which is independent of the amount of lithogenic particles (Bertrand et al., 2012; see Section 3.3.1).

Likewise, projecting the mineralogical composition on the geochemistry-based PCA (Fig. 9c,d) confirms that Si is mostly associated with quartz and that plagioclase does not play a significant role in controlling the concentrations of any of the measured elements (Fig. 9d). Note that the interpretation of geochemical and mineralogical data from PCA biplots should not only be based on the correlations between variables but should also consider mineral chemistry (e.g., Table 4; Deer et al., 2013).

The statistical analyses mentioned above are relatively simple and can be rapidly achieved with most statistical software. For their ease of use, we recommend XLStat (an Excel add-on), Past, or the R "compositions" package (van den Boogaart and Tolosana-Delgado, 2008). The

Table 4
Chemical composition of the most common rock-forming minerals, organized by decreasing order of abundance in the Earth's crust.

Mineral name	Chemical formula
Plagioclase (albite – anorthite)	$NaAlSi_3O_8$ – $CaAl_2Si_2O_8$
Potassium feldspar (orthoclase)	$KAlSi_3O_8$
Quartz	SiO_2
Pyroxene (clino- – ortho-)	$Ca(Mg,Fe)Si_2O_6$ – $(Mg,Fe)_2Si_2O_6$
Amphibole (hornblende)	$(Ca,Na)_{2-3}(Mg,Fe,Al)_5(Al,Si)_8O_{22}OH_2$
Mica (biotite-muscovite)	$KAl_2AlSi_3O_{10}(OH)_2$ – $K(Mg,Fe)_3AlSi_3O_{10}(OH)_2$
Olivine	$(Mg,Fe)_2SiO_4$
Kaolinite	$Al_2Si_2O_5(OH)_4$
Calcite / Aragonite	$CaCO_3$
Dolomite	$CaMg(CO_3)_2$

latter also includes clr-transformation of the geochemical data, which can otherwise be done manually (see Section 2.2.2) or using CoDaPack. The main difference between these is that only a few of them have the option to plot supplementary variables, for which XLStat is particularly handy. Note that other variables such as grain-size mean or mode (expressed in phi), grain size fractions, magnetic parameters, etc. can also be projected as supplementary variables in PCA biplots. Here too, the compositional data (e.g., grain-size classes) should be clr-transformed before analysis. For non-compositional data (e.g., grain-size mean, magnetic parameters), it is important to ensure that the software used for PCA analysis normalizes the data (e.g., *Z*-score) before analysis since these supplementary variables are expressed on a different scale.

3.2.3. *Concentrations or accumulation rates?*

As mentioned at the start of Section 3.2, geochemical data are compositional, i.e., the concentration of any element is relative to the concentration of all the others. This means that a change in the concentration of one element automatically results in a change in the concentration of the others. For example, an increase in biogenic silica concentrations in a sediment core could result from an increase in biogenic productivity, or from a decrease in terrigenous sediment supply (decreased dilution).

In multivariate statistics, this closed-sum problem is generally solved using log ratios. Another way to circumvent the closed-sum effect in paleolimnology is to calculate elemental fluxes instead of using concentrations directly. The latter requires having access to a relatively precise chronology and dry bulk density data, from which mass accumulation rates can be computed. When these measurements are available, the mass accumulation rate of any element or component of the sediment can be calculated as follows:

$$MAR_{elt} = SR \times BDD \times [elt] \times 10^2$$

where MAR_{elt} is the mass accumulation rate of the element (in g m^{-2} yr^{-1}), SR is the linear sedimentation rate (in cm yr^{-1}), BDD is the dry bulk density in g cm^{-3}; and [elt] is the concentration of the element of interest (in wt%).

To illustrate how the use concentrations and fluxes can result in different interpretations, Fig. 10 compares downcore variations in bioSi concentrations and accumulation rates, for a 550-yr long sediment core from Lake Puyehue, Chile. BioSi concentrations were calculated every 1 cm by normative calculation based on XRF-WD measurements and corroborated with values obtained by alkaline extraction (Bertrand et al., 2005). Core chronology is based on a combination of radionuclide analysis (Arnaud et al., 2006) and varve-counting (Boës and Fagel, 2008).

The results show that between the bottom of the core (~1450 CE) and 1900 CE, bioSi concentrations roughly doubled, from ~15% to 30% (Fig. 10a). At first glance, this increase could be interpreted as a gradual increase in lake productivity. However, a more detailed analysis shows that total mass accumulation rates roughly decreased by a factor of two during the same period (Fig. 10b). Therefore, once bioSi is expressed as MAR (Fig. 10c), it shows very little change through time, reflecting a relatively stable lake productivity between 1450 and 1900 CE. Using concentrations directly can therefore be misleading. When the quality of the age model allows, interpretations should be based on accumulation rates of elements or of sediment components.

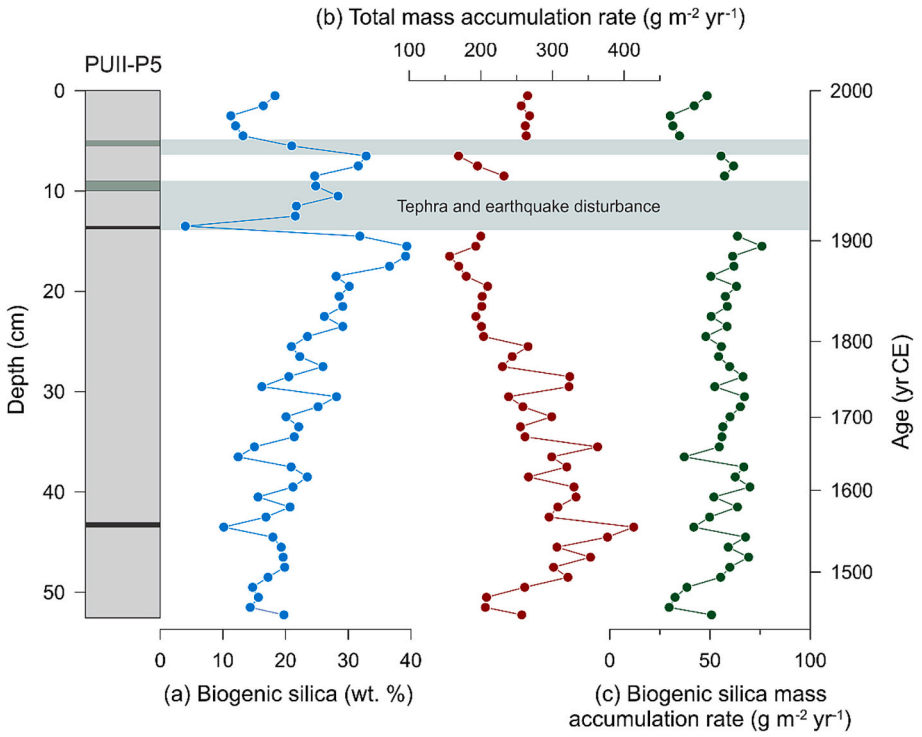

Fig. 10. Comparison between biogenic silica concentrations and mass accumulation rates in a sediment core from Lake Puyehue, Chile (Bertrand et al., 2005).

3.2.4. Additional techniques

In addition to the data exploration techniques mentioned above, more complex mathematical processing can be used to extract specific information from bulk geochemical data. This includes end-member modeling, which can be particularly useful to disentangle sedimentary processes from complex lake sediment records (Weltje, 1997). This technique was recently applied successfully to XRF-CS data (Morlock et al., 2021). Another approach involves cluster analysis, which is increasingly used to identify and classify specific groups of samples, including event deposits (e.g., Kaboth-Bahr et al., 2019; Liu, 2020).

3.3. Origin of changes in lithogenic elements

Lithogenic particles tend to dominate the composition of sediments deposited in freshwater lakes. Some inorganic geochemical elements, such as Al, Fe, Ti, Zr, Rb, and K occur entirely within the lithogenic fraction. In theory, downcore changes in the abundance of any of these elements can therefore reflect changes in the proportion of lithogenic particles. In practice, however, the concentration of lithogenic elements in the lithogenic fraction itself varies with grain size, provenance, and, to a lesser extent, diagenesis and weathering (e.g., K is more soluble than Zr). The extent to which these variables affect the concentration of each element is highly variable. Elements such as Al and Rb tend to be the most conservative, i.e. the most representative of the lithogenic fraction and the least affected by changes in grain size, provenance, and diagenesis. Others, such as Zr, tend to vary by up to an order of magnitude with grain size (see 3.3.1). As a result, downcore changes in the concentration of the most conservative elements (Al and Rb) generally provide a good estimate of the lithogenic content of the sediment. Variations in the abundance of most other elements tend to reflect changes in grain size and provenance, which are discussed in more details below.

3.3.1. Grain size

Many lithogenic elements tend to be enriched in a specific grain-size fraction of the sediment, due to their association with minerals of different sizes and refractoriness (e.g., Table 4). In river sediments, Si is generally associated with quartz and aluminosilicates and tends to increase with sediment grain size (Fig. 11). The latter represents the great hardness of quartz, and therefore its resistance to physical erosion. Likewise, Zr mostly occurs in the heavy mineral zircon, which is highly enriched in the coarse silt and fine sand fraction of sediments (Fig. 11). Potassium, on the other hand, is mostly associated with clay minerals and therefore tends to be enriched in the fine fraction of sediments. Elements such as Al and Rb occur in a large variety of minerals and therefore show relatively little variations with grain size.

The association of elements with specific grain-size fractions of the sediment has been frequently used in paleolimnology to estimate downcore variations in sediment grain size (e.g., Cuven et al., 2010). Zirconium and Ti are the most abundantly used (e.g., Davies et al., 2015). Silicon is rarely used since in most lake sediments, total Si concentrations are also influenced by biogenic sources (see 3.1.2). To discard the influence of dilution by other components of the sediment, the classical approach is to use the ratio (or better log-ratio) of an element varying with grain size (e.g., Zr, Ti) to a mostly conservative element (e.g., Al, Rb). In the literature, Ti/Al, Zr/Al and Zr/Rb are the most frequently used (e.g., Wu et al., 2020; Cuven et al., 2010; Davies et al., 2015). Aluminum is commonly used as conservative element when using ICP-OES and WD-XRF datasets, but since it is a light element that cannot be measured with high precision by XRF-CS (see 2.2), it is generally replaced by Rb when using XRF-CS data.

An alternative method that is sometimes used in the literature is dividing an element enriched in the coarse fraction of the sediment (e.g., Zr) by an element mostly represented in the fine fraction (e.g., K). These ratios can be particularly effective at detecting event deposits (e.g., Wilhelm et al., 2012a, 2013). Indiscriminately applying any of these

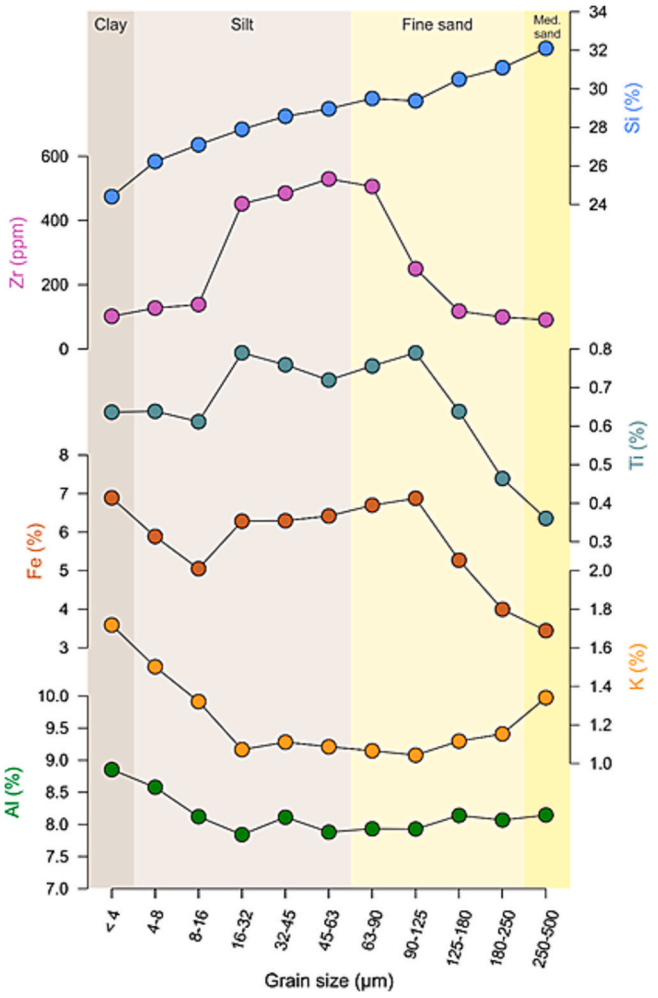

Fig. 11. Variations in element concentrations of river sediment samples according to grain size. Each dot corresponds to an average of 7 different rivers from Chilean Patagonia (data partly published in Liu et al., 2019).

elements or elemental ratios as grain-size proxies is, however, particularly risky since the association of elements with specific grain-size fractions of the sediment highly depends on mineralogy, and therefore on the geology of the lake watershed. There is therefore no element ratio that is universally applicable to represent grain size. Our recommendation is to conduct a series of grain-size measurements at low resolution along any new sediment core and investigate the relationship between the grain-size parameter of interest (generally mean grain size) and element concentration (clr in case of XRF-CS data) and/or ratios. The latter can easily be done using either a correlation matrix, or a PCA with grain size plotted as a supplementary variable (see 3.2).

Using a single element or elemental ratio as a grain-size proxy assumes that variations in the concentration of the element, or in elemental ratio, are linearly related to grain size over the entire range of grain sizes occurring in the sediment core. In practice, this is rarely the case since each element is sensitive in a specific grain-size fraction. Zr, for example, is particularly sensitive to grain size in the coarse silt fraction but totally insensitive to particle size in fine silts and clays (Fig. 11). In sands, it actually decreases with grain size (Fig. 11). In other words, no element is linearly related to grain size from clay to sand. The only possible exception is Si, but the presence of biogenic silica in the sediments of most lakes precludes using Si as a grain-size proxy.

To circumvent this issue, several lithogenic elements need to be used together. Such a technique was proposed by Liu et al. (2019), who developed a simple grain-size prediction model based on partial least

square regression. The method only requires a small set (~10) of calibration samples, and it can be applied to geochemical datasets generated with traditional techniques (ICP-OES, WD-XRF) and core scanners (see example in Section 4.2 below). The method weighs the different lithogenic elements automatically and it provides quantitative, i.e., not only relative as when using elemental ratios, grain-size results. When working on several sediment cores from the same lake, a prediction model developed for one core can be applied to any other core from the same basin, providing that the source(s) of sediment do not significantly vary across the lake.

3.3.2. *Provenance*

In addition to grain size, the geochemistry of the lithogenic fraction of lake sediments is also largely controlled by sediment provenance. Deciphering the influence of grain size and provenance on the abundance of different elements can be particularly challenging but a first analysis of the data using simple multivariate statistics generally allows identifying groups of elements that may reflect provenance (see Section 3.2). When the geochemical composition of the sediment sources is not fully characterized, i.e., if samples from the lake watershed are not available, qualitative changes in provenance visible as element associations on PCA biplots can generally be interpreted using geological maps of the lake watershed. Such an example is presented in Section 4.3.

On the other hand, when quantitative geochemical data are available on both lake sediments and on the sediment sources it becomes possible to estimate variations in the contribution of each source through time. The latter can be done by fingerprint the sediment sources, and then unmixing the lake sediment samples (e.g., Pulley et al., 2015; Lizaga et al., 2020).

Geochemically fingerprinting sediment sources is generally done by analyzing the geochemical composition of river sediment samples (bulk or suspended), or bedrock and soil samples. The advantage of using river sediment samples is that they integrate all possible sediment sources within their specific sub-watersheds. However, the composition of suspended river sediments can change throughout the year, requiring several sampling campaigns to capture the complete range of geochemical compositions (e.g., Stutenbecker et al., 2023). Bulk river sediment samples do not suffer from this problem but they require separating and analyzing a grain-size fraction that is representative of what is transported by rivers (generally <63 μm) to limit the influence of grain size on the geochemical characterization of the sediment sources (see Section 3.3.1). Elements used to fingerprint sediment sources should (a) be able to uniquely identify and differentiate between possible sources, and (b) be stable during transfer from source to sink (Collins et al., 2020). Evaluating the capability of elements to discriminate between sources is generally done using a series of statistical tests (Kruskal-Wallis H-test, tracer variability ratios, discriminant analysis), which are described in detail in Pulley et al. (2015), Collins et al. (2017), and Lizaga et al. (2020). In practice, conservative inorganic tracers such as Si, Al, Ti and Zr are the most commonly used.

The second step consists in estimating the contribution of each source using a multivariate unmixing model. This can be done manually using a discriminant analysis or through the use of software or packages built specifically for this purpose such as Fingerpro (Lizaga et al., 2020) or SIFT (Pulley and Collins, 2018). Since the concentration of the elements used to reconstruct provenance is also affected by grain size (see Section 3.3.1), some models include particle size corrections (Collins et al., 1998).

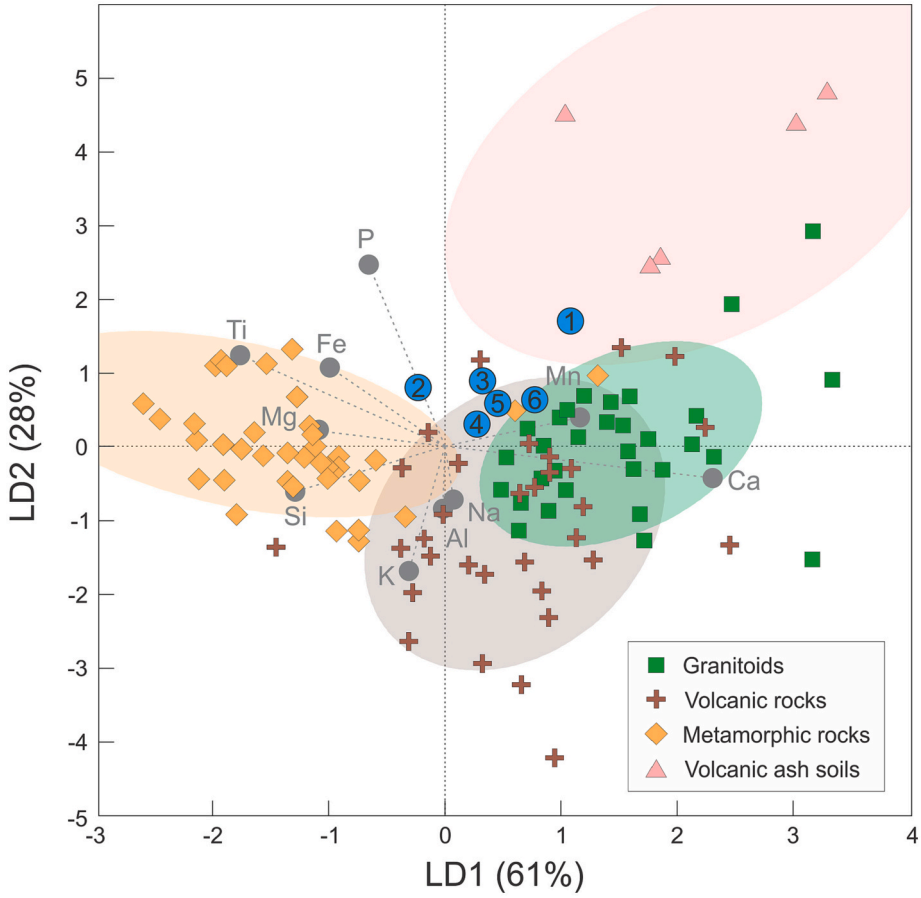

Fig. 12. Linear discriminant biplot of sediment sources (105 bedrock samples and 5 soil samples) from Chilean Patagonia (Liu et al., 2020). The ellipses represent the confidence intervals (1 sigma). The blue circles correspond to river sediment samples draining different watersheds. The plot shows that sample 1 has a distinct provenance and is particularly enriched in volcanic ash soil material. Figure modified from Liu et al. (2020).

An example of source discrimination for provenance analysis is presented in Fig. 12. In this example, 105 bedrock samples and 5 soil samples from a ~ 50,000 km^2 area in Chilean Patagonia were used to evaluate the possibility to discriminate between three different bedrock types and volcanic soils, based on major elements only (Al, Ca, Fe, K, Mg, Mn, Na, P, Si and Ti; Liu et al., 2020). After application of the Kruskal-Wallis test, Al was discarded as it was not able to discriminate between the four sediment sources and therefore added noise to the dataset. A linear discriminant analysis (LDA) was then applied to all the other elements (after clr-transformation). Similar to PCA, LDA is a multivariate dimension reduction technique, but it focuses on maximizing the separability of pre-defined groups (here lithologies; Schuenemeyer and Drew, 2011). The LDA results show that major elements were able to differentiate between the four source groups, with relatively little overlap between them (Fig. 12). Any sediment sample can then be projected on the LDA biplot, allowing to estimate the contribution of each of the four sediment sources.

Although major element geochemistry generally provides acceptable results in terms of fingerprinting and provenance quantification, more accurate results may be obtained in combination with isotope tracers such as Sr, Nd, Pb or Hf (e.g., Liu et al., 2022), or clay minerals. However, it is worth noting that grain size also influences provenance estimates based on radiogenic isotopes (Meyer et al., 2011). For best results, it is generally recommended to use a combination of tracers (Pulley et al., 2015; Collins et al., 2020).

3.3.3. *Weathering*

In sedimentary geochemistry, weathering is often considered as another important variable controlling the bulk inorganic geochemistry of sediments. For recent sediment records, however, the influence of weathering is generally very limited, and often masked by the much stronger influence of grain size, and possibly provenance (e.g., Nesbitt and Young, 1996; Guo et al., 2018; Hatano et al., 2019). As a result, downcore variations in grain size tend to overwhelm any weathering intensity information that may be contained in commonly used indices such as the Chemical Index of Alteration (CIA; Nesbitt and Young, 1982), Chemical Index of Weathering (CIW), or Weathering Index of Parker (WIP). The reason behind this strong grain-size influence is that the weathering indices rely on elements that are highly mobile during weathering, such as Al, Ca and K (Eq. (3)). These elements, however, also significantly co-vary with grain size (Fig. 11), independently of weathering intensity.

$$\mathrm{CIA} = \frac{\mathrm{Al_2O_3}}{\mathrm{Al_2O_3} + \mathrm{CaO^*} + \mathrm{Na_2O} + \mathrm{K_2O}}\ x\ 100 \quad (3)$$

The predominant influence of grain size on weathering indices is illustrated in Fig. 13, which uses river sediment samples separated into distinct grain-size fractions. Since all grain-size fractions represent sediments produced under the same climate conditions, any weathering index should in theory show constant values. In practice, however, all traditional weathering indices vary significantly with grain size (Fig. 13). Values obtained for medium silts (16–32 μm) tend to represent fresh material (CIA and CIW < 50), whereas values calculated for clays and sands correspond to more weathered material. Interpreting these weathering indices from recent lake sediment cores without considering the influence of grain size would therefore result in misinterpretations in terms of weathering intensity. On short (~millennial) timescales, the influence of grain size dominates over any weathering signal. Therefore, the use of indices such as CIA, CIW or CIP as weathering intensity indicators is not recommended for recent lake sediments.

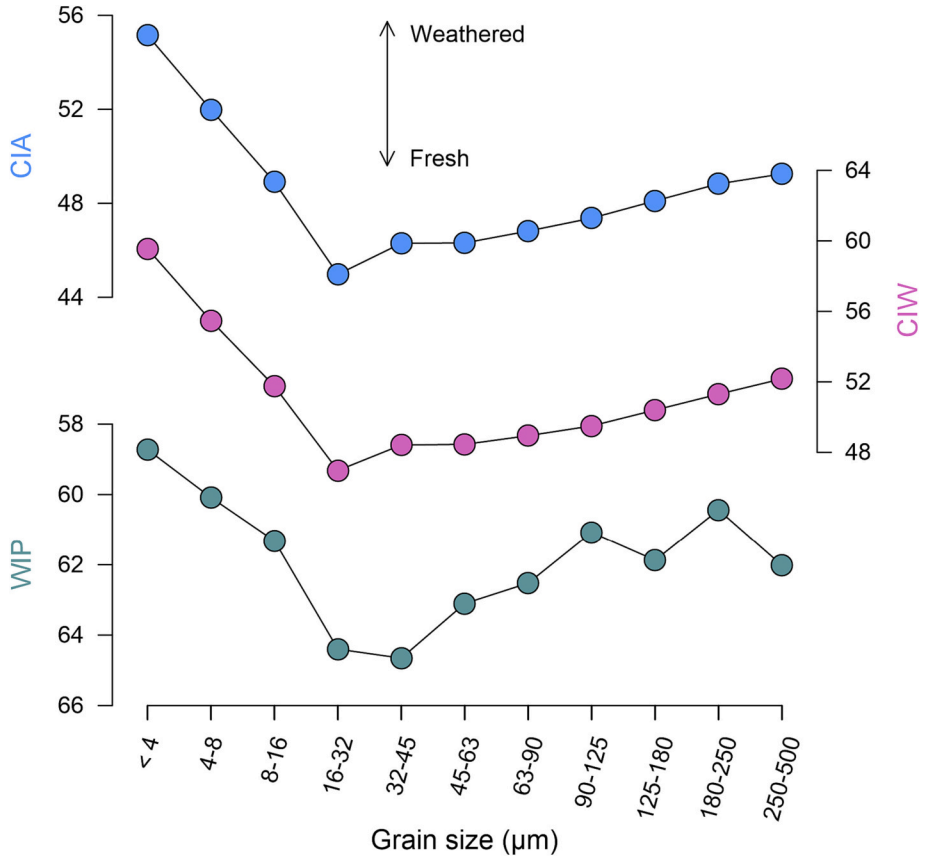

Fig. 13. Weathering indices calculated on eleven grain-size fractions of river sediment samples from Chilean Patagonia (the average of 7 river sediment samples is shown). The main source of sediments corresponds to granitoids. The samples are the same as those presented in Fig. 11. This figure illustrates the dominant influence of grain size on weathering indices.

4. Applications

Lake sediment inorganic geochemistry generally reflects a series of processes (e.g., changes in productivity, grain size, provenance) that may be difficult to disentangle. Generally, variations in some well-chosen elements or elemental ratios, possibly supported by multivariate statistical analyses, can be used to reconstruct a specific process, independently of the others. Although element selection can be challenging, a good understanding of the four sediment components mentioned above, the possible processes at play, and the regional geology is the best place to start. Below are examples of such applications where carefully selected elements were used to reconstruct a specific process. These examples serve as guidelines on how to interpret inorganic geochemical data from lake sediments.

4.1. Main components of the sediment

4.1.1. Carbonates

Carbonates are one of the four main components of lake sediments (Section 3.1). Lake carbonates can either be biogenic, authigenic (formed within the lake) or detrital (supplied through erosion of carbonate-rich rocks and/or soils in the watershed). The element that is generally analyzed to quantify carbonate content in sediments is Ca (Fig. 4). However, Ca can be associated with carbonate minerals (calcite and aragonite) and with a variety of non-carbonate rock-forming minerals such as plagioclase, especially in siliciclastic rocks (Table 4). In many lakes, Ca is therefore associated with both the carbonate and siliciclastic fractions of the sediment (Fig. 4), making this element relatively difficult to interpret. In lakes dominated by authigenic carbonate sedimentation, however, Ca concentrations can provide a direct estimate of the carbonate content of the sediment. This is the case of hardwater Lake Le Bourget, NW Alps.

Overall, the Holocene sediments of Lake Le Bourget are dominated by carbonates (50–90%), which largely control the total Ca abundance. This is supported by the very similar trends in carbonate content measured by Rock-Eval analysis and Ca abundance, whether it is quantified by ED-XRF on discrete samples or measured by XRF-CS (Fig. 14a). As discussed in Section 2.2.2, expressing the XRF-CS Ca counts in terms of clr is recommended to avoid the influence of matrix effects and changes in physical properties of the sediments on the geochemical results. For the sediments of Lake Le Bourget, the clr transformation is supported by the much stronger correlation between the XRF-CS data and the ED-XRF measurements (both clr-transformed; $r = 0.93$; $p < 0.0001$) than between the raw Ca counts and ED-XRF measurements ($r = 0.86$; $p < 0.0001$) (Fig. 14b). The effect of the clr transformation is particularly pronounced for the samples in the upper ~30 cm of the sediment core, where the raw Ca counts are anomalously low, due to high water content (Giguet-Covex et al., 2010). The clr Ca values of those samples, on the other hand, accurately reflect the Ca concentrations obtained by ED-XRF, which significantly increase towards the top of the core (Fig. 14 a, b).

A direct comparison of the Ca concentrations measured by ED-XRF with the carbonate content of the sediments quantified by RockEval analysis shows that the bulk Ca concentrations are almost entirely driven by the carbonate content of the sediment (Fig. 14c). This also applies to the clr Ca data measured by XRF-CS, which indicates that, in Lake Le Bourget, clr Ca can be used as a high-resolution indicator of the carbonate content of the sediment. In this specific lake, the correlation between Ca and carbonate content is consistently high, even at lower carbonate contents (Fig. 14c), suggesting that the amount of Ca originating from siliciclastic rocks is negligible. The Ca values therefore reflect the abundance of authigenic carbonates in the sediments. The decrease in Ca values in the upper 400 cm of the core was interpreted as a period of higher terrigenous input from the Rhône river, which is the only one supplying the lake with significant amounts of silicate minerals (Arnaud et al., 2012).

Although this case study shows that Ca can simply be used as a proxy for carbonate content in the sediments of Lake Le Bourget, this relation cannot be generalized to all lakes. It only applies to lakes where the sedimentation is dominated by carbonates (whether they are authigenic or not), which should be verified by comparing carbonate content and Ca measurements obtained on a series of discrete samples, ideally covering the entire range of observed concentrations. In most lakes, Ca represents a mixture of carbonate and non-carbonate sources and can therefore not be interpreted as reflecting one single component of the sediment.

4.1.2. Biogenic silica

Biogenic silica (composed of diatom and radiolarian tests, sponge spicules, and phytoliths) is another major component of lake sediments (Section 3.1), which is best quantified by alkaline extraction (see Section 3.1.2). This method, however, is labor-intensive and destructive. Estimation of bioSi from XRF-CS data thus offers substantial benefits, but it requires a number of assumptions and normalizations.

Since XRF-CS data are bulk measurements, the silicon measured by XRF-CS includes both bioSi and Si associated with clastic minerals. Therefore, it is important to select an appropriate element to normalize for clastic components of the sediment. The best clastic proxy varies from site to site, but K, Al, Rb, and Ti are typically used (Brown, 2015). Aluminum is the logical choice as a proxy for clastic sediment, as it is conservative and relatively independent of grain size (Fig. 11). In practice, however, its concentration in sediments may be low relative to XRF-CS detection limits, and its signal may be subject to random background noise or to variations in XRF response associated with bulk sediment physical properties and chemical composition. Titanium may be a good alternative since it is well-measured by XRF-CS and nearly immobile during chemical weathering and diagenesis. Although it typically shows some enrichment in heavy minerals and hence varies as a function of grain size (Fig. 11), this may not be a serious issue for low energy offshore depositional environments in large lakes, where sediments have relatively modest grain-size variations. Likewise, K is entirely lithogenic and may be used to represent the lithogenic fraction of the sediments, although it may be enriched in the fine-fraction of sediments (Fig. 11) and confounded by the presence of volcanic materials (Brown et al., 2007). In large lakes, Ti and K are commonly used to represent the clastic fraction of the sediment, particularly for sites dominated by pelagic sedimentation.

This application is illustrated here using sediments from northern Lake Malawi, East Africa. BioSi was determined at 1-cm resolution in 50-cm long core M98-10MCB, using a modified version of the Mortlock and Froelich (1989) alkaline extraction method (Johnson et al., 2002; Fig. 15a). A replicate core from the same multicorer deployment (M98-10MCA) underwent XRF scanning on an Itrax XRF core scanner at 2 mm resolution. Simple Si:Ti and Si:K ratios provide a first order estimate of sediments enriched in bioSi, as values above a specific threshold represent “excess silica”, i.e., silica not associated with lithogenic particles (hence, of biogenic origin). In Lake Malawi, Si:Ti displays the best overall relationship with bioSi, but other elements may be better suited in other lakes depending on possible variations in provenance, grain size, etc. (Brown et al., 2007).

Biogenic silica quantification may be improved by using a variation of the excess silica technique (Leinen, 1977), adapted for XRF-CS measurements (Brown, 2015). This requires characterizing the Si:Ti ratio of a purely clastic component, which can be obtained either by scanning a core section barren of bioSi or through the intercept of a bioSi vs Si:Ti plot. This approach generally improves the correlation between the XRF-based estimates and bioSi values obtained by alkaline extraction (Fig. 15b), particularly when applied to lakes where carbonates and organic matter have a low abundance. Theoretically, the best approach to estimate biogenic silica from XRF-CS measurements is to apply the excess silica technique to fully calibrated XRF-CS data (Section 2.2.2c). To our knowledge, this approach has yet to be applied to lake sediments.

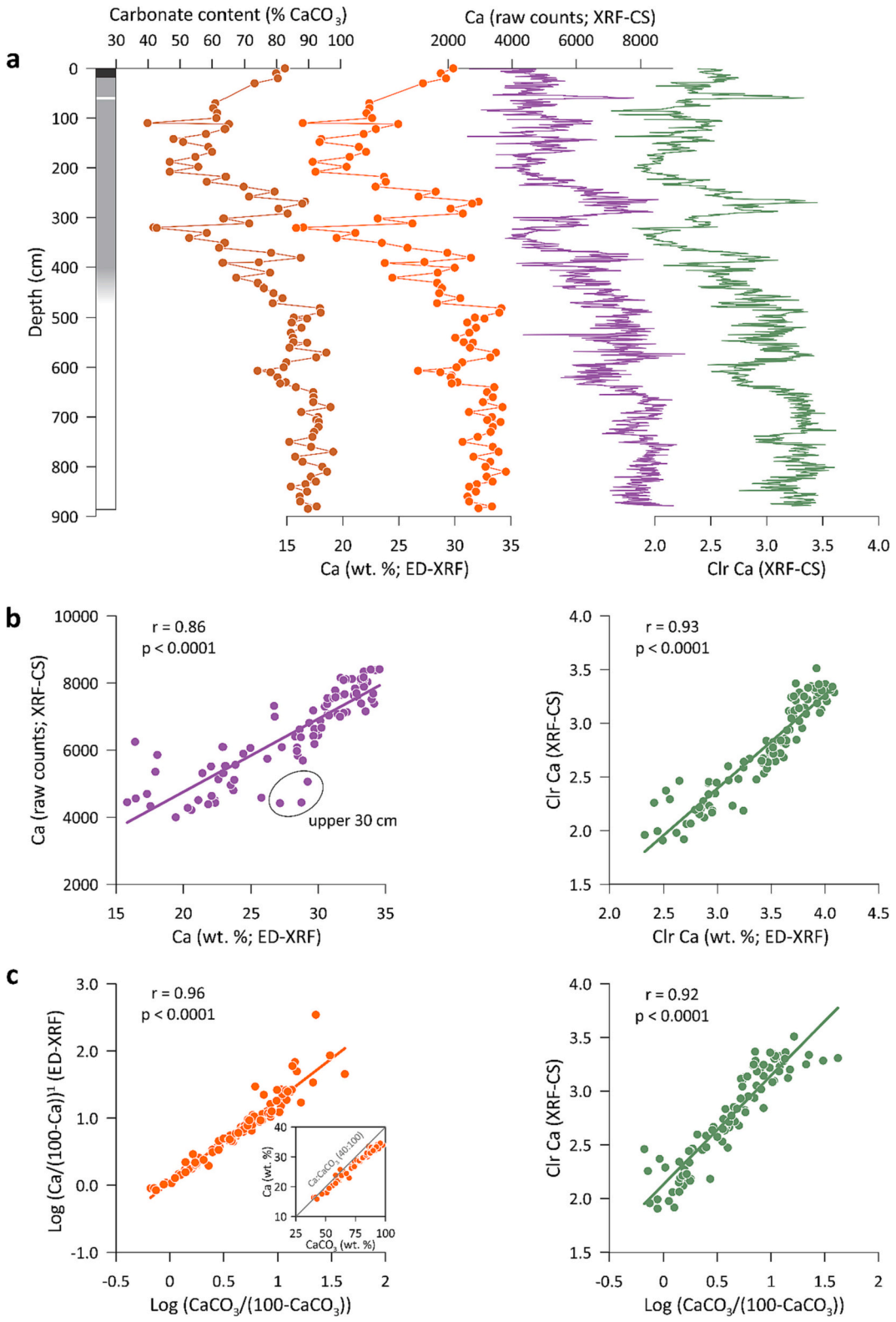

Fig. 14. Carbonate content and Ca abundance in the sediments of Lake Le Bourget. (a) Carbonate content obtained by Rock-Eval analysis compared with Ca abundance measured by ED-XRF (both at 10 cm resolution; Arnaud et al., 2005) and XRF-CS (5 mm resolution; raw counts and centered log ratio[clr]; Arnaud et al., 2012). (b) Comparison between Ca measured by XRF-CS (raw counts and clr) and calcium concentrations obtained by ED-XRF. (c) Ca abundance (ED-XRF and XRF-CS expressed in clr) compared to the carbonate content obtained by Rock-Eval. The comparisons in (b) show that transforming the data in clr results in a much better correlation with the quantitative Ca measurements obtained by ED-XRF. The biplots in (c) show that Ca is mostly associated with carbonates in the sediments of Lake Le Bourget. The carbonate content was apparently overestimated by Rock-Eval analysis (i.e., the 100% $CaCO_3$ intercept corresponds to ~ 35% Ca instead of the theoretical 40%; see section 3.1.3). [1]Log (Ca/(100-Ca)) is preferred over clr for datasets with one overly dominant element (in this case Ca). It also allows comparing datasets with the same transformation on both axes. For the XRF-CS data, the clr transformation is applied since it also accounts for downcore variation in water content physical properties of the sediment. For the ED-XRF data, Ca concentrations were normalized to 100% before calculation.

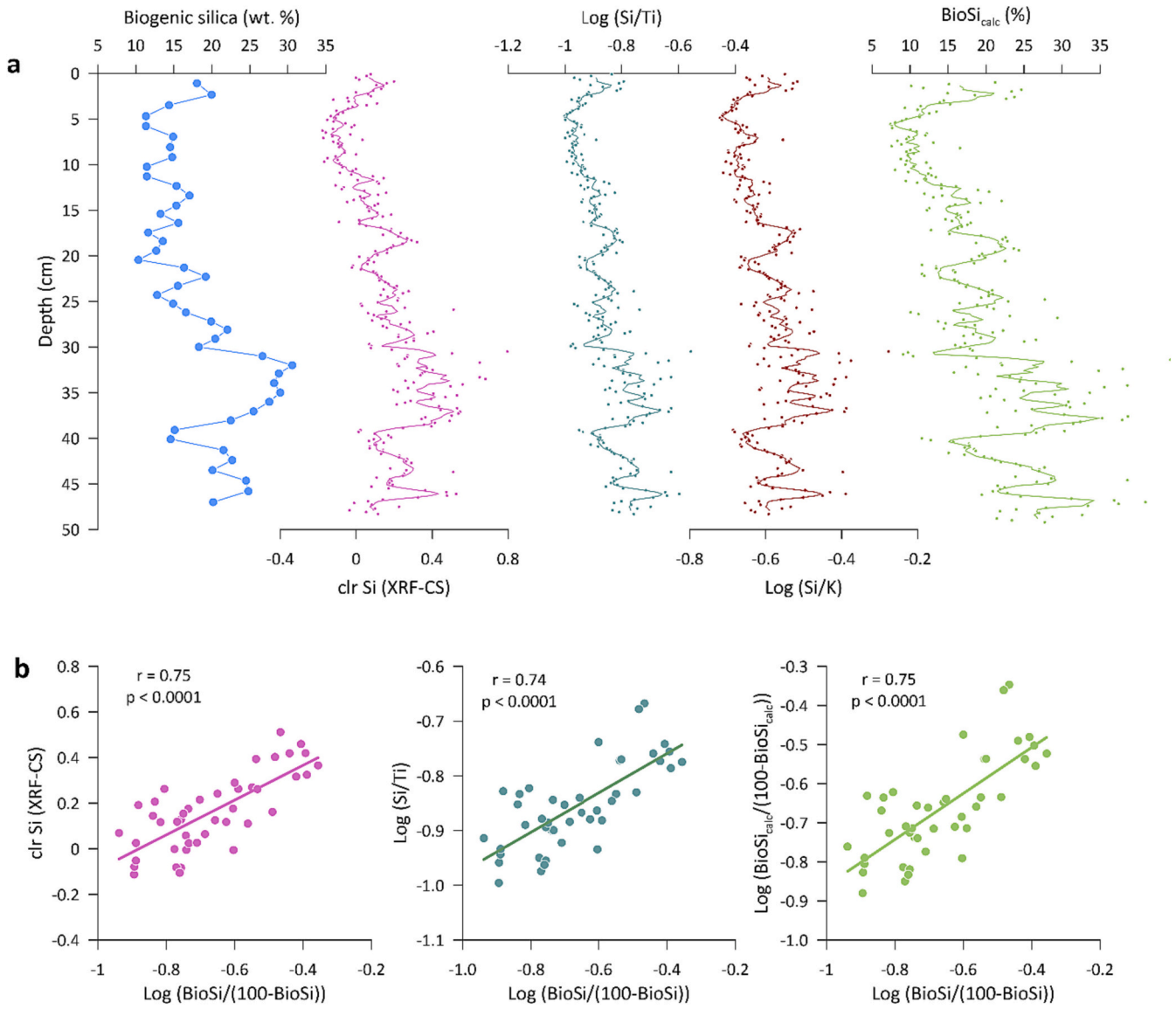

Fig. 15. Biogenic silica (bioSi) estimates based on XRF-CS data. (a) BioSi quantified by alkaline extraction (1 cm resolution) compared with clr Si, log (Si/Ti) and log (Si/K) measured by XRF-CS at 2 mm resolution, and BioSi calculated with the formulate of Brown (2015) (BioSi$_{calc}$), with 5-point running average (data partly published in Brown, 2015). (b) Biplots of clr Si, log (Si/Ti), and BioSi$_{calc}$ measured by XRF-CS against BioSi measured by alkaline extraction. The XRF-CS measurements were obtained with a 60 s counting time, using a Cr X-ray tube with a current of 15 mA and voltage of 30 kV.

4.2. Grain size

As mentioned in Section 3.3.1, the inorganic geochemical composition of lake sediments is significantly influenced by grain size. In lakes dominated by lithogenic particles, inorganic geochemistry can be used to reconstruct sediment grain size and, which, in turn, can be used, for example, to identify event deposits. Often, a single element or elemental ratio reflecting grain size is used (e.g., Cuven et al., 2010). A better approach to improve the relation across the entire grain-size spectrum is to predict sediment grain size using multi-elemental techniques (Liu et al., 2019).

Fig. 16 shows the application of the geochemical ratio Ca/K as a grain-size proxy for a sediment core from Lake Allos, French Alps, which contains a series of flood turbidites (Wilhelm et al., 2022). The ratio Ca/K was used by Wilhelm et al. (2022) based on the observation that the coarse bases of the turbidites are enriched in (detrital) Ca and the fine tops are enriched in K.

Further, a grain-size prediction model was built based on the grain-size analysis of 12 calibration samples from across the 150 cm long core. It was subsequently applied to XRF-CS data obtained every 1 mm and the prediction results were compared to mean grain size measured by laser diffraction every 5 mm. The predicted values show a highly significant positive correlation ($r = 0.87$; $p < 0.001$) with the measured values, and they allow identifying flood turbidites at very high resolution. It is more powerful than the Ca/K ratio ($r = 0.65$; $p < 0.001$; Fig. 16).

In the specific case of Lake Allos, seven lithogenic elements that were well measured by XRF-CS were used for grain-size prediction (Sr, Si, K, Ti, Ca, Fe, and Zr). Silicon and Ca were included since the lake does not contain biogenic silica or authigenic carbonates. The results show that the prediction is mostly based on elements Sr, Si, K and Ti (Fig. 16b). Although the selection of elements is done manually (see explanation in Liu et al., 2019), the model automatically weighs them based on their importance in the prediction. This weighing mostly reflects the nature of the sediment sources. In the case of Lake Allos, the main sediment source

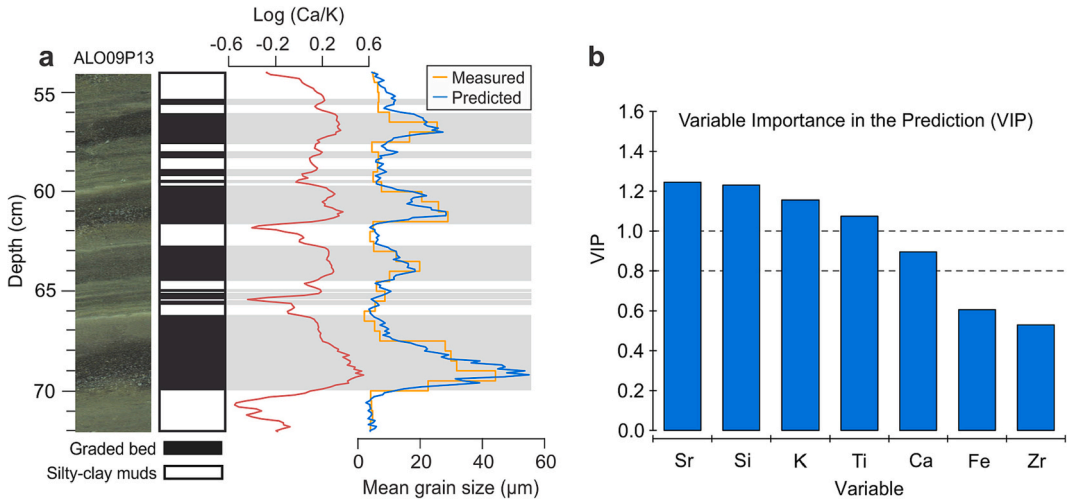

Fig. 16. Application of the grain-size prediction method of Liu et al. (2019) to a sediment core from Lake Allos, French Alps. (a) Mean sediment grain size measured by laser diffraction (resolution 5 mm) and predicted from XRF core scanner data (resolution 1 mm), compared to the Ca/K ratio used in Wilhelm et al. (2022). The results are plotted along a core picture and a representation of the core lithology (from Wilhelm et al., 2012b). Note that the grain-size prediction model is based on 12 data points obtained along the sediment core and that none of them is from the 54–72 cm interval presented here. (b) Importance of the different lithogenic elements included in the grain-size prediction. Values above 1 indicate the most influential elements.

is composed of glacial sediments originating from the erosion of conglomerates composed of siliceous rocks (quartzite and granite) in a carbonate matrix, and marine carbonates.

This application illustrates the potential of high-resolution XRF-CS data to compute grain-size values at high resolution. Although the prediction does not always perform as well as in the case presented here, its main advantage is that the same model can be applied to other cores from the same lake without measuring additional samples for grain size (Liu, 2020). Ultimately, the predictions are of high quality for sites where the sediment is mostly lithogenic, and for which provenance remains relatively constant, including that of event deposits. Future research should determine whether predicting other statistical parameters of the grain-size distributions (mode, sorting, specific percentiles) is also feasible.

4.3. Provenance

In addition to grain size, sediment inorganic geochemistry is also highly controlled by sediment provenance. In lakes with watersheds of variable lithology, rivers draining different areas and/or processes affecting parts of the watershed only may therefore result in the deposition of sediments that bear distinctive geochemical signatures. This also applies to event deposits, whose geochemical signature may reveal the specific area that was affected by the event. A good illustration of the use of major elements to reconstruct provenance is the abundance of Ca in the background sediments and event deposits of Martinez Channel, Chilean Patagonia (Liu, 2020).

Virtually all the sediments that are deposited in Martinez Channel originate from the Baker River, which drains a watershed composed of two distinct lithologies: granitoids in the northwest and metamorphic rocks in the southeast (Fig. 17a). The northwestern watershed is covered by a large icefield, whereas the southeastern watershed is mostly ice-free. Using a combination of X-ray CT-scan images, grain-size analysis, and Zr concentrations, Vandekerkhove et al. (2021) identified a series of flood deposits in the sediments of Martinez Channel. However, those parameters were not able to indicate if the event deposits originated from the northwestern watershed, in which case the floods were glacial in origin, or if they were derived from the southeastern watershed, and hence meteorological in origin.

A linear discriminant analysis of the dominant bedrock lithologies in the watershed clearly highlighted that Ca was the most suited element to differentiate between the granitoids and metamorphic rocks occurring in the area (Fig. 12; Liu et al., 2020). The metamorphic rocks are poor in Ca, whereas the granitoids are characterized by high Ca concentrations, mostly due to abundant Ca-rich plagioclase. Since carbonates do not occur in the sediments of Martinez Channel and that, in this setting, Ca variations are independent of grain-size (Fig. 17b), variations in clr Ca can be used to identify changes in sediment provenance. Using this approach, Liu (2020) was able to show that the background sediment and most of the event deposits recorded in the sediments of Martinez Channel are rich in Ca, and therefore originate from the northwestern side of the watershed (Fig. 17c). The flood deposit at 66–70 cm, on the other hand, displays a sharp drop in Ca abundance, suggesting an origin from the Ca-poor metamorphic rocks in the southeastern part of the watershed (Fig. 17c).

The changes in sediment provenance that were identified based on Ca abundance were confirmed using Sr and Nd isotope analysis on selected samples (Liu et al., 2022; Fig. 17d). The sediment isotopic signatures clearly show that the background sediments and most flood deposits originated from the area of the watershed dominated by granitoids, whereas the flood deposit at 66–70 cm matches the isotopic signature of the metamorphic rocks. Based on these results, Liu et al. (2022) were able to attribute the flood deposit at 66–70 cm to a meteorological flood that affected the eastern side of the watershed, and all other flood deposits to glacier lake outburst floods originating from the icefield in the northwestern part of the watershed. This interpretation was additionally supported by an excellent chronological match between flood deposits and historical chronicles and river discharge measurements (Liu et al., 2022). Ultimately, these results allowed Liu (2020) to use clr Ca values in other sediment cores from the same basin to identify the provenance of flood deposits throughout the basin, without additional ground-truthing.

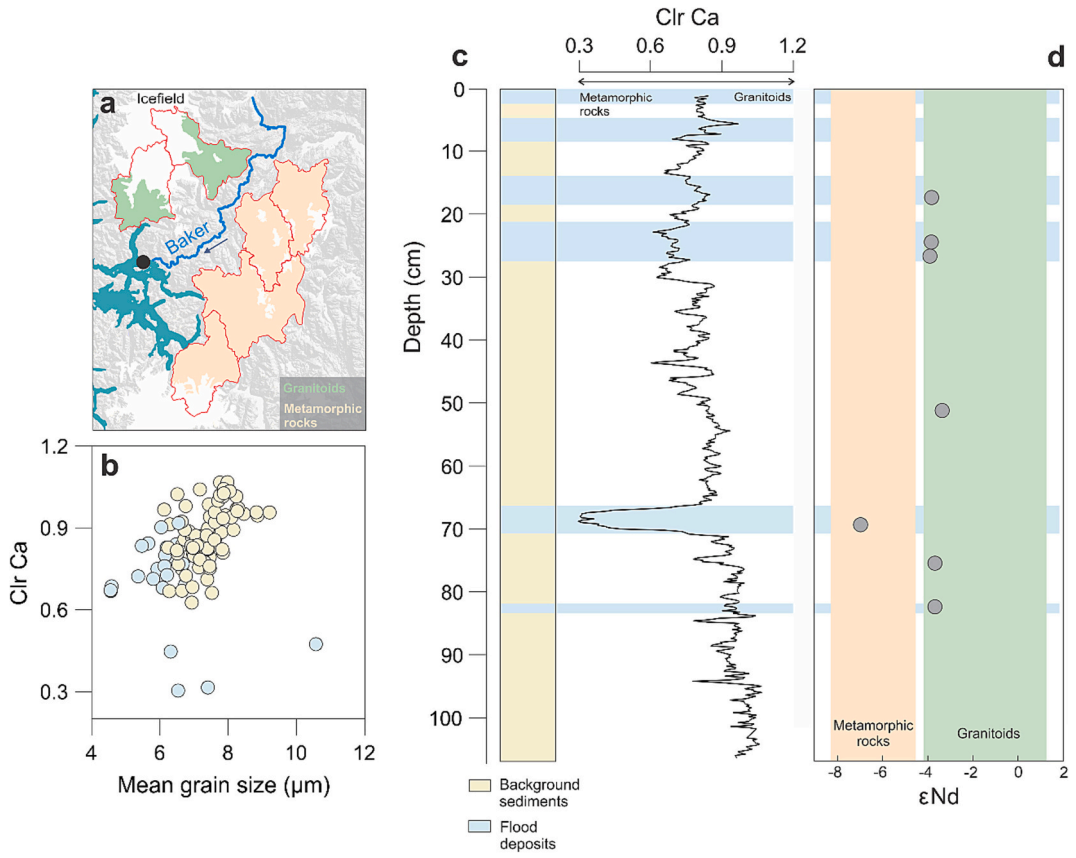

Fig. 17. Provenance of flood deposits in the sediments of Martinez Channel based on Ca abundance (Liu, 2020; Amann et al., in prep.). (a) Geological map showing the distribution of Ca-rich granitoids and Ca-poor metamorphic rocks. See also Fig. 12. The black dot represents the location of the sediment core. (b) Clr Ca versus mean grain size, providing evidence for a lack of relation between the two parameters. Ca abundance is therefore not controlled by grain size and can be used as a provenance tracer. (c) Event deposits in the sediment core (from Vandekerkhove et al., 2021) and Ca abundance measured by XRF-CS. (d) Provenance of the event deposits based on Nd isotopes (Liu et al., 2022).

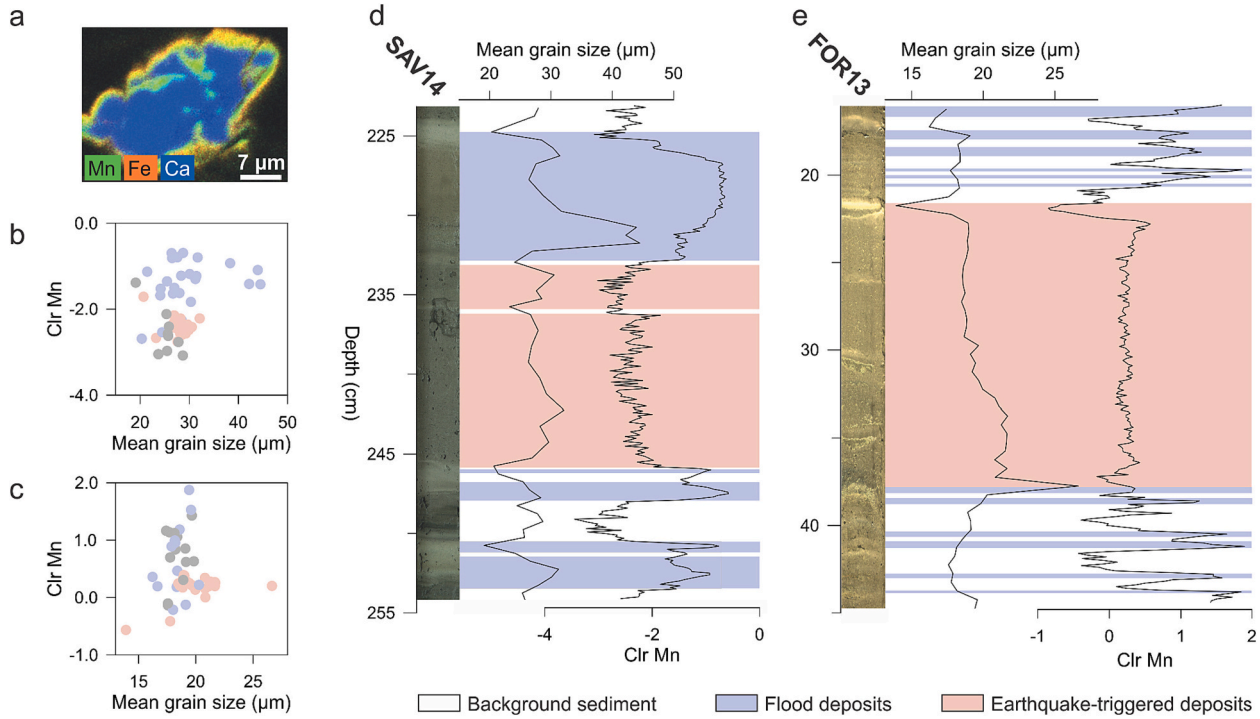

Fig. 18. Distinction between event layers induced by floods and earthquakes based on the paleo-oxygenation of the lake bottom waters tracked with changes in Mn content. (a) SEM-EDX image of a particle from the sediments of Savine Lake. (b,c) Clr Mn plotted against sediment grain size (geometric mean) for lakes Savine and Foréant. These plots show that Mn is not significantly correlated to sediment grain size (at $p < 0.01$), indicating that Mn is independent of grain size in these two lakes. (d, e) Sediment sequences of lakes Savine (Sabatier et al., 2017) and Foréant (Wilhelm et al., 2016) with a core picture, geometric mean grain size, and Mn abundance measured by XRF-CS.

4.4. Lake-specific processes

4.4.1. Distinguishing flood and earthquake-triggered turbidites

Lake sediment sequences often contain several types of event deposits, resulting from e.g. earthquake-triggered subaquatic mass movements and flood events. The sedimentological characteristics of these event deposits are generally very similar, making it challenging to distinguish their respective triggers (e.g., Wilhelm et al., 2022; Sabatier et al., 2022). Inorganic geochemistry may help attribute a triggering mechanism to these event deposits, independently of the provenance of the sediments.

Such an application makes use of elements that have multiple oxidation states (e.g., Mn, Fe) as these may provide evidence of the temporary oxygenation of the bottom waters. During a flood, river water generally plunges when entering a lake, ultimately supplying oxygen to the deep basin. In lakes where bottom waters are anoxic, this process can result in a temporary oxygenation, which can in turn lead to the precipitation of e.g., Mn-Ca carbonates (Calvert and Pedersen, 1993) and/or Mn oxides (Elbaz-Poulichet et al., 2014; Fig. 18a). Those minerals are generally preserved when the lake returns to anoxic conditions because they are immediately buried by the flood deposits. This results in enrichments in Mn at the base, or within, flood layers. In lakes where Mn is not controlled by sediment grain size, such as in Lake Savine (Fig. 18b) and Foréant (Fig. 18c), French Alps, Mn can therefore be used to identify flood events (blue layers in Fig. 18d,e; Wilhelm et al., 2016; Sabatier et al., 2017). By comparison, subaquatic mass movements of slope sediments do not supply oxygen to the lake bottom, resulting in low and constant Mn values (pink layers in Fig. 17d,e).

Note that the use of Mn and/or Fe concentrations, or their ratio, to reconstruct redox conditions is not universal. In most lakes, variations in Fe and Mn concentrations reflect changes in sediment grain-size and/or provenance (e.g., Figs. 11 and 12). Therefore, a sound interpretation of downcore changes in these elements also requires a good understanding of their association with specific minerals or grain-size fractions, as illustrated in Fig. 18 a–c.

4.4.2. Biological activity

Inorganic geochemistry has a strong potential to reconstruct biological activity, even when the biologically-produced particles only constitute a minor fraction of the sediment. In addition to biogenic silica and carbonate production (see Section 4.1), it has been used to track penguin colony size, based on the principle that guano contains significantly elevated concentrations of 'bio-elements' such as As, Ba, Ca, Cd, Cu, P, S, Se, Sr, and Zn and that the erosion of guano-enriched material and subsequent deposition into lakes is proportional to colony size (Sun et al., 2000).

The sediments of Ardley Lake, Antarctic Peninsula, constitute a particularly clear example (Roberts et al., 2017). Ardley Lake is the largest lake on Ardley Island, which is currently home to the Antarctic Peninsula's largest breeding population of gentoo penguins (Liu et al., 2011; MAPPPD, Mapping Application for Penguin Populations and Projected Dynamics). To reconstruct the regional penguin colonization history, Roberts et al. (2017) used the concentrations of Ca and P in a sediment core extracted from Ardley Lake to quantify hydroxyapatite

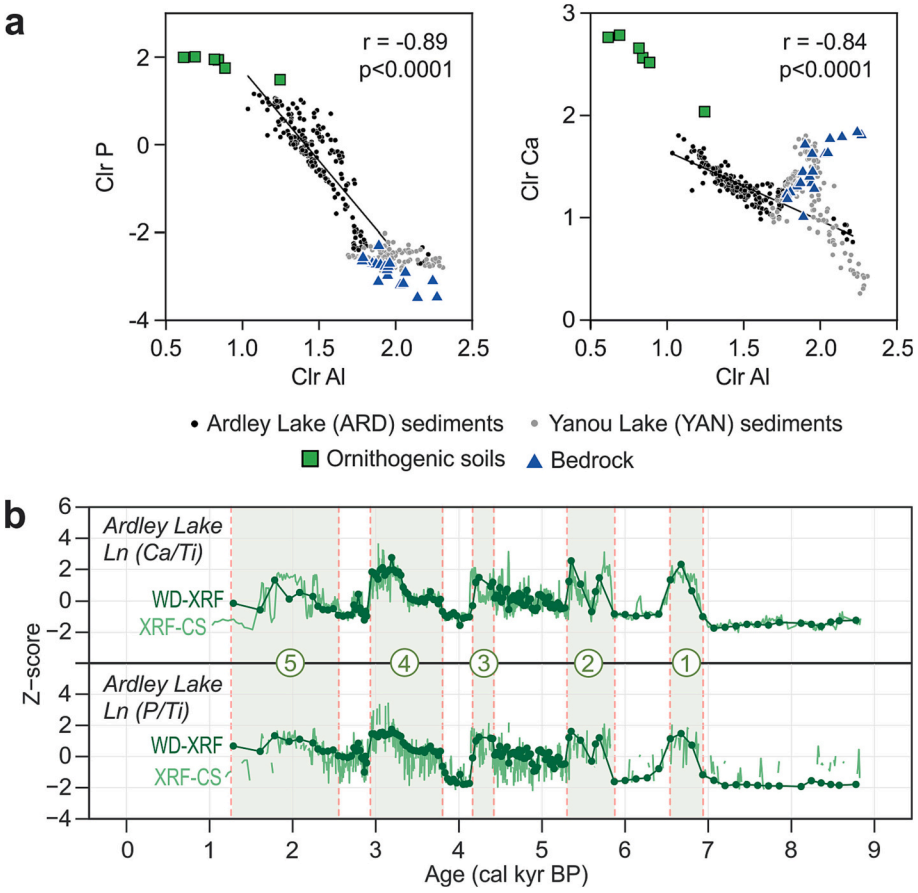

Fig. 19. Use of Ca and P to reconstruct penguin colonization history from the sediments of Ardley Lake, Antarctic Peninsula (Roberts et al., 2017). (a) Biplots of P and Ca versus Al measured by WD-XRF for Ardley Lake sediments, ornithogenic soils (Tatur et al., 1997) and local bedrock (Machado et al., 2005). Yanou Lake sediments are also plotted for comparison as they represent sediments from a lake in a similar geological setting but with no known history of penguin occupation. (b) Profiles of Ti-normalized ln P and Ca measured by WD-XRF and XRF-CS plotted as Z-scores, which highlight guano zones 1–5 (green shading). Z-scores are used to show phases enriched in guano (values > 0).

[$(Ca_{10}(PO_4)_6(OH)_2$], which is the main phosphate mineral found in guano and ornithogenic soils (Tatur and Barczuk, 1985).

Quantitative inorganic geochemical results obtained by WD-XRF show that the sediments from Ardley Lake are enriched in Ca and P compared to the regional bedrock (Fig. 19a). They are also richer in Ca and P than the sediments of Yanou Lake, a lake from the South Shetland Islands with similar underlying volcanic bedrock but no known history of penguin occupation (Fig. 19a). Compared to the bedrock, the local ornithogenic soils are also strongly enriched in Ca and P (Fig. 19a), indicating that these two elements are suitable to reconstruct penguin colonization history on Ardley Island. A mixing model based on Al-normalized P and Ca was then used to determine the fraction of ornithologically-influenced sediment in Ardley Lake (Roberts et al., 2017).

In the Ardley Lake sediment record, Ca and P correlate strongly with other bio-elements measured by WD-XRF (Ba, Sr) and ICP-MS (As, Cd, Cu, S, Se, and Zn), and they are negatively correlated to the lithogenic elements Al, Ti, and Si, supporting their association with sediments originating from ornithogenic soils throughout the record. In addition, the downcore profiles of Ca and P are similar to those of total C, N and S, which reflect organic matter content, suggesting that excess Ca and P is likely driven by the presence of hydroxyapatite in the Ardley Lake guano phases.

XRF-CS data were then used to estimate changes in excess Ca and P at high temporal resolution, based on the P/Ti and Ca/Ti ratios. Titanium was used here as the normalizer since the XRF-CS counts for Al, which is generally the best element to normalize overall (Section 3), were too low and noisy. In this case, Ti is often a good alternative, unless large grain-size changes are observed. Correlations of the log Ca/Ti and P/Ti obtained by XRF-CS and WD-XRF for all data from Ardley Lake were positive and significant ($r = 0.83$ and 0.73, respectively; $p < 0.0001$). XRF-CS data can therefore be used to rapidly identify lake sediments influenced by guano (Fig. 19b).

These XRF-CS data and the fraction of ornithologically-influenced sediment (based on Al-normalized P and Ca measured by WD-XRF) were then used to define five of 13 geochemical zones in the Ardley Lake record as 'guano zones', using constrained cluster analysis (CONISS) (Fig. 19b). In Fig. 19b, z-scores are used to show the phases enriched in guano (values >0) but the same trends are visible when plotting log ratios.

The data was used to show that penguins first colonized Ardley Island ~7000 years ago. In addition, the record revealed that the five guano zones (labeled 1–5; Fig. 18b) were formed during warmer climate conditions and local relative sea level fall, making more land on Ardley Island available for nesting. The most sustained colony between ~3800–2900 years ago (zone 4) coincided with the locally warmest part of the late Holocene.

4.4.3. Hydroclimatology in arid environments

Lakes in arid environments are predominantly saline. Sedimentation, and therefore sediment geochemistry, in those lakes is dominated by evaporites, often alternating with detrital particles of aeolian or river origin. The mineralogical composition of the evaporites is variable and mostly reflects the chemistry of the saline lake water and the intensity of evaporation (Deocampo and Jones, 2014). The most common sequence of precipitates as evaporation progresses is calcium carbonate, followed by gypsum, and then halite until the lake completely dries out. The geochemical composition of those deposits can therefore be used to reconstruct variations in aridity through time.

This is illustrated here using a sediment core from the western Dead Sea margin. The Dead Sea is a hyper-saline terminal lake, with a water level that is strongly controlled by precipitation in the Levant and evaporation (Ben Dor et al., 2019; Müller et al., 2022). The dominant source of freshwater is the Jordan River, although there are also several small ephemeral rivers and streams around the lake (Enzel et al., 2003). The strong and partly seasonal evaporation of the Dead Sea results in the deposition of annually-laminated evaporites composed of authigenic aragonite, gypsum, or even halite (Ben Dor et al., 2019).

Using geochemical data from sediment core DSEn, Neugebauer et al. (2015) demonstrated the presence of period of severe drought between 3.0 and 2.5 cal kyr BP, which is recorded as downcore changes in the nature of the evaporitic minerals. A PCA analysis of the clr-transformed XRF-CS data (Fig. 20a) allows distinguishing between aragonite (Sr-rich carbonate), gypsum ($CaSO_4$), and detrital sediments (siliciclastics). Since Ca occurs in all three sediment fractions, it has no clear positive loading on any of the PC axes and can be used to normalize Sr, S, and Si (or Ti, Fe) to represent variations in the abundance of aragonite, gypsum, and detrital minerals, respectively.

The sediment types are further supported by a Ward's hierarchical cluster analysis (Fig. 20a), which is designed to identify groups of similar composition (Martin-Puertas et al., 2017). Sediments dominated by detrital siliciclastics are represented by cluster 1, aragonite-rich sediments correspond to cluster 2, and gypsum-rich sediments compose cluster 3. The two additional clusters (4 and 5) represent intermediate sediment types, composed of a mixture of detrital particles with significant amounts of gypsum and aragonite, respectively.

Downcore variations in log(Si/Ca), log(Sr/Ca), and log(S/Ca), as well as the cluster stratigraphy, reflect changes in the hydroclimate of the Dead Sea area during the late Holocene (Fig. 20b). During the dry season, the seasonal deposition of aragonite is typical in the Dead Sea area but increasing aridity results in the deposition of gypsum (Müller et al., 2022). Periods of extreme aridity are therefore represented by cluster 3, which corresponds to low log(Sr/Ca) and high log(S/Ca) values. This cluster is particularly present between 3.0 and 2.5 cal kyr BP, representing a distinct period of increased aridity (Neugebauer et al., 2015). During the same period, thick siliciclastic detrital layers represented by cluster 1 and high log(Si/Ca) values are also observed (Fig. 20b). These thick detrital layers are interbedded with the gypsum layers, and they are the result of flash floods that form during extreme rainfall events (Ahlborn et al., 2018). These results allowed Neugebauer et al. (2015) to show that strong flood events occurred sporadically during the period of intensified aridity between 3.0 and 2.5 cal kyr BP. The presence of such floods deposits during a regional drought indicates a shift in synoptic atmospheric circulation patterns, which decreased the passage of eastern Mediterranean cyclones, leading to drier conditions, but favored rainstorms triggered by the Active Red Sea Trough (Ahlborn et al., 2018; Neugebauer et al., 2015).

4.4.4. Metal pollution

Concentrations of Pb and other trace metal pollutants (e.g., Zn, Cu, Ni) in lake sediments are often used to identify pollution patterns over time or space. These elements are generally immobile after deposition and their concentrations are high enough to be measured with classical techniques such as WD-XRF, ICP-OES and ICP-MS. In Sweden, for example, Renberg et al. (1994) used Pb concentrations in multiple lake-sediment records to demonstrate the occurrence of long-range atmospherically-transported Pb pollution, starting with the Greek and Roman cultures. Thanks to the consistency of the broad temporal pattern among lakes, as well as peat records, it was even possible to use the Pb concentration profiles to support radiocarbon-dated chronologies and to estimate sediment ages (Renberg et al., 2016).

In general, the most prominent peak in Pb concentrations in lake sediments represents the 20th century increase in fossil fuel consumption (starting in 1920–1930 CE), which is often followed by a decrease in the 1970s due to the introduction of unleaded gasoline (Callender, 2003). The increase in Pb concentrations in the 20th century tends to be so large that it is frequently also visible in XRF-CS data (e.g., Miller et al., 2014).

With the greater availability of multi-element analyzers, such as ICP-OES, ICP-MS and WD-XRF, and the increased use of multivariate statistics, much more information about pollution and landscape evolution can now be extracted from lake sediment records (e.g., Myrstener et al.,

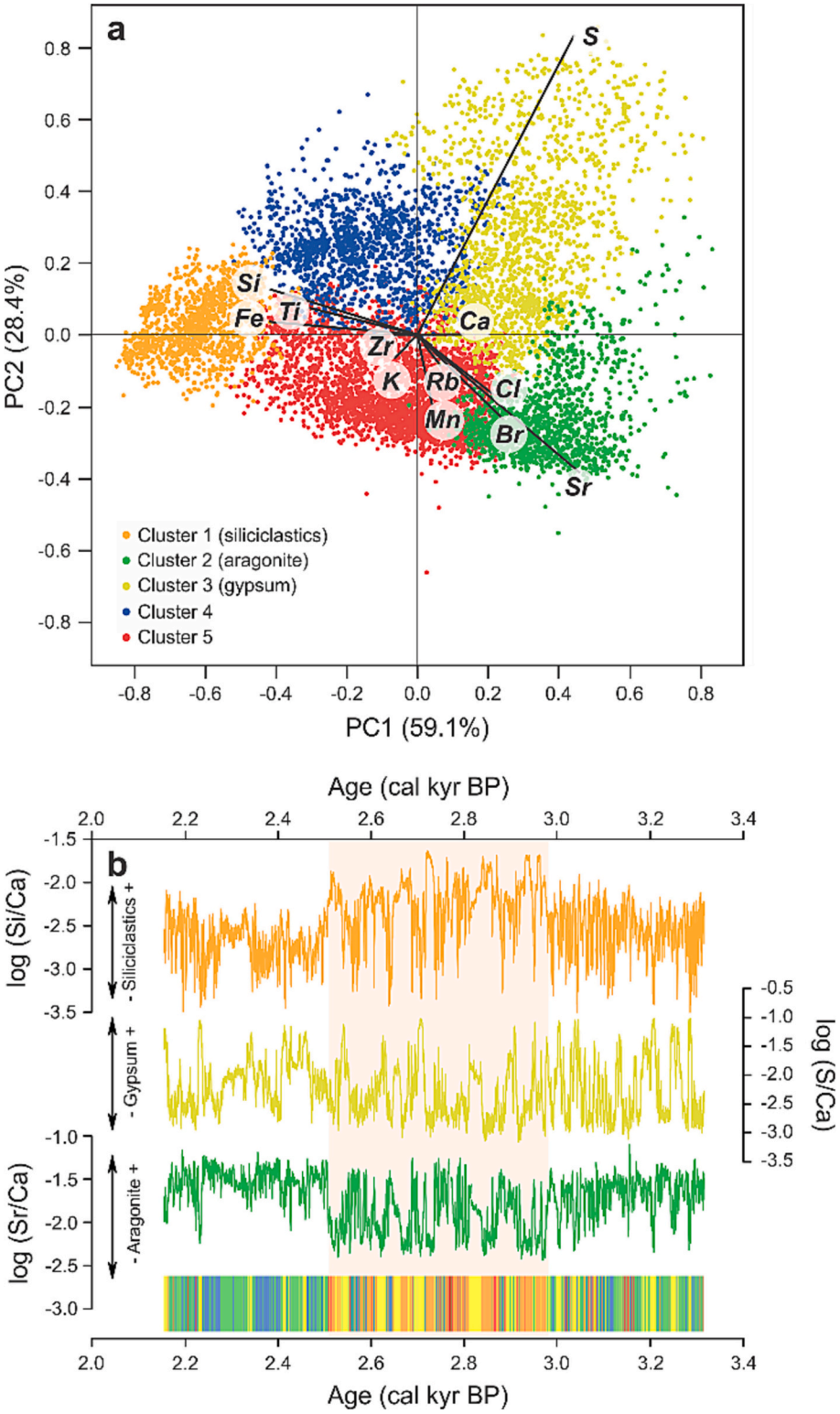

Fig. 20. Late Holocene arid period recorded in Dead Sea sediments. (a) PCA biplot of the clr-transformed XRF-CS data. The elements Sr and S are indicative of aragonite and gypsum, respectively. Note the high positive correlation between Si, Ti, and Fe, representing detrital siliciclastics. The color of the dots corresponds to the clusters obtained with a Ward's hierarchical analysis. (b) Downcore variations in detrital siliciclastics (log(Si/Ca)), gypsum (log(S/Ca)), and aragonite (log(Sr/Ca)) plotted along the cluster stratigraphy. The color legend is the same as in (a).

2019; Thevenon et al., 2011). This is demonstrated here using a multi-element record from Hyttgölen (*hytt* – smelter; *göl* – pond), a small lake in southeastern Sweden, where a series of iron blast furnaces and copper smelters were in use along the lake inlet (Karlsson et al., 2015).

Lead and Cu concentrations alone (presented here as enrichment factors; see e.g., Boës et al., 2011), reveal a valuable but limited history of metal contamination (Karlsson et al., 2015; Fig. 21a). The Pb data indicate only a small increase after ~1700 CE, which, examined alone, would be assumed to result only from diffuse long-range atmospheric transport. Cu concentrations, however, display a rapid increase from

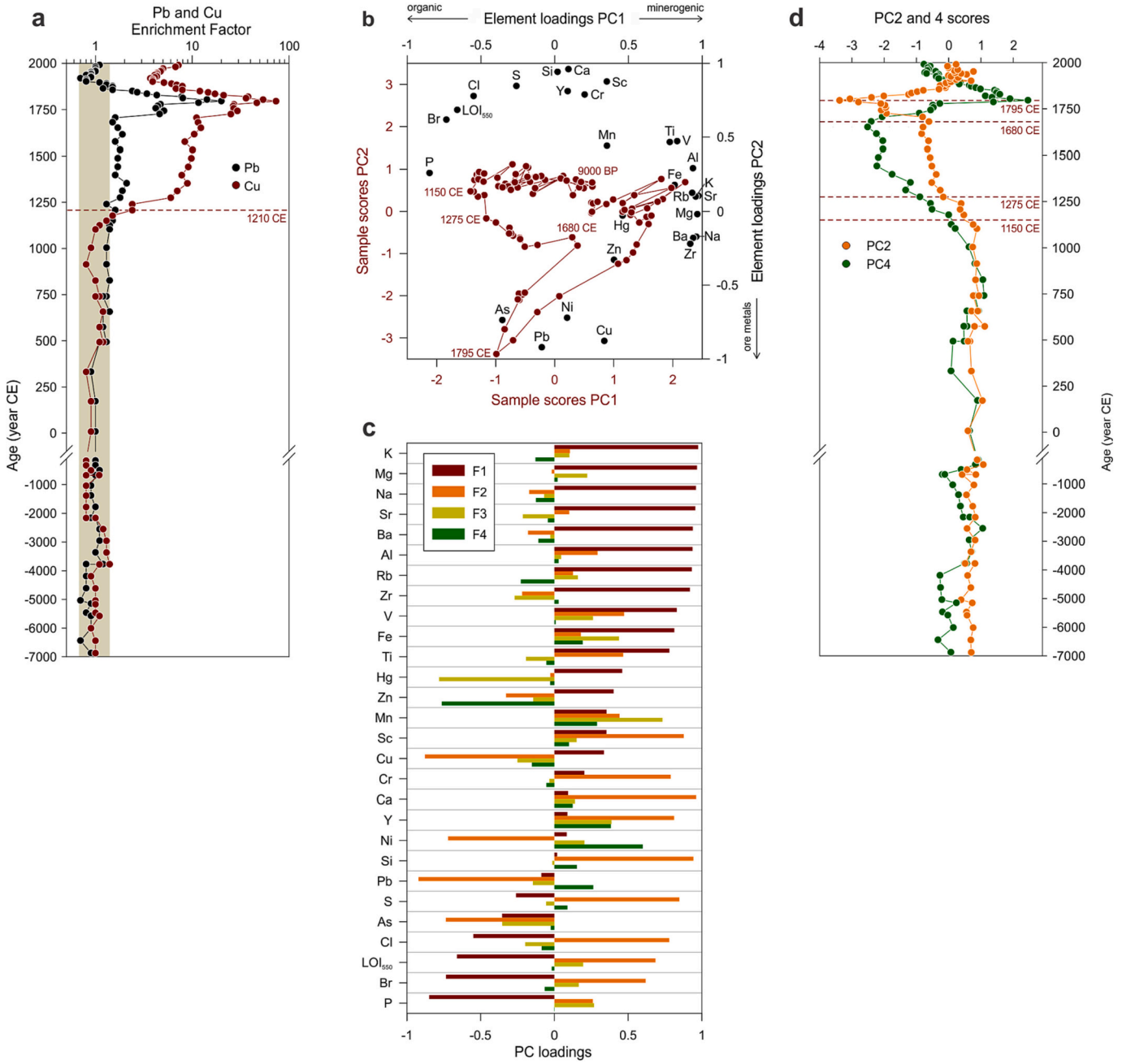

Fig. 21. Holocene metal pollution history of southeastern Sweden reconstructed from major and trace elements (WD-XRF analysis) in the sediments of lake Hyttgölen (Karlsson et al., 2015). (a) Downcore profiles of the enrichment factors (EF) for Pb and Cu. The light brown rectangle represents natural abundance values. (b) PCA biplot showing the evolution of the sample scores through time, superimposed on the element loadings. (c) Loadings of the 27 measured elements and LOI_{550} on the four principal components (F1–F4). (d) Downcore profiles of PC2 (on which Pb, Cu, Ni, and As load negatively) and PC4 (on which Zn loads particularly low) sample scores.

1210 CE, providing evidence for local input. From the two elements, it could be inferred that some form of metal processing occurred as early as 1210 CE, which is 300 years earlier than the oldest documented reference to mining and metallurgy in the area.

A PCA of the multi-element data set (27 elements plus LOI_{550}) reveals even more information about the local pollution history, as well as the evolution of the lake. The PCA (made on clr-transformed data) indicates four main principal components, which capture 92% of the total variance (Fig. 21b). As often in paleolimnology, the first component (PC1; 43.4% of the total variance) represents the lithogenic material (e.g., K, Mg, Na, Fe, Al; positive PC1 loadings) versus organic matter (e.g., P, Br, LOI_{550}; negative PC1 loadings) (Fig. 21b and c). Most of the variability in the lake dataset from c. 9000 BP to c. 1100 CE occurs along PC1 (Fig. 21b). The gradual evolution of the PC1 scores towards negative values during that period indicates an increasingly organic sedimentation, likely due to the development of mature forests and soils that resulted in reduced erosion and transport of mineral matter, in addition to the build up of terrestrial organic matter (cf. Engstrom et al., 2000).

The natural Holocene landscape evolution is interrupted from 1150 CE, as indicated by a small but distinct negative shift along PC2 (35% of the total variance), which reflects the contribution of ore-related metals (Fig. 21b), namely: Pb (85% of its total variance), Cu (77%), As (54%), Ni (52%) and to a lesser extent Zn (11%). This shift, which is also visible when PC2 scores are plotted downcore (Fig. 21d), reveals an even earlier

start of metallurgical activities than suggested by Cu and Pb concentrations alone (1210 CE; Fig. 21a). It is inferred to represent the establishment of a furnace or smelter near the lake, coinciding with the earliest known phase of iron-ore mining and metallurgy in Sweden, where the oldest known iron-ore blast furnace (Lapphyttan) is dated to the late-1100's (Magnusson, 1984). Both PC3 (not shown) and PC4 (Fig. 21d) show a similar departure from the long-term pattern at ~1150 CE. These two components are interpreted to represent the complexity of the ores, with PC3 mostly reflecting changes in Mn, Fe, Hg and As, and PC4 changes in Zn and Ni (Fig. 21c).

From 1275 CE the changes in sediment composition include not only a further negative shift along PC2 (ore-related metals), but also a shift along PC1 towards the elements characteristic of lithogenic material, which could result both from construction or renovation of a furnace or smelter or from channelization of the inlet stream. This dual shift represents more intense activities at the furnace site from 1275 CE, but also suggests a change to processing Cu ores, instead of Fe ores, in agreement with historical data. This is indicated by the particularly low PC2 scores, on which Cu and As load heavily, and by the shift in PC4 (Zn). The lowest PC2 scores occur during 1725–1825 CE. They are consistent with expanded Cu production in the area, which involved the processing of ores with high As contents. Mining then declined and ore processing moved away from the lake shores in the 19th century, resulting in a return of the Cu concentrations and PC scores to near-natural levels (Fig. 21a, d).

The multi-element dataset of the Hyttgölen sediment record and its analysis by PCA demonstrate how lake sediment geochemical records can reveal important details about the environmental evolution of a site. Those results complement and, more importantly, extend, what might be known from archaeological and historical contexts. This example also illustrates the need to investigate principal components beyond PC1, as secondary variations in lake sediment geochemistry may hold more information about the processes of interest than PC1 scores. Here, the varied history of ore processing is reflected in the variations in three components (PC2–4), in agreement with the historical record.

5. Conclusions

The use of inorganic geochemical data in paleolimnology has significantly increased in the 21st century, particularly due to the development of XRF core scanners. These instruments allow the rapid acquisition of elemental profiles along sediment cores non-destructively and at high resolution. Although XRF-CS are currently superseding traditional data acquisition techniques such as WD-XRF and ICP-OES, the latter remain fundamental to generate high-quality quantitative data. The high resolution that can be achieved with XRF-CS is particularly attractive to paleolimnologists but the results require more intense data processing, which is not yet routinely done by all laboratories. In particular, we recommend avoiding the use of raw XRF-CS data. Instead, we recommend using elemental log ratios and/or centered log ratios of single elements when working with XRF-CS data, which is a simple and efficient way to significantly reduce most of the limitations that are inherent to XRF-CS analysis.

In parallel to technical developments, the high number of lake sediment records generated over the last decades provided clear evidence that inorganic geochemical proxies are not universally applicable but should be evaluated on a lake-by-lake basis. The best data exploration approach involves a combination of multivariate statistics with quantification of the main components of the sediment (organic matter, biogenic silica, carbonates and lithogenic particles) and/or mineralogical assemblages. After proper processing of the compositional data, this approach allows associating elements with one or several components of the sediment, resulting in a rigorous interpretation of the geochemical results.

In lake sediments, inorganic elements are predominantly hosted in the lithogenic fraction. Their abundance is mostly driven by changes in grain size and provenance, which offers opportunities to use major element geochemistry to estimate variations in sediment grain-size and sediment provenance at high resolution. Although elemental ratios have often been used as grain-size indicators, simple prediction techniques are now able to generate more accurate downcore grain-size profiles from multi-elemental data. In addition, weathering indices tend to be unsuitable for lake sediments due to the overwhelming influence of grain size on major element geochemistry.

In the future, we expect that the use of inorganic geochemical data will continue increasing in paleolimnology, particularly to obtain more quantitative reconstructions of the processes occurring in lake watersheds. This will require additional data processing efforts, but it has the potential to increase the use of lake sediments as high-resolution archives of climate and environmental change, including in natural hazard research. Although most of the examples presented in this review correspond to lake and fjord sediments, the principles presented here also apply to other sedimentary environments.

Declaration of Competing Interest

The authors declare that they have no known competing financial interests or personal relationships that could have appeared to influence the work reported in this paper.

Data availability

This review paper uses previously-published examples, for which the data is already available online

Acknowledgements

This review results from enlightening discussions with many paleolimnologists and geochemists over the last decade. Katleen Wils, Jana Molenaar, Loic Piret, and Matthias Troch are thanked for constructive comments on an earlier version of this manuscript. Dawei Liu is acknowledged for providing the data used to make Figs. 12 and 17. We wish to thank Gert-Jan Weltje for convincing us of the need to use log-ratios for compositional data analysis. SB acknowledges the French Ministry of Higher Education, Research, and Innovation and the *Agence Nationale de la Recherche* (*ANR*), France, for financing his research chair at Paris-Saclay University. The authors are also grateful to the three anonymous reviewers for their constructive suggestions. This article is dedicated to the memory of Bruno Wilhelm, who tragically passed away during the writing of this manuscript.

Appendix A. Supplementary data

Supplementary data to this article can be found online at https://doi.org/10.1016/j.earscirev.2023.104639.

References

Ahlborn, M., Armon, M., Ben Dor, Y., Neugebauer, I., Schwab, M.J., Tjallingii, R., Shoqeir, J.H., Morin, E., Enzel, Y., Brauer, A., 2018. Increased frequency of torrential rainstorms during a regional late Holocene eastern Mediterranean drought. Quat. Res. 89, 425–431. https://doi.org/10.1017/qua.2018.9.

Aitchison, J., 1982. The statistical analysis of compositional data. J. R. Stat. Soc. Ser. B Methodol. 44, 139–177.

Aitchison, J., 1986. The Statistical Analysis of Compositional Data. Chapman and Hall, London; New York, p. 416.

Amann, B., Bertrand, S., Liu, D., Vandekerkhove, E., Troch, M., in prep. Identification and provenance of Baker river flood deposits in fjord sediments based on inorganic geochemistry (Chilean Patagonia, 48°S). Geochem. Geophys. Geosyst. in preparation.

Arnaud, F., 2005. Discriminating bio-induced and detrital sedimentary processes from particle size distribution of carbonates and non-carbonates in hard water lake sediments. J. Paleolimnol. 34, 519–526. https://doi.org/10.1007/s10933-005-6787-1.

Arnaud, F., Revel, M., Chapron, E., Desmet, M., Tribovillard, N., 2005. 7200 years of Rhone river flooding activity in Lake Le Bourget, France: a high-resolution sediment

record of NW Alps hydrology. The Holocene 15, 420–428. https://doi.org/10.1191/0959683605hl801rp.
Arnaud, F., Magand, O., Chapron, E., Bertrand, S., Boës, X., Charlet, F., Mélières, M.A., 2006. Radionuclide dating (^{210}Pb, ^{137}Cs, ^{241}Am) of recent lake sediments in a highly active geodynamic setting (Lakes Puyehue and Icalma—Chilean Lake District). Sci. Total Environ. 366, 837–850. https://doi.org/10.1016/j.scitotenv.2005.08.013.
Arnaud, F., Révillon, S., Debret, M., Revel, M., Chapron, E., Jacob, J., Giguet-Covex, C., Poulenard, J., Magny, M., 2012. Lake Bourget regional erosion patterns reconstruction reveals Holocene NW European Alps soil evolution and paleohydrology. Quat. Sci. Rev. 51, 81–92. https://doi.org/10.1016/j.quascirev.2012.07.025.
Arnaud, F., Poulenard, J., Giguet-Covex, C., Wilhelm, B., Révillon, S., Jenny, J.-P., Revel, M., Enters, D., Bajard, M., Fouinat, L., Doyen, E., Simonneau, A., Pignol, C., Chapron, E., Vannière, B., Sabatier, P., 2016. Erosion under climate and human pressures: an alpine lake sediment perspective. Quat. Sci. Rev. 152, 1–18. https://doi.org/10.1016/j.quascirev.2016.09.018.
Arndt, S., Jørgensen, B.B., LaRowe, D.E., Middelburg, J.J., Pancost, R.D., Regnier, P., 2013. Quantifying the degradation of organic matter in marine sediments: a review and synthesis. Earth Sci. Rev. 123, 53–86. https://doi.org/10.1016/j.earscirev.2013.02.008.
Baudin, F., Disnar, J.-R., Aboussou, A., Savignac, F., 2015. Guidelines for Rock–Eval analysis of recent marine sediments. Org. Geochem. 86, 71–80. https://doi.org/10.1016/j.orggeochem.2015.06.009.
Baxter, M.J., Freestone, I.C., 2006. Log-ratio compositional data analysis in archaeometry. Archaeometry 48, 511–531. https://doi.org/10.1111/j.1475-4754.2006.00270.x.
Ben Dor, Y., Neugebauer, I., Enzel, Y., Schwab, M.J., Tjallingii, R., Erel, Y., Brauer, A., 2019. Varves of the Dead Sea sedimentary record. Quat. Sci. Rev. 215, 173–184. https://doi.org/10.1016/j.quascirev.2019.04.011.
Bertrand, S., Boës, X., Castiaux, J., Charlet, F., Urrutia, R., Espinoza, C., Lepoint, G., Charlier, B., Fagel, N., 2005. Temporal evolution of sediment supply in Lago Puyehue (Southern Chile) during the last 600 yr and its climatic significance. Quat. Res. 64, 163–175. https://doi.org/10.1016/j.yqres.2005.06.005.
Bertrand, S., Hughen, K.A., Sepulveda, J., Pantoja, S., 2012. Geochemistry of surface sediments from the fjords of Northern Chilean Patagonia (44-47°S): Spatial variability and implications for paleoclimate reconstructions. Geochim. Cosmochim. Acta 76, 125–146. https://doi.org/10.1016/j.gca.2011.10.028.
Bertrand, S., Hughen, K., Sepulveda, J., Pantoja, S., 2014. Late Holocene covariability of the southern westerlies and sea surface temperature in northern Chilean Patagonia. Quat. Sci. Rev. 105, 195–208. https://doi.org/10.1016/j.quascirev.2014.09.021.
Bertrand, S., Hughen, K., Giosan, L., 2015. Limited influence of sediment grain size on elemental XRF core scanner measurements. In: Croudace, I.W., Rothwell, R.G. (Eds.), Micro-XRF Studies of Sediment Cores: Applications of a Non-destructive Tool for the Environmental Sciences. Springer, Dordrecht, pp. 473–490. https://doi.org/10.1007/978-94-017-9849-5_19.
Boës, X., Fagel, N., 2008. Relationships between southern Chilean varved lake sediments, precipitation and ENSO for the last 600 years. J. Paleolimnol. 39, 237–252. https://doi.org/10.1007/s10933-007-9119-9.
Boës, X., Rydberg, J., Martinez-Cortizas, A., Bindler, R., Renberg, I., 2011. Evaluation of conservative lithogenic elements (Ti, Zr, Al, and Rb) to study anthropogenic element enrichments in lake sediments. J. Paleolimnol. 46, 75–87. https://doi.org/10.1007/s10933-011-9515-z.
Bonk, A., Müller, D., Ramisch, A., Kramkowski, M.A., Noryśkiewicz, A.M., Sekudewicz, I., Gąsiorowski, M., Luberda-Durnaś, K., Słowiński, M., Schwab, M., Tjallingii, R., Brauer, A., Błaszkiewicz, M., 2021. Varve microfacies and chronology from a new sediment record of Lake Gościąż (Poland). Quat. Sci. Rev. 251, 106715 https://doi.org/10.1016/j.quascirev.2020.106715.
Bonk, A., Piotrowska, N., Żarczyński, M., Enters, D., Makohonienko, M., Rzodkiewicz, M., Tylmann, W., 2023. Limnological responses to environmental changes during the last 3,000 years revealed from a varved sequence of Lake Lubińskie (western Poland). Catena 226, 107053. https://doi.org/10.1016/j.catena.2023.107053.
Brodie, C.R., Leng, M.J., Casford, J.S.L., Kendrick, C.P., Lloyd, J.M., Zong, Y.Q., Bird, M. I., 2011. Evidence for bias in C and N concentrations and δ13C composition of terrestrial and aquatic organic materials due to pre-analysis acid preparation methods. Chem. Geol. 282, 67–83. https://doi.org/10.1016/j.chemgeo.2011.01.007.
Brown, E.T., 2015. Estimation of biogenic silica concentrations using scanning XRF: Insights from studies of Lake Malawi sediments. In: Croudace, I.W., Rothwell, R.G. (Eds.), Micro-XRF Studies of Sediment Cores: Applications of a Non-destructive Tool for the Environmental Sciences. Springer, Dordrecht, pp. 267–277. https://doi.org/10.1007/978-94-017-9849-5_9.
Brown, E.T., Johnson, T.C., Scholz, C.A., Cohen, A.S., King, J.W., 2007. Abrupt change in tropical African climate linked to the bipolar seesaw over the past 55,000 years. Geophys. Res. Lett. 34 https://doi.org/10.1029/2007gl031240.
Callender, E., 2003. 9.03 - Heavy metals in the environment—Historical trends. In: Holland, H.D., Turekian, K.K. (Eds.), Treatise on Geochemistry. Pergamon, Oxford, pp. 67–105. https://doi.org/10.1016/B0-08-043751-6/09161-1.
Calvert, S.E., Pedersen, T.F., 1993. Geochemistry of recent oxic and anoxic marine sediments - Implications for the geological record. Mar. Geol. 113, 67–88. https://doi.org/10.1016/0025-3227(93)90150-T.
Cantera, C., Ozán, I.L., 2022. Applicability of calcimetry in low-calcium carbonate sediments. Latin Am. J. Sedimentol. Basin Anal. 29, 83–95.
Cevik, U., Akbulut, S., Makarovska, Y., Van Grieken, R., 2013. Polarized-beam high-energy EDXRF in geological samples. Spectrosc. Lett. 46, 36–46. https://doi.org/10.1080/00387010.2012.661015.
Chawchai, S., Kylander, M.E., Chabangborn, A., Löwemark, L., Wohlfarth, B., 2016. Testing commonly used X-ray fluorescence core scanning-based proxies for organic-rich lake sediments and peat. Boreas 45, 180–189. https://doi.org/10.1111/bor.12145.
Collins, A.L., Walling, D.E., Leeks, G.J.L., 1998. Fingerprinting the origin of fluvial suspended sediment in larger river basins: combining assessment of spatial provenance and source type. Geogr. Annal. Ser. A Phys. Geogr. 79, 239–254. https://doi.org/10.1111/j.0435-3676.1997.00020.x.
Collins, A.L., Pulley, S., Foster, I.D., Gellis, A., Porto, P., Horowitz, A.J., 2017. Sediment source fingerprinting as an aid to catchment management: a review of the current state of knowledge and a methodological decision-tree for end-users. J. Environ. Manag. 194, 86–108. https://doi.org/10.1016/j.jenvman.2016.09.075.
Collins, A.L., Blackwell, M., Boeckx, P., Chivers, C.A., Emelko, M., Evrard, O., Foster, I., Gellis, A., Gholami, H., Granger, S., Harris, P., Horowitz, A.J., Laceby, J.P., Martinez-Carreras, N., Minella, J., Mol, L., Nosrati, K., Pulley, S., Silins, U., da Silva, Y.J., Stone, M., Tiecher, T., Upadhayay, H.R., Zhang, Y., 2020. Sediment source fingerprinting: benchmarking recent outputs, remaining challenges and emerging themes. J. Soils Sediments 20, 4160–4193. https://doi.org/10.1007/s11368-020-02755-4.
Craigie, N., 2018. Sampling, sample preparation and analytical techniques. In: Principles of Elemental Chemostratigraphy. Springer Cham, pp. 9–37. https://doi.org/10.1007/978-3-319-71216-1_2.
Croudace, I.W., Gilligan, J.M., 1990. Versatile and accurate trace element determinations in iron-rich and other geological samples using x-ray fluorescence analysis. X-Ray Spectrom. 19, 117–123. https://doi.org/10.1002/xrs.1300190307.
Croudace, I.W., Rothwell, R.G., 2015. Micro-XRF studies of sediment cores: Applications of a non-destructive tool for the environmental sciences. In: Developments in Paleoenvironmental Research, 1st ed. Springer, Dordrecht. https://doi.org/10.1007/978-94-017-9849-5. 656 p.
Croudace, I.W., Rindby, A., Rothwell, R.G., 2006. ITRAX: description and evaluation of a new multi-function X-ray core scanner. Geol. Soc. Lond. Spec. Publ. 267, 51–63. https://doi.org/10.1144/GSL.SP.2006.267.01.04.
Croudace, I.W., Löwemark, L., Tjallingii, R., Zolitschka, B., 2019. Current perspectives on the capabilities of high resolution XRF core scanners. Quat. Int. 514, 5–15. https://doi.org/10.1016/j.quaint.2019.04.002.
Cuven, S., Francus, P., Lamoureux, S.F., 2010. Estimation of grain size variability with micro X-ray fluorescence in laminated lacustrine sediments, Cape Bounty, Canadian High Arctic. J. Paleolimnol. 44, 803–817. https://doi.org/10.1007/s10933-010-9453-1.
Davies, S.J., Lamb, H.F., Roberts, S.J., 2015. Micro-XRF core scanning in palaeolimnology: Recent developments. In: Croudace, I.W., Rothwell, R.G. (Eds.), Micro-XRF Studies of Sediment Cores : Applications of a Non-Destructive Tool for the Environmental Sciences, pp. 189–226. https://doi.org/10.1007/978-94-017-9849-5_7.
Deer, W.A., Howie, R.A., Zussman, J., 2013. An introduction to the rock-forming minerals, 3rd ed. Mineralogical Society of Great Britain and Ireland. https://doi.org/10.1180/DHZ.
Deocampo, D.M., Jones, B.F., 2014. Geochemistry of saline lakes. In: Holland, H.D., Turekian, K.K. (Eds.), Treatise on Geochemistry, Second edition. Elsevier, Oxford, pp. 437–469. https://doi.org/10.1016/B978-0-08-095975-7.00515-5.
Duchesne, J.C., Bologne, G., 2009. XRF major and trace element determination in Fe-Ti oxide minerals. Geol. Belg. 12, 205–212.
Dunlea, A.G., Murray, R.W., Tada, R., Alvarez-Zarikian, C.A., Anderson, C.H., Gilli, A., Giosan, L., Gorgas, T., Hennekam, R., Irino, T., Murayama, M., Peterson, L.C., Reichart, G.J., Seki, A., Zheng, H.B., Ziegler, M., 2020. Intercomparison of XRF core scanning results from seven labs and approaches to practical calibration. Geochem. Geophys. Geosyst. 21 https://doi.org/10.1029/2020GC009248.
El Bilali, L., Rasmussen, P.E., Hall, G.E.M., Fortin, D., 2002. Role of sediment composition in trace metal distribution in lake sediments. Appl. Geochem. 17, 1171–1181. https://doi.org/10.1016/s0883-2927(01)00132-9.
Elbaz-Poulichet, F., Sabatier, P., Dezileau, L., Freydier, R., 2014. Sedimentary record of V, U, Mo and Mn in the Pierre-Blanche lagoon (Southern France) - evidence for a major anoxia event during the Roman period. The Holocene 24, 1384–1392. https://doi.org/10.1177/0959683614540957.
Engstrom, D.R., Fritz, S.C., Almendinger, J.E., Juggins, S., 2000. Chemical and biological trends during lake evolution in recently deglaciated terrain. Nature 408, 161–166. https://doi.org/10.1038/35041500.
Enzel, Y., Bookman, R., Sharon, D., Gvirtzman, H., Dayan, U., Ziv, B., Stein, M., 2003. Late Holocene climates of the Near East deduced from Dead Sea level variations and modern regional winter rainfall. Quat. Res. 60, 263–273. https://doi.org/10.1016/j.yqres.2003.07.011.
Espitalie, J., Deroo, G., Marquis, F., 1985. Rock-Eval pyrolysis and its applications (part two). Revue de l'Institut Français du Pétrole 40, 755–784. https://doi.org/10.2516/ogst:1985045.
Ferreira, S.L.C., Bezerra, M.A., Santos, A.S., dos Santos, W.N.L., Novaes, C.G., de Oliveira, O.M.C., Oliveira, M.L., Garcia, R.L., 2018. Atomic absorption spectrometry – a multi element technique. Trac-Trends Anal. Chem. 100, 1–6. https://doi.org/10.1016/j.trac.2017.12.012.
Giguet-Covex, C., Arnaud, F., Poulenard, J., Enters, D., Reyss, J.-L., Millet, L., Lazzaroto, J., Vidal, O., 2010. Sedimentological and geochemical records of past trophic state and hypolimnetic anoxia in large, hard-water Lake Bourget, French Alps. J. Paleolimnol. 43, 171–190. https://doi.org/10.1007/s10933-009-9324-9.
Gilfedder, B.S., Petri, M., Wessels, M., Biester, H., 2011. Bromine species fluxes from Lake Constance's catchment, and a preliminary lake mass balance. Geochim. Cosmochim. Acta 75, 3385–3401. https://doi.org/10.1016/j.gca.2011.03.021.

Gill, R., 2014. Modern Analytical Geochemistry: An Introduction to Quantitative Chemical Analysis Techniques for Earth, Environmental and Materials Scientists. Taylor & Francis. https://doi.org/10.4324/9781315844381, 342 p.
Gregory, B.R.B., Patterson, R.T., Reinhardt, E.G., Galloway, J.M., Roe, H.M., 2019. An evaluation of methodologies for calibrating Itrax X-ray fluorescence counts with ICP-MS concentration data for discrete sediment samples. Chem. Geol. 521, 12–27. https://doi.org/10.1016/j.chemgeo.2019.05.008.
Grosjean, M., Von Gunten, L., Trachsel, M., Kamenik, C., 2009. Calibration-in-time: Transforming biogeochemical lake sediment proxies into quantitative climate variables. PAGES News 108–110. https://doi.org/10.22498/pages.17.3.108.
Guo, Y., Yang, S., Su, N., Li, C., Yin, P., Wang, Z., 2018. Revisiting the effects of hydrodynamic sorting and sedimentary recycling on chemical weathering indices. Geochim. Cosmochim. Acta 227, 48–63. https://doi.org/10.1016/j.gca.2018.02.015.
Hahn, A., Kliem, P., Oehlerich, M., Ohlendorf, C., Zolitschka, B., 2014. Elemental composition of the Laguna Potrok Aike sediment sequence reveals paleoclimatic changes over the past 51 ka in southern Patagonia, Argentina. J. Paleolimnol. 52, 349–366. https://doi.org/10.1007/s10933-014-9798-y.
Hatano, N., Yoshida, K., Sasao, E., 2019. Effects of grain size on the chemical weathering index: a case study of Neogene fluvial sediments in Southwest Japan. Sediment. Geol. 386, 1–8. https://doi.org/10.1016/j.sedgeo.2019.03.017.
Heiri, O., Lotter, A.F., Lemcke, G., 2001. Loss on ignition as a method for estimating organic and carbonate content in sediments: reproducibility and comparability of results. J. Paleolimnol. 25, 101–110. https://doi.org/10.1023/A:1008119611481.
Huang, S.L., Sholkovitz, E.R., Conte, M.H., 2007. Application of high-temperature fusion for analysis of major and trace elements in marine sediment trap samples. Limnol. Oceanogr. Methods 5, 13–22. https://doi.org/10.4319/lom.2007.5.13.
Hunt, J.E., Croudace, I.W., MacLachlan, S.E., 2015. Use of calibrated ITRAX XRF data in determining turbidite geochemistry and provenance in Agadir Basin, Northwest African passive margin. In: Croudace, I.W., Rothwell, R.G. (Eds.), Micro-XRF Studies of Sediment Cores: Applications of a Non-destructive Tool for the Environmental Sciences. Springer, Dordrecht, pp. 127–146. https://doi.org/10.1007/978-94-017-9849-5_4.
Jansen, J.H.F., Van der Gaast, S.J., Koster, B., Vaars, A.J., 1998. CORTEX, a shipboard XRF-scanner for element analyses in split sediment cores. Mar. Geol. 151, 143–153. https://doi.org/10.1016/S0025-3227(98)00074-7.
Jenkins, R., de Vries, J.L., 1970. Practical x-Ray Spectrometry. Philips Technical Library, Eindhoven, 190 p.
Johnson, T.C., Brown, E.T., McManus, J., Barry, S., Barker, P., Gasse, F., 2002. A high-resolution paleoclimate record spanning the past 25,000 years in southern East Africa. Science 296, 113–132. https://doi.org/10.1126/science.1070057.
Jokinen, S.A., Jilbert, T., Tiihonen-Filppula, R., Koho, K., 2020. Terrestrial organic matter input drives sedimentary trace metal sequestration in a human-impacted boreal estuary. Sci. Total Environ. 717, 137047 https://doi.org/10.1016/j.scitotenv.2020.137047.
Jones, A.F., Turner, J.N., Daly, J.S., Francus, P., Edwards, R.J., 2019. Signal-to-noise ratios, instrument parameters and repeatability of Itrax XRF core scan measurements of floodplain sediments. Quat. Int. 514, 44–54. https://doi.org/10.1016/j.quaint.2018.09.006.
Kaboth-Bahr, S., Denis, V., Su, C., O'Regan, M., Gyllencreutz, R., Jakobsson, M., Löwemark, L., 2019. Deciphering ~45.000 years of Arctic Ocean lithostratigraphic variability through multivariate statistical analysis. Quat. Int. 514, 141–151. https://doi.org/10.1016/j.quaint.2018.11.043.
Karlsson, J., Segerström, U., Berg, A., Mattielli, N., Bindler, R., 2015. Tracing modern environmental conditions to their roots in early mining, metallurgy, and settlement in Gladhammar, Southeast Sweden: vegetation and pollution history outside the traditional Bergslagen mining region. The Holocene 25, 944–955. https://doi.org/10.1177/0959683615574586.
Kennedy, D.M., Woods, J.L.D., 2013. Determining organic and carbonate content in sediments. In: Shroder, J.F. (Ed.), Treatise on Geomorphology. Academic Press, San Diego, pp. 262–273. https://doi.org/10.1016/B978-0-12-374739-6.00389-4.
Kido, Y., Koshikawa, T., Tada, R., 2006. Rapid and quantitative major element analysis method for wet fine-grained sediments using an XRF microscanner. Mar. Geol. 229, 209–225. https://doi.org/10.1016/j.margeo.2006.03.002.
Klöcking, M., Wyborn, L., Lehnert, K.A., Ware, B., Prent, A.M., Profeta, L., Kohlmann, F., Noble, W., Bruno, I., Lambart, S., Ananuer, H., Barber, N.D., Becker, H., Brodbeck, M., Deng, H., Deng, K., Elger, K., de Souza Franco, G., Gao, Y., Ghasera, K. M., Hezel, D.C., Huang, J., Kerswell, B., Koch, H., Lanati, A.W., ter Maat, G., Martínez-Villegas, N., Yobo, L.N., Redaa, A., Schäfer, W., Swing, M.R., Taylor, R.J. M., Traun, M.K., Whelan, J., Zhou, T., 2023. Community recommendations for geochemical data, services and analytical capabilities in the 21st century. Geochim. Cosmochim. Acta 351, 192–205. https://doi.org/10.1016/j.gca.2023.04.024.
Kylander, M.E., Ampel, L., Wohlfarth, B., Veres, D., 2011. High-resolution X-ray fluorescence core scanning analysis of Les Echets (France) sedimentary sequence: new insights from chemical proxies. J. Quat. Sci. 26, 109–117. https://doi.org/10.1002/jqs.1438.
Kylander, M.E., Lind, E.M., Wastegard, S., Lowemark, L., 2012. Recommendations for using XRF core scanning as a tool in tephrochronology. The Holocene 22, 371–375. https://doi.org/10.1177/0959683611423688.
Lafargue, E., Marquis, F., Pillot, D., 1998. Rock-Eval 6 applications in hydrocarbon exploration, production, and soil contamination studies. Revue de l'Institut Français du Pétrole 53, 421–437. https://doi.org/10.2516/ogst:1998036.
Last, W.M., 2002. Geolimnology of salt lakes. Geosci. J. 6, 347–369. https://doi.org/10.1007/bf03020619.
Leinen, M., 1977. Normative calculation technique for determining opal in deep-sea sediments. Geochim. Cosmochim. Acta 41, 671–676. https://doi.org/10.1016/0016-7037(77)90304-0.
Liu, D., 2020. Integrating Sediment Grain Size and Inorganic Geochemistry: Implications for Paleohydrological Research in Patagonia. PhD thesis.. Ghent University, Belgium, 165 p.
Liu, X.D., Sun, L.G., Li, D., Wang, Y.H., 2011. Rare earth elements in the ornithogenic sediments from the Maritime Antarctic: a potential new palaeoecology proxy. Geochem. J. 45, 15–26. https://doi.org/10.2343/geochemj.1.0087.
Liu, D.W., Bertrand, S., Weltje, G.J., 2019. An empirical method to predict sediment grain size from inorganic geochemical measurements. Geochem. Geophys. Geosyst. 20, 3690–3704. https://doi.org/10.1029/2018gc008154.
Liu, D., Bertrand, S., Villaseñor, T., Van Dijck, T., Fagel, N., Mattielli, N., 2020. Provenance of northwestern Patagonian river sediments (44–48°S): a critical evaluation of mineralogical, geochemical and isotopic tracers. Sediment. Geol. 408, 105744 https://doi.org/10.1016/j.sedgeo.2020.105744.
Liu, D., Bertrand, S., Vandekerkhove, E., Renson, V., 2022. Provenance of Baker River sediments (Chile, 48°S): implications for the identification of flood deposits in fjord sediments. Earth Surf. Process. Landf. 47 (3), 825–838. https://doi.org/10.1002/esp.5287.
Lizaga, I., Latorre, B., Gaspar, L., Navas, A., 2020. FingerPro: an R package for tracking the provenance of sediment. Water Resour. Manag. 34, 3879–3894. https://doi.org/10.1007/s11269-020-02650-0.
Loring, D.H., Rantala, R.T.T., 1992. Manual for the geochemical analyses of marine sediments and suspended particulate matter. Earth Sci. Rev. 32, 235–283. https://doi.org/10.1016/0012-8252(92)90001-a.
Lowemark, L., Chen, H.F., Yang, T.N., Kylander, M., Yu, E.F., Hsu, Y.W., Lee, T.Q., Song, S.R., Jarvis, S., 2011. Normalizing XRF-scanner data: a cautionary note on the interpretation of high-resolution records from organic-rich lakes. J. Asian Earth Sci. 40, 1250–1256. https://doi.org/10.1016/j.jseaes.2010.06.002.
Machado, A., Lima, E.F., Chemale, F., Morata, D., Oteiza, O., Almeida, D.P.M., Figueiredo, A.M.G., Alexandre, F.M., Urrutia, J.L., 2005. Geochemistry constraints of Mesozoic-Cenozoic calc-alkaline magmatism in the South Shetland arc, Antarctica. J. S. Am. Earth Sci. 18, 407–425. https://doi.org/10.1016/j.jsames.2004.11.011.
Magnusson, G., 1984. Lapphyttan – en medeltida masugn i Karbennings socken. In: Norberg (Ed.), Särtryck ur Karbenning. En bergslagssocken. Norbergs kommun, pp. 60–85.
Martin-Puertas, C., Tjallingii, R., Bloemsma, M., Brauer, A., 2017. Varved sediment responses to early Holocene climate and environmental changes in Lake Meerfelder Maar (Germany) obtained from multivariate analyses of micro X-ray fluorescence core scanning data. J. Quat. Sci. 32, 427–436. https://doi.org/10.1002/jqs.2935.
Meyer, I., Davies, G.R., Stuut, J.-B.W., 2011. Grain size control on Sr-Nd isotope provenance studies and impact on paleoclimate reconstructions: an example from deep-sea sediments offshore NW Africa. Geochem. Geophys. Geosyst. 12 https://doi.org/10.1029/2010GC003355.
Miller, H., Croudace, I.W., Bull, J.M., Cotterill, C.J., Dix, J.K., Taylor, R.N., 2014. A 500 year sediment lake record of anthropogenic and natural inputs to Windermere (English Lake District) using double-spike lead isotopes, radiochronology, and sediment microanalysis. Environ. Sci. Technol. 48, 7254–7263. https://doi.org/10.1021/es5008998.
Morlock, M.A., Vogel, H., Russell, J.M., Anselmetti, F.S., Bijaksana, S., 2021. Quaternary environmental changes in tropical Lake Towuti, Indonesia, inferred from end-member modelling of X-ray fluorescence core-scanning data. J. Quat. Sci. 36, 1040–1051. https://doi.org/10.1002/jqs.3338.
Mörth, C.-M., Backman, J., 2011. Practical steps for improved estimates of calcium carbonate concentrations in deep sea sediments using coulometry. Limnol. Oceanogr. Methods 9, 565–570. https://doi.org/10.4319/lom.2011.9.565.
Mortlock, R.A., Froelich, P.N., 1989. A simple method for the rapid determination of biogenic opal in pelagic marine sediments. Deep-Sea Res. Part a-Oceanogr. Res. Pap. 36, 1415–1426. https://doi.org/10.1016/0198-0149(89)90092-7.
Müller, D., Neugebauer, I., Ben Dor, Y., Enzel, Y., Schwab, M.J., Tjallingii, R., Brauer, A., 2022. Phases of stability during major hydroclimate change ending the Last Glacial in the Levant. Sci. Rep. 12, 6052. https://doi.org/10.1038/s41598-022-10217-9.
Murdmaa, I., Borisov, D., Dorokhova, E., Dara, O., 2021. Lithology. In: Murdmaa, I., Ivanova, E. (Eds.), The Ioffe Drift. Springer, pp. 53–97. https://doi.org/10.1007/978-3-030-82871-4_6.
Murray, R., Miller, D., Kryc, K., 2000. Analysis of major and trace elements in rocks, sediments, and interstitial waters by inductively coupled plasma–atomic emission spectrometry (ICP-AES). ODP Tech. Note 1–27.
Myrbo, A., Morrison, A., McEwan, R., 2011. Tool for Microscopic Identification (TMI). https://tmi.csd.umn.edu.
Myrstener, E., Biester, H., Bigler, C., Lidberg, W., Meyer-Jacob, C., Rydberg, J., Bindler, R., 2019. Environmental footprint of small-scale, historical mining and metallurgy in the Swedish boreal forest landscape: the Moshyttan blast furnace as microcosm. The Holocene 29, 578–591. https://doi.org/10.1177/0959683618824741.
Nesbitt, H., Young, G., 1982. Early Proterozoic climates and plate motions inferred from major element chemistry of lutites. Nature 299, 715–717. https://doi.org/10.1038/299715a0.
Nesbitt, H., Young, G., 1996. Petrogenesis of sediments in the absence of chemical weathering: effects of abrasion and sorting on bulk composition and mineralogy. Sedimentology 43, 341–358. https://doi.org/10.1046/j.1365-3091.1996.d01-12.x.
Neugebauer, I., Brauer, A., Schwab, M.J., Dulski, P., Frank, U., Hadzhiivanova, E., Kitagawa, H., Litt, T., Schiebel, V., Taha, N., Waldmann, N.D., 2015. Evidences for centennial dry periods at ~3300 and ~2800 cal. yr BP from micro-facies analyses of

the Dead Sea sediments. The Holocene 25, 1358–1371. https://doi.org/10.1177/0959683615584208.
Ohlendorf, C., Sturm, M., 2007. A modified method for biogenic silica determination. J. Paleolimnol. 39, 137–142. https://doi.org/10.1007/s10933-007-9100-7.
Ohlendorf, C., Wennrich, V., Enters, D., 2015. Experiences with XRF-scanning of long sediment records. In: Croudace, I.W., Rothwell, R.G. (Eds.), Micro-XRF Studies of Sediment Cores: Applications of a Non-destructive Tool for the Environmental Sciences. Springer, Dordrecht, pp. 351–372. https://doi.org/10.1007/978-94-017-9849-5_13.
Ordoñez, L., Vogel, H., Sebag, D., Ariztegui, D., Adatte, T., Russell, J.M., Kallmeyer, J., Vuillemin, A., Friese, A., Crowe, S.A., Bauer, K.W., Simister, R., Henny, C., Nomosatryo, S., Bijaksana, S., 2019. Empowering conventional Rock-Eval pyrolysis for organic matter characterization of the siderite-rich sediments of Lake Towuti (Indonesia) using End-Member Analysis. Org. Geochem. 134, 32–44. https://doi.org/10.1016/j.orggeochem.2019.05.002.
Pillot, D., Deville, E., Prinzhofer, A., 2014. Identification and quantification of carbonate species using rock-eval pyrolysis. Oil & Gas Science and Technology – Revue d'IFP Energies nouvelles 69, 341–349. https://doi.org/10.2516/ogst/2012036.
Potts, P.J., 1987. A Handbook of Silicate Rock Analysis. Chapman and Hall, Glasgow, New York. https://doi.org/10.1007/978-94-015-3988-3, 622 p.
Pribyl, D.W., 2010. A critical review of the conventional SOC to SOM conversion factor. Geoderma 156, 75–83. https://doi.org/10.1016/j.geoderma.2010.02.003.
Pulley, S., Collins, A.L., 2018. Tracing catchment fine sediment sources using the new SIFT (SedIment Fingerprinting Tool) open source software. Sci. Total Environ. 635, 838–858. https://doi.org/10.1016/j.scitotenv.2018.04.126.
Pulley, S., Foster, I., Antunes, P., 2015. The uncertainties associated with sediment fingerprinting suspended and recently deposited fluvial sediment in the Nene river basin. Geomorphology 228, 303–319. https://doi.org/10.1016/j.geomorph.2014.09.016.
Rebolledo, L., Bertrand, S., Lange, C.B., Tapia, F.J., Quiroga, E., Troch, M., Silva, N., Cárdenas, P., Pantoja, S., 2019. Compositional and biogeochemical variations of sediments across the terrestrial-marine continuum of the Baker-Martínez fjord system (Chile, 48°S). Prog. Oceanogr. 174, 89–104. https://doi.org/10.1016/j.pocean.2018.12.004.
Renberg, I., Persson, M.W., Emteryd, O., 1994. Pre-industrial atmospheric lead contamination detected in Swedish lake sediments. Nature 368, 323–326. https://doi.org/10.1038/368323a0.
Renberg, I., Bindler, R., Brännvall, M.-L., 2016. Using the historical atmospheric lead-deposition record as a chronological marker in sediment deposits in Europe. The Holocene 11, 511–516. https://doi.org/10.1191/095968301680223468.
Richter, T.O., Gaast, S.V.D., Koster, B., Vaars, A., Gieles, R., Stigter, H.C.D., Haas, H.D., Weering, T.C.E.V., Rothwell, R.G., 2006. The Avaatech XRF Core Scanner: Technical Description and Applications to NE Atlantic Sediments, New Techniques in Sediment Core Analysis. Geological Society of London, p. 0. https://doi.org/10.1144/gsl.sp.2006.267.01.03.
Roberts, S.J., Monien, P., Foster, L.C., Loftfield, J., Hocking, E.P., Schnetger, B., Pearson, E.J., Juggins, S., Fretwell, P., Ireland, L., Ochyra, R., Haworth, A.R., Allen, C.S., Moreton, S.G., Davies, S.J., Brumsack, H.J., Bentley, M.J., Hodgson, D.A., 2017. Past penguin colony responses to explosive volcanism on the Antarctic Peninsula. Nat. Commun. 8 https://doi.org/10.1038/ncomms14914.
Rothwell, R.G., 2006. New Techniques in Sediment Core Analysis, vol. 267. Geological Society of London. https://doi.org/10.1144/gsl.sp.2006.267, 266 p.
Rothwell, R.G., Croudace, I.W., 2015. Twenty years of XRF core scanning marine sediments: What do geochemical proxies tell us? In: Croudace, I.W., Rothwell, R.G. (Eds.), Micro-XRF Studies of Sediment Cores: Applications of a Non-Destructive Tool for the Environmental Sciences. Springer Dordrecht, pp. 25–102. https://doi.org/10.1007/978-94-017-9849-5_2.
Rudnick, R.L., Gao, S., 2014. Composition of the Continental Crust, pp. 1–51. https://doi.org/10.1016/B978-0-08-095975-7.00301-6.
Rydberg, J., 2014. Wavelength dispersive X-ray fluorescence spectroscopy as a fast, non-destructive and cost-effective analytical method for determining the geochemical composition of small loose-powder sediment samples. J. Paleolimnol. 52, 265–276. https://doi.org/10.1007/s10933-014-9792-4.
Sabatier, P., Wilhelm, B., Ficetola, G.F., Moiroux, F., Poulenard, J., Develle, A.-L., Bichet, A., Chen, W., Pignol, C., Reyss, J.-L., Gielly, L., Bajard, M., Perrette, Y., Malet, E., Taberlet, P., Arnaud, F., 2017. 6-kyr record of flood frequency and intensity in the western Mediterranean Alps – Interplay of solar and temperature forcing. Quat. Sci. Rev. 170, 121–135. https://doi.org/10.1016/j.quascirev.2017.06.019.
Sabatier, P., Moernaut, J., Bertrand, S., Van Daele, M., Kremer, K., Chaumillon, E., Arnaud, F., 2022. A review of event deposits in lake sediments. Quaternary 5, 34. https://doi.org/10.3390/quat5030034.
Sakamoto, T., Kuroki, K., Sugawara, T., Aoike, K., Iijima, K., Sugisaki, S., 2006. Non-destructive x-ray fluorescence (XRF) core-imaging scanner, TATSCAN-F2. Sci. Drill. 2, 37–39. https://doi.org/10.5194/sd-2-37-2006.
Schillereff, D.N., Chiverrell, R.C., Croudace, I.W., Boyle, J.F., 2015. An inter-comparison of μXRF scanning analytical methods for lake sediments. In: Croudace, I.W., Rothwell, R.G. (Eds.), Micro-XRF Studies of Sediment Cores: Applications of a Non-destructive Tool for the Environmental Sciences. Springer, Dordrecht, pp. 583–600. https://doi.org/10.1007/978-94-017-9849-5_24.
Schuenemeyer, J.H., Drew, L.J., 2011. Statistics for Earth and Environmental Scientists. Wiley, Hoboken, N.J, 420 p.
Sholkovitz, E.R., 1990. Rare-Earth elements in marine sediments and geochemical standards. Chem. Geol. 88, 333–347. https://doi.org/10.1016/0009-2541(90)90097-Q.
Stutenbecker, L., Scheuvens, D., Hinderer, M., Hornung, J., Petschick, R., Raila, N., Schwind, E., 2023. Temporal variability of fluvial sand composition: an annual time series from four rivers in SW Germany. J. Geophys. Res. Earth 128. https://doi.org/10.1029/2023jf007138.
Sun, L.G., Xie, Z.Q., Zhao, J.L., 2000. A 3,000-year record of penguin populations. Nature 407, 858. https://doi.org/10.1038/35038163.
Tatur, A., Barczuk, A., 1985. Ornithogenic phosphates on King George Island in the maritime Antarctic, 163–168. https://doi.org/10.1007/978-3-642-82275-9_22.
Tatur, A., Myrcha, A., Niegodzisz, J., 1997. Formation of abandoned penguin rookery ecosystems in the maritime Antarctic. Polar Biol. 17, 405–417. https://doi.org/10.1007/s003000050135.
Thevenon, F., Guédron, S., Chiaradia, M., Loizeau, J.-L., Poté, J., 2011. (Pre-) historic changes in natural and anthropogenic heavy metals deposition inferred from two contrasting Swiss Alpine lakes. Quat. Sci. Rev. 30, 224–233. https://doi.org/10.1016/j.quascirev.2010.10.013.
Thomson, J., Croudace, I.W., Rothwell, R.G., 2006. A geochemical application of the ITRAX scanner to a sediment core containing eastern Mediterranean sapropel units. Geol. Soc. Lond. Spec. Publ. 267, 65–77. https://doi.org/10.1144/gsl.sp.2006.267.01.05.
Tjallingii, R., Rohl, U., Kolling, M., Bickert, T., 2007. Influence of the water content on X-ray fluorescence core-scanning measurements in soft marine sediments. Geochem. Geophys. Geosyst. 8 https://doi.org/10.1029/2006gc001393.
van den Boogaart, K.G., Tolosana-Delgado, R., 2008. "Compositions": a unified R package to analyze compositional data. Comput. Geosci. 34, 320–338. https://doi.org/10.1016/j.cageo.2006.11.017.
Vandekerkhove, E., Bertrand, S., Torrejón, F., Kylander, M.E., Reid, B., Saunders, K.M., 2021. Signature of modern glacial lake outburst floods in fjord sediments (Baker River, southern Chile). Sedimentology 68, 2798–2819. https://doi.org/10.1111/sed.12874.
Verardo, D.J., Froelich, P.N., Mcintyre, A., 1990. Determination of organic-carbon and nitrogen in marine-sediments using the Carlo-Erba-Na-1500 analyzer. Deep-Sea Res. Part a-Oceanogr. Res. Pap. 37, 157–165. https://doi.org/10.1016/0198-0149(90)90034-S.
Wattripont, A., Baudin, F., de Rafelis, M., Deconinck, J.-F., 2019. Specifications for carbonate content quantification in recent marine sediments using Rock-Eval pyrolysis. J. Anal. Appl. Pyrolysis 140, 393–403. https://doi.org/10.1016/j.jaap.2019.04.019.
Weltje, G.J., 1997. End-member modeling of compositional data: numerical-statistical algorithms for solving the explicit mixing problem. Math. Geol. 29, 503–549. https://doi.org/10.1007/Bf02775085.
Weltje, G.J., Tjallingii, R., 2008. Calibration of XRF core scanners for quantitative geochemical logging of sediment cores: theory and application. Earth Planet. Sci. Lett. 274, 423–438. https://doi.org/10.1016/j.epsl.2008.07.054.
Weltje, G.J., Bloemsma, M.R., Tjallingii, R., Heslop, D., Röhl, U., Croudace, I.W., 2015. Prediction of geochemical composition from XRF core scanner data: a new multivariate approach including automatic selection of calibration samples and quantification of uncertainties. In: Croudace, I.W., Rothwell, R.G. (Eds.), Micro-XRF Studies of Sediment Cores: Applications of a Non-destructive Tool for the Environmental Sciences. Springer, Dordrecht, pp. 507–534. https://doi.org/10.1007/978-94-017-9849-5_21.
Wien, K., Wissmann, D., Kölling, M., Schulz, H.D., 2005. Fast application of X-ray fluorescence spectrometry aboard ship: how good is the new portable Spectro Xepos analyser? Geo-Mar. Lett. 25, 248–264. https://doi.org/10.1007/s00367-004-0206-x.
Wilhelm, B., Arnaud, F., Enters, D., Allignol, F., Legaz, A., Magand, O., Revillon, S., Giguet-Covex, C., Malet, E., 2012a. Does global warming favour the occurrence of extreme floods in European Alps? First evidences from a NW Alps proglacial lake sediment record. Clim. Chang. 113, 563–581. https://doi.org/10.1007/s10584-011-0376-2.
Wilhelm, B., Arnaud, F., Sabatier, P., Crouzet, C., Brisset, E., Chaumillon, E., Disnar, J.R., Guiter, F., Malet, E., Reyss, J.L., Tachikawa, K., Bard, E., Delannoy, J.J., 2012b. 1400 years of extreme precipitation patterns over the Mediterranean French Alps and possible forcing mechanisms. Quat. Res. 78, 1–12. https://doi.org/10.1016/j.yqres.2012.03.003.
Wilhelm, B., Arnaud, F., Sabatier, P., Magand, O., Chapron, E., Courp, T., Tachikawa, K., Fanget, B., Malet, E., Pignol, C., Bard, E., Delannoy, J.J., 2013. Palaeoflood activity and climate change over the last 1400 years recorded by lake sediments in the north-west European Alps. J. Quat. Sci. 28, 189–199. https://doi.org/10.1002/jqs.2609.
Wilhelm, B., Vogel, H., Crouzet, C., Etienne, D., Anselmetti, F.S., 2016. Frequency and intensity of palaeofloods at the interface of Atlantic and Mediterranean climate domains. Clim. Past 12, 299–316. https://doi.org/10.5194/cp-12-299-2016.
Wilhelm, B., Amann, B., Corella, J.P., Rapuc, W., Giguet-Covex, C., Merz, B., Støren, E., 2022. Reconstructing paleoflood occurrence and magnitude from lake sediments. Quaternary 5, 9. https://doi.org/10.3390/quat5010009.
Wilkin, R.T., Barnes, H.L., Brantley, S.L., 1996. The size distribution of framboidal pyrite in modern sediments: an indicator of redox conditions. Geochim. Cosmochim. Acta 60, 3897–3912. https://doi.org/10.1016/0016-7037(96)00209-8.
Wohlfarth, B., Veres, D., Ampel, L., Lacourse, T., Blaauw, M., Preusser, F., Andrieu-Ponel, V., Keravis, D., Lallier-Verges, E., Bjorck, S., Davies, S.M., de Beaulieu, J.L., Risberg, J., Hormes, A., Kasper, H.U., Possnert, G., Reille, M., Thouveny, N., Zander, A., 2008. Rapid ecosystem response to abrupt climate changes during the last glacial period in western Europe, 40-16 ka. Geology 36, 407–410. https://doi.org/10.1130/G24600a.1.
Woodward, C.A., Gadd, P.S., 2019. The potential power and pitfalls of using the X-ray fluorescence molybdenum incoherent: coherent scattering ratio as a proxy for

sediment organic content. Quat. Int. 514, 30–43. https://doi.org/10.1016/j.quaint.2018.11.031.
Wu, L., Wilson, D.J., Wang, R., Yin, X., Chen, Z., Xiao, W., Huang, M., 2020. Evaluating Zr/Rb ratio from XRF scanning as an indicator of grain-size variations of glaciomarine sediments in the Southern Ocean. Geochem. Geophys. Geosyst. 21 https://doi.org/10.1029/2020GC009350 e2020GC009350.
Zhan, X., 2005. Application of polarized EDXRF in geochemical sample analysis and comparison with WDXRF. X-Ray Spectrom. 34, 207–212. https://doi.org/10.1002/xrs.794.